The Effect of Ethanol on the Differentiation of C2C12 Mouse Myogenic Cells

A dissertation

submitted by

Michelle A. Arya

In fulfillment of the requirements

for the degree of

Doctor of Philosophy

in

Genetics

TUFTS UNIVERSITY

Sackler School of Graduate Biomedical Sciences

August, 2012

ADVISER: Gordon S. Huggins, M.D.

Abstract

The loss of muscle mass in alcoholic myopathy may reflect alcohol inhibition of myogenic cell differentiation into myotubes. In order to examine this possibility, the effects of alcohol on the mouse C2C12 cell line, an established model of myogenic cell differentiation, was measured through the use of a custom high content immunocytochemical assay. Exposure to ethanol caused shorter and thinner myotubes to form and inhibited the myogenic fusion index (MFI) ($p<0.05$).

Ethanol reduced levels of the muscle regulatory factors (MRFs), Myf5, MyoD and myogenin ($p<0.05$) during differentiation. Transcriptional profiling over three days identified genes significantly altered by alcohol during differentiation compared with control treated cells and MyoD was found to be significantly associated with ethanol driven C2C12 differentiation ($p=8.7 \times 10^{-4}$). The microarray also predicted activation of the Notch signaling pathway ($p=4.35 \times 10^{-3}$). Notch signaling has been shown to inhibit muscle differentiation.

The Notch effectors, Hes-1 and Hey-1 were consistently up-regulated by alcohol treatment and ethanol increased activity of the proximal Hes-1 gene promoter which contains the CBF-1/RBP-Jk response element ($p \leq 0.05$). Blocking Notch signaling with a ɣ-secretase inhibitor (GSI) abrogated the ethanol induced increase in Hes-1 and partly restored MyoD levels ($p<0.05$).

The GSI completely restored the myogenic fusion index (MFI) in C2C12 cells differentiating in the presence of ethanol and modest improvements were seen in all other cellular parameters measured in the immunocytochemical assay (p<0.05).

Signaling through Notch1 is required to maintain the satellite cell pool in post-natal myogenesis. Ethanol reduced levels of activated Notch1 (N1-ICD) during C2C12 differentiation (p<0.05) and tended to decrease the number of quiescent CD34- cells which are reported to express Notch 1 (p=0.08).

My results suggest that ethanol inhibits C2C12 differentiation by reducing MyoD, blocks myoblast fusion events by activating Notch signaling and decreases Notch1 to attenuate maintenance of the satellite cell pool.

Dedication

This thesis is dedicated to Jason Altom (1971-1998) who made the ultimate

sacrifice to improve the lives of graduate students.

The man [woman] who stands for nothing will fall for anything.

Malcolm X (1925-1965)

THE BLIND MEN AND THE ELEPHANT

A Hindoo Fable

A Poem by John Godfrey Saxe

(1816-1887)

I.

It was six men of Indostan

To learning much inclined,

Who went to see the Elephant

(Though all of them were blind),

That each by observation

Might satisfy his mind.

II.

The *First* approached the Elephant,

And happening to fall

Against his broad and sturdy side,

At once began to bawl:

"God bless me!--but the Elephant

Is very like a wall!"

III.

The *Second*, feeling of the tusk,

Cried:"Ho!-what have we here

So very round and smooth and sharp?

To me 't is mighty clear

This wonder of an Elephant

Is very like a spear!"

IV.

The *Third* approached the animal,

And happening to take

The squirming trunk within his hands,

Thus boldly up and spake:

"I see," quoth he, "the Elephant

Is very like a snake!"

V.

The *Fourth* reached out his eager hand,

And felt about the knee.

"What most this wondrous beast is like

Is mighty plain," quoth he;

"T is clear enough the Elephant

Is very like a tree!"

VI.

The *Fifth*, who chanced to touch the ear,

Said: "E'en the blindest man

Can tell what this resembles most;

Deny the fact who can,

This marvel of an Elephant

Is very like a fan!"

VII.

The *Sixth* no sooner had begun

About the beast to grope,

Then, seizing on the swinging tail

That fell within his scope,

"I see," quoth he, "the Elephant

Is very like a rope!"

VIII.

And so these men of Indostan

Disputed loud and long,

Each in his own opinion

Exceeding stiff and strong,

Though each was partly in the right,

And all were in the wrong!

MORAL.

So, oft in theologic wars

The disputants, I ween,

Rail on in utter ignorance

Of what each other mean,

And prate about an Elephant

Not one of them has seen!

Acknowledgments

"I start where the last man left off," spoke Thomas Edison and my work began where that of my thesis advisor, Dr. Gordon Huggins left off. I would like to thank him for writing the grant proposal funded by NIH (R01-AA014140, G.S.H.) which contained the seed for my fascinating project. I would like to thank Elena Kudryavtseva for showing me how to culture the C2C12 cells and how to perform the initial Troponin T assay to quantify myotube formation using ImageJ which I adapted for use in my thesis work.

I would like thank the committee, my chair, Dr. Pam Yelick, Dr. Phil Hinds, whom I considered like my second thesis advisor, and Dr. Claire Moore for their guidance and support over the years. I would like to thank Dr. Erik Selsing and Dean Kathryn Lange for their support. I would like to thank Dr. Matt Layne for serving as my outside examiner.

I consider myself incredibly lucky to be married to Paul Taslimi, who is a brilliant scientist. He has been a scientific mentor to me throughout most of our relationship and bouncing ideas off him and getting his input has made this a much better endeavor then I could have accomplished on my own. He is a wonderful husband and amazing father to our children and without his support I would not have been able to come this far.

In 2002 when my son, Severin was born I became a mother and in 2005 my daughter, Claire followed. In my darkest days, their presence and love gave me the inspiration and strength to continue the fight to build a better future for them.

Table of Contents

List of Figures

Chapter 1

Chapter 3

Chapter 4

Chapter 5

Chapter 6

List of Tables

Chapter 5

Chapter One

Myogenesis

The Origin of the Muscle Satellite (Stem) Cells

Formation of the mesoderm and the neural tube occurs during gastrulation[1]. The mesoderm gives rise in turn to skeletal muscle. Flanking either side of the neural tube lie thick bands of non-segmented mesodermal cells[1]. The paraxial mesoderm (area which forms lateral to both sides of the neural tube) is cleaved into somites [1]. As the somite matures, subdivisions are formed (**Figure 1.1**)[1]. The ventral-medial epithelial cells of the somite (cells located furthest from the back but closest to the neural tube) i.e. the sclerotome divide and dedifferentiate to become mesenchymal (unspecialized mesodermal) cells again[1]. These mesenchymal cells give rise to chondrocytes (cartilage cells) of the vertebrae and ribs[1]. The central zone of the dorsal layer of the dermamyotome, called the dermatome, forms the dermis (mesenchymal connective tissue of the back skin)[1]. Cells in the two lateral regions of the epithelium make up the primary myotome, a muscle-forming region[1]. The cells of the myotome produce a lower layer of muscle precursor cells, the myoblasts[1]. The resulting double-layered structure is called the dermamyotome[1].

Those myoblasts made from the region closest to the neural tube will form the primaxial (epaxial) muscles[1]. These muscles lie between the ribs and the deep back muscles[1]. Myoblasts made in the region farthest from the neural tube will make up the abaxial (hypaxial) muscles of the body wall, limbs and tongue[1]. These myoblasts move away from the center and differentiate within

(A) 2-day embryo
- Epidermis
- Neural tube
- Somite
- Notochord

(B) 3-day embryo
- Epidermis
- Dermamyotome
- Neural tube
- Sclerotome
- Notochord

(C) 4-day embryo
- Epidermis
- Epaxial dermamyotome lip
- Neural tube
- Epaxial myotome
- Sclerotome cells
- Notochord
- Central dermamyotome region
- Hypaxial myotome
- Hypaxial dermamyotome lip

(D) Late 4-day embryo
- Epidermis
- Epaxial dermamyotome lip
- Dorsal root ganglia
- Neural tube
- Myotome
- Notochord
- Sclerotome
- Central dermamyotome region
- Hypaxial somitic bud

Gilbert 2006

Figure 1.1: Somite specification in chick embryo on days 2-4. (A) On day 2 the sclerotome cells are visible. (B) On day 3, the scleretome cells detach from one another and migrate to the neural tube. (C) On day 4 the rest of the cells divide. The medial cells construct a primaxial myotome beneath the dermamyotome and the lateral cells construct the abaxial myotome. (D) The myotome (muscle cell precursors) forms under the epithelial dermamyotome[1].

the lateral plate-derived dermis[1]. After formation of the primary myotome is complete, cells detach from the central most region of the dermamyotome and join the cells of the primary myotome to form a secondary myotome (usually called the myotome)[1]. These central cells differ from the marginal myoblasts by being undifferentiated, and they undergo rapid cell division to make up most of the myoblast cell population[1]. The majority of these cells will differentiate to form muscle, however some will remain undifferentiated and reside around the muscle[1]. These undifferentiated cells give rise to the satellite (stem) cells which are responsible for postnatal muscle growth and repair[1]. These satellite cells express the transcription factors, Pax3 and/or Pax7 and they remain quiescent until late fetal myogenesis or until they differentiate into myogenic cells whereupon they induce Myf5 and MyoD[3]. Lineage tracing studies suggest that Pax3+ cells provide embryonic myoblasts and endothelial cells whereas Pax7+ cells furnish fetal myogenic cells [3].

The Formation of Skeletal Muscle

The primaxial myoblasts are specified by factors from the neural tube, perhaps Wnt1 and Wnt3a and Shh[1]. The abaxial myoblasts are likely specified by Wnt proteins from the epidermis and BMP4 from the lateral plate mesoderm[1]. Paracrine factors in the lateral part of the dermamyotome induce the transcription factor, Pax3, which then activates the MyoD gene to form the hypaxial muscles[1]. In the central part of the dermamyotome paracrine factors induce Myf5 which activates MyoD to form the epaxial muscles[1].

To form skeletal muscle, MyoD is active throughout the differentiation program[1]. First, it directly activates muscle-specific genes necessary for skeletal muscle formation[1]. MyoD also directly activates its own gene[1]. Secondly MyoD can activate non-muscle specific genes, the products of which help MyoD bind enhancers that activate a second group of muscle-specific genes[1].

Commitment of cells to the myoblast lineage is mediated by the activation of MyoD and Myf5 and terminal differentiation is mediated by myogenin. This stage is followed by the formation of multinucleated myotube cells (**Figure 1.2**). Myotubes are formed by the fusion of several myoblasts to each other and the dissolution of the cell membranes between them[1]. Once the myoblasts stop dividing the events leading to cell fusion will begin. The first step involves exit from the cell cycle when the supply of growth factors, in particular FGF (fibroblast growth factor) is exhausted[1]. The myoblasts then secrete fibronection into their extracellular matrix and bind to it through α5β1 integrin, their principal fibronectin receptor[1]. The second step involves alignment of the myoblasts into series mediated by cell membrane glycoproteins, including several cadherins and CAMs (cell adhesion molecules)[1]. The third step is the cell fusion event itself. Calcium ions are critical, and fusion can be activated by ionophores which transport Ca^{2+} across cell membranes[1]. Fusion is also likely mediated by metalloproteinases called meltrins[1]. After the myotube is formed, the myotube secretes IL4 which engages other myoblasts to fuse with the tube[1].
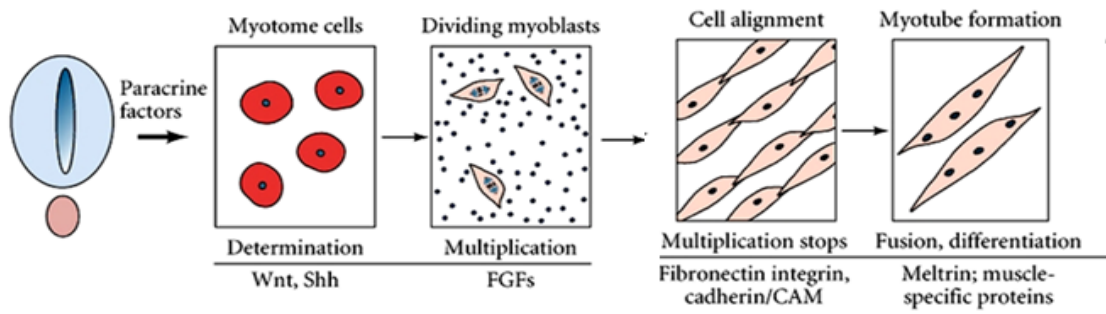
Gilbert 2006

Figure 1.2: Myoblast differentiation into myotubes in culture. Paracrine factors determine the myotome cells. Committed myoblasts continue cycling in the presence of mitogens (FGFs). Upon growth factor withdrawal, the myoblasts exit the cell cycle, align and fuse into myotubes. The myotubes organize into muscle fibers which contract (not shown)[1].

The Role of Satellite Cells in Post-Natal Myogenesis

Skeletal muscle in the mouse is determined from embryonic day 8.5/9 (E8.5/9) to E18.5 and following birth to about 19 days [4, 5]. Muscle maturation occurs for approximately three weeks during the postnatal period mostly due to hypertrophy (enlargement) of myofibers [4, 5].

The satellite cells which are lodged in the hollows between the muscle cell membrane and the basal lamina give rise to new myofibers during the perinatal period and to new myofibers in response to injury or exercise in adults[1, 6, 7]. Satellite cells account for the principal means by which adult muscle is formed[8]. Satellite cell nuclei drop from about 30% to about 5% in the 2 month old mouse due to fusion into new or resident myofibers[8]. Pax3 expression disappears from satellite cells after birth[3]. Pax7 expression is seen in satellite cells and proliferating myoblasts and it disappears before differentiation[3]. Pax7 is necessary for the formation of satellite cells as Pax7-knock-out mice do not contain satellite cells and Pax3 cannot compensate for the absence of Pax7[3]. Interestingly, molecular mechanisms of satellite cell regulation may be different in the post-natal period compared with during embryonic development. Pax7 and Pax3 may not be necessary for post-natal muscle regeneration since skeletal muscle regeneration was shown to be unimpaired in mice when Pax7 and Pax3 were conditionally knocked out [9]. However a requirement for Pax7 was seen until postnatal day 21 suggesting that Pax7 is necessary for formation of the satellite cell pool [9]. The finding that Pax7 is unnecessary for post-natal regeneration is considered controversial and unresolved[3].

Adult muscle turns over slowly so satellite cells remain quiescent unless activated by exercise or injury[3]. Removal of satellite cells under physiological conditions does not escalate loss of muscle mass[3]. This is in contrast to degenerative muscle diseases such as Duchenne muscular dystrophy (DMD) where continuous muscle regeneration causes increased proliferation of satellite cells which eventually exhausts the stem cell pool[3]. A more toxic phenotype of muscle wasting is seen in the mdx mouse, a model for DMD in which satellite cell function is further disrupted suggesting that satellite cells are indispensable for regeneration. The profound phenotypes that result from loss of satellite cells in disease suggests there is no compensatory mechanism to produce muscle in this instance[3].

Activation of Satellite Cells

When activated, satellite cells proliferate and divide for many cycles before they fuse with each other or the injured myofibers[8, 10]. Satellite cells recruited to injured adult skeletal muscle rely on the sequential expression of MyoD and myogenin to activate expression of skeletal muscle genes [11-13]. MyoD controls commitment of myoblasts to differentiation and myogenin controls terminal differentiation[12]. Growth of the satellite cell pool requires activation of Notch signaling which causes expression of transcriptional repressors of myogenesis including Hey1, Hes1 and MyoR to inhibit MyoD and myogenin. Termination of Notch signaling allows differentiation to proceed[14-20].

Wnt proteins have been shown to be critical players in satellite cell commitment and self-renewal during post-natal myogenesis[13]. After Notch

signaling expands the progenitor pool, canonical Wnt3a signaling is necessary for effective muscle differentiation and regeneration[13]. Wnt7a mediates expansion of the satellite cell pool and has been shown to augment regeneration in injured muscle[13]. Other factors important in the regulation of satellite cells include HGF, FGFs, IGF-1, myostatin and TGF-β [13, 21].

Quiescent Satellite Cells

Satellite cells that do not fuse with myotubes enter a quiescent state which depends on Notch signaling[3]. In mice knocked out for the Notch targets, Hesr1 (Hey1) and Hesr3 (Heyl), quiescent satellite cells cannot form [3, 22]. Blocking Notch signaling in quiescent satellite cells causes their premature differentiation and fusion[3]. Quiescent satellite cells express Pax7, α7β1 integrin, CD34, syndecan 3, syndecan 4, myotubule cadherin (M-cadherin), caveolin 1, CXC chemokine receptor 4 (CXCR4) and calcitonin receptor (CTR)[3, 10]. Lineage tracing experiments performed in mice in which cells that had expressed Myf5 were labeled with yellow fluorescent protein (YFP) have shown that a tenth of the Pax7 expressing cells expressed Pax7 but not YFP indicating they never expressed Myf5 [3]. The less committed Pax7+, YFP- cells gave rise to YFP+ satellite cells and were able to resist differentiation[3]. These YFP- cells expressed Notch3 whereas the activated and hence more committed YFP+ cells expressed Delta[23]. Inhibition of Notch signaling with a ɣ-secretase inhibitor reduced the number of YFP- cells and caused appearance of more MyoD+ cells l.positing a role for Notch in maintenance of the quiescent stem cell state[23]. Furthermore the YFP- cells underwent symmetric division in response to

9

cardiotoxin which suggests that quiescent satellite cells undergo asymmetric cell division to maintain their numbers and to maintain tissue homeostasis, but in response to injury, they undergo symmetric cell division for the purpose of tissue repair[23].

Reversible Quiescence

To maintain its numbers, the satellite cell pool needs a mechanism by which to be activated, proliferate and then return to quiescence[3]. When satellite cells were isolated from myofibers and cultured in growth medium they became activated and expressed Pax7 and MyoD, however 72 hours later a subpopulation of cells stopped expressing MyoD but still expressed Pax7[24]. The majority of Pax7+/Myf5- satellite stem cells correspond to this subpopulation of cells and MyoD and myogenin are not expressed in this population when cultured on myofibers[3]. A similar phenomenon is observed in the murine myoblast C2C12 cell line derived from activated satellite cells[25]. In this cell line, MyoD is down-regulated in a subpopulation of 'reserve' cells upon transfer to differentiation medium[7]. One mechanism proposed for reversible quiescence implicates Notch signaling in a subpopulation of satellite cells to cause down-regulation of MyoD and hence resistance to differentiation[24]. Other studies have implicated the ERK pathway as a modulator of reversible quiescence and calpain3, a calcium-dependent cysteine protease that was recently reported to down-regulate MyoD during C2C12 differentiation to maintain the reserve cell population[3, 26].

The Myogenic Regulatory Factors (MRFs)

The myogenic regulatory factors (MRFs) are a group of bHLH transcription factors that are critical for cell fate commitment and differentiation into muscle[1]. The four proteins are MyoD, Myf5, myogenin, and MRF4 (Myf6)[12]. Transfection of a MRF into myriad non-muscle cell types will convert them into muscle cells[1]. Each MRF has a conserved DNA binding domain that binds to CANNTG (E box) consensus sequences located in the promoters and enhancers of genes expressed in muscle[12]. Mice lacking both Myf5 and MyoD do not develop skeletal muscle and mice lacking either Myf5 or MyoD seem to undergo normal muscle development but display defects symptomatic of lineage progression down epaxial and hypaxial lineages[12, 21]. Mice in which myogenin has been knocked out possess myoblasts but no myofibers suggesting that myogenin is necessary for the terminal differentiation of myoblasts [12, 21, 27]. MRF4 expression is expressed during the commitment and differentiation phases of muscle development suggesting it plays a role in both commitment and terminal differentiation of myoblasts[12]. Adult MyoD knock-out mice have defects in muscle regeneration presumably due to diminished differentiation of satellite cells[28]. In culture, the satellite cells display increased proliferation and delayed differentiation[21].

The MRFs associate with the Mef2 family of transcription factors to facilitate expression of muscle specific genes[12]. Mef2 proteins belong to the MADS box-containing transcription factor family[12]. There are four Mef2 family members (A-D)[12]. Mef2 genes are not only expressed in muscle, they are also

expressed in all tissues during development but only induced in developing cardiac, skeletal and smooth muscles [12, 27]. Mef2 proteins bind to the DNA sequence element (C/TTA(A/T)$_4$TAG/A) present in promoters of many muscle-specific genes[12]. On its own Mef2 does not have an ability to enforce the myogenic program but it has been shown to act co-operatively with MyoD[12]. The Mef2C knock-out mouse does not show defects in skeletal muscle but it has a defect in cardiac morphogenesis[12]. Mef2C, 2A and 2D are expressed in skeletal muscle and the splice isoforms and their expression changes in response to MyoD[12].

MyoD activation induces expression of myogenin, M-cadherin, myosin heavy and light chains, and muscle creatine kinase[12]. MyoD also up-regulates p21$^{Waf/Cip1}$, which causes the exit of differentiating cells from the cell cycle[12]. Chromatin immunoprecipitation experiments show that MyoD binds promoters of genes necessary throughout the differentiation program[12].

Histone acetyltransferases (HATs) and histone deacetylases (HDACs) interact with MyoD[12]. HAT activity goes up during myoblast differentiation and the HAT protein p300/CBP is necessary for induction of muscle-specific genes[12]. In differentiating C2C12 cells, MyoD is found in a complex with p300 and PCAF, also a HAT protein and the interaction between the three proteins has been confirmed in an in vitro transcription system[12]. The histone deacetylases, HDACs 4 and 5 interact with Mef2 proteins which then blocks transcriptional activation of Mef2 binding sites on promoters[12]. HDAC1 interacts with MyoD,

which can cause deacetylation of MyoD in vitro and MyoD has been found complexed with HDAC1 in myoblasts but not in myotubes[12].

Signaling Pathways that Modulate Myogenesis

Wnt Signaling Pathway

Activation of Wnt signaling causes the Wnt protein to bind to the Frizzled receptor which activates Dishevelled (Dsh) to inhibit GSK-3β[27, 29]. This in turn stabilizes β-catenin and with the help of T-cell factor (Tcf) activates Myf5 expression [27, 29]. Non-canonical Wnt signaling induces Pax3 transcriptional activity which then induces MyoD and myogenesis[28]. Wnt signaling has recently been shown to be important in post-natal myogenesis since Wnt signaling gets activated in injured muscle and over-activation of Wnt signaling causes significant increases in muscle regeneration[29]. Notch has been shown to antagonize Wnt signaling by activating GSK3β [14].

The FOXOs

Muscle repair and hypertrophy depends on anabolic and catabolic pathways [11, 21]. The transcription factor forkhead box O1 (FOXO1) and FOXO3A regulate catabolic pathways[11]. Phosphorylated FOXOs are kept in the cytoplasm whereas dephosphorylated FOXOs translocate to the nucleus to activate target genes[11]. The atrogenes (atrophy related genes) for example, Atrogin-1 and the MURF (muscle-up regulated RING finger) are among the downstream targets of the FOXOs[11]. Atrogenes target transcriptional proteins, metabolic and myofibrillar proteins for degradation by the autophagy-lysosomal

or the ubiquitin-proteasome system[11]. FOXO3A is the prevalent FOXO protein present in muscle[11].

Signaling through IGF-1 and protein tyrosine kinases activates the phosphoinositide 3-kinase (PI3K)-AKT pathway, an anabolic pathway in muscle which directly stimulates protein synthesis by inducing mammalian target of rapamycin (mTOR) and its downstream effectors[11]. AKT phosphorylates FOXO1 and FOXO3A[11].

Atrogin-1 can amplify catabolic pathways by stimulating the degradation of calcineurin which blocks transcriptional signals from the calcineurin-NFAT pathway, an anabolic pathway[11]. Neuronal activity relayed to muscle fibers leads to different membrane potentials and hence altered intracellular Ca^{2+} levels[11]. Ca^{2+} changes are sensed by the Ca^{2+}-activated Ser phosphatase calcineurin which dephosphorylates and activates NFAT and in the nucleus NFAT interacts with Myf5 to mediate expression of fast and slow twitch muscle isoforms[11]. NF-κB signaling regulates expression of some atrogenes for instance through TNF thus inducing catabolism [11]. Myostatin activity in differentiated fibers antagonizes IGF1 and negatively regulates muscle mass by activating SMAD2 and 3 which causes atrophy through the FOXO proteins[11].

Growth Factors in Signaling

Injured muscle causes the secretion of biologically active factors which aid in satellite cell activation and proliferation[21]. Fibroblast growth factors (FGFs), transforming growth factor-β (TGF-β), Insulin like growth factors (IGF), hepatocyte growth factor (HGF), tumor necrosis factor-α (TNF-α), interleukin-6

14

(IL-6) cytokine, neural derived factors, nitric oxide and ATP have been shown in culture systems to be important for maintaining balance between growth and differentiation of satellite cells to maintain homeostasis in muscle[21].

HGF increases in the early phases of muscle regeneration and activates quiescent satellite cells causing them to proliferate[21]. Injection of HGF into injured muscle inhibits repair while increasing the number of satellite cells[21].

IGF-I and –II have been shown in culture to change the expression of MRFs and promote proliferation and differentiation[21]. These hormones are controlled by paracrine and autocrine regulation[21]. Induction of IGF-1 in vivo causes increases in muscle mass due to increases in protein and DNA content[21]. The augmentation of muscle mass is caused both by satellite cell activation which leads to their proliferation thereby providing new myofibers and also by hypertrophy[21]. IGF-I and –II levels are increased in regenerated muscle and IGF-II improves aged muscle and dystrophic muscle in mdx mice and is induced in the later stages of muscle regeneration[21]. IGF-I acts via PI3-K pathway and Akt activation to promote cell survival[21]. As mentioned above, Akt plays a role through modification of the FOXOs[21].

TGF-β cytokines are growth factors that bind a receptor pair on the cell membrane causing the phosphorylation of SMAD proteins which then translocate to the nucleus leading to gene activation[21]. These cytokines have varied roles and can inhibit both proliferation and differentiation[21].

Myostatin (MSTN), or growth and differentiation factor-8 (GDF-8), belongs to the TGF-β family[21]. The muscles of MSTN knockout mice show a

hypertrophic and hyperplasic (increased fiber number) phenotype[21]. MSTN

may function as an inhibitor of satellite cell proliferation and regulator of fiber

growth by causing their withdrawal from the cell cycle and muscle differentiation

in the embryo[21, 28].

The Notch Signaling Pathway

The Notch signaling pathway is evolutionarily conserved among

metazoans[14]. It controls development and tissue regeneration dependent on

the context in which it acts[30]. Notch signaling controls genes involved in

proliferation, differentiation and apoptosis [2, 31]. Notch receptors are single

pass Type I trans-membrane proteins and four homologues are present in

mammals containing both redundant and separate activities[2].

The Notch Protein, Processing and Activation

The Notch protein is a single pass transmembrane protein that undergoes

glycosylation in the ER and proteolysis in the Golgi apparatus by a furin like

convertase to form the functional, mature receptor[14, 30]. After this processing,

the receptor is transported to the cell membrane as a heterodimer held together

by non-covalent interactions[2].

The extracellular domain contains 29-36 epidermal growth factor (EGF)-

like repeats[30]. Dynamic trans-interactions occur via repeats 11-12 and when

ligand and receptor are expressed in the same cell, inhibitory (cis) interactions

occur via repeats 24-29[2, 30]. Most of the EGF repeats bind calcium affecting

ligand binding and hence signaling [2, 30]. Following the EGF repeats is a

negative regulatory region (NRR) containing three cysteine-rich Lin12-Notch

repeats unique to all Notch receptors [2, 30]. The transmembrane domain

contains a small extracellular domain that includes two conserved cysteine

residues and the intracellular domain contains a RAM (RBPjκ association

module) domain, followed by a nuclear localizing sequence (NLS) that connects

to six to seven ankyrin repeats.[2, 30]. The ANK domain is followed by two NLS

domains, and at the C-terminus, a proline/glutamic acid/serine/threonine-rich

motif (PEST) acts as a signal peptide for the degradation of the intracellular

domain[2, 30]. The Notch heterodimer is held together by a non-covalent

interaction between the N and C terminal halves [2, 30]. After S1 cleavage the

extracellular domain and the intracellular domain are held together non-

covalently [2, 30].

The Notch ligands are also Type I transmembrane proteins [2]. The most

abundant family of Notch ligands contains an N-terminal DSL

(Delta/Serrate/LAG-2) motif, a unique series of EGF repeats called the DOS

domain (Delta and OSM-11-like proteins) followed by EGF-like repeats (both

calcium and non-calcium binding)[2]. The DSL and DOS domains mediate

receptor binding with the former involved in trans and cis interactions[2].

Jagged/Serrate ligands additionally contain a cysteine-rich domain[2].

A series of proteolytic events lead to Notch receptor activation[2]. Upon

ligand binding, Notch is cleaved by ADAM metalloproteases at a site just before

the TMD called site 2 (S2)[2, 14]. This cleavage causes the release of the Notch

ectodomain causing it to become a substrate for γ-secretase which cleaves at S3

within the transmembrane domain[2]. γ-secretase is made up of 4 membrane

proteins, the catalytic component presenilin and three limiting co-factors, NCT, Pen2 and Aph1[2]. Since there are 2 presenilin and 2-3 APH proteins, multiple enzyme complexes may form, each exhibiting different activities[2]. After cleavage, the Notch intracellular domain (NICD) translocates to the nucleus where it interfaces with the DNA binding protein CSL (CBF1/RBPjκ/Su(H)/Lag-1) through its RAM domain[2]. This is followed by an interaction between the ANK domain and CSL which recruits the co-activator Mastermind/Lag-3 and then recruits the MED8 mediator complex causing up-regulation of target genes (**Figure 1.3**) [2].

In the nucleus NICD is incapable of recognizing or binding DNA by itself but with the help of CSL it is guided to target genes[2]. The nuclear environment determines what CSL will bind to and hence what will be activated by Notch[2]. In Drosophila, Su(H) represses its target promoters when NICD is not present, but in mammals RBPjκ can complex with many ubiquitous co-repressors such as CIR, FLH1C/KyoT2 and NCoR/SMRT and SHARP/MINT/SPEN with the last considered the principal repressor of the target genes of Notch[2].

Most Notch mediated events require a short burst of activity, therefore NICD half-life is three hours[2]. While NICD is activating transcription it is phosphorylated on its PEST domain by CDK8 kinase and is tagged by the E3 ubiquitin ligase Sel10/Fbw7 for proteasomal degradation[2]. Several E3 ubiquitin ligases – Deltex, Nedd3, Su(Dx)/Itch and Cbl - regulate Notch receptor trafficking towards either lysosomal degradation or recycling which influences receptor half-life[2].
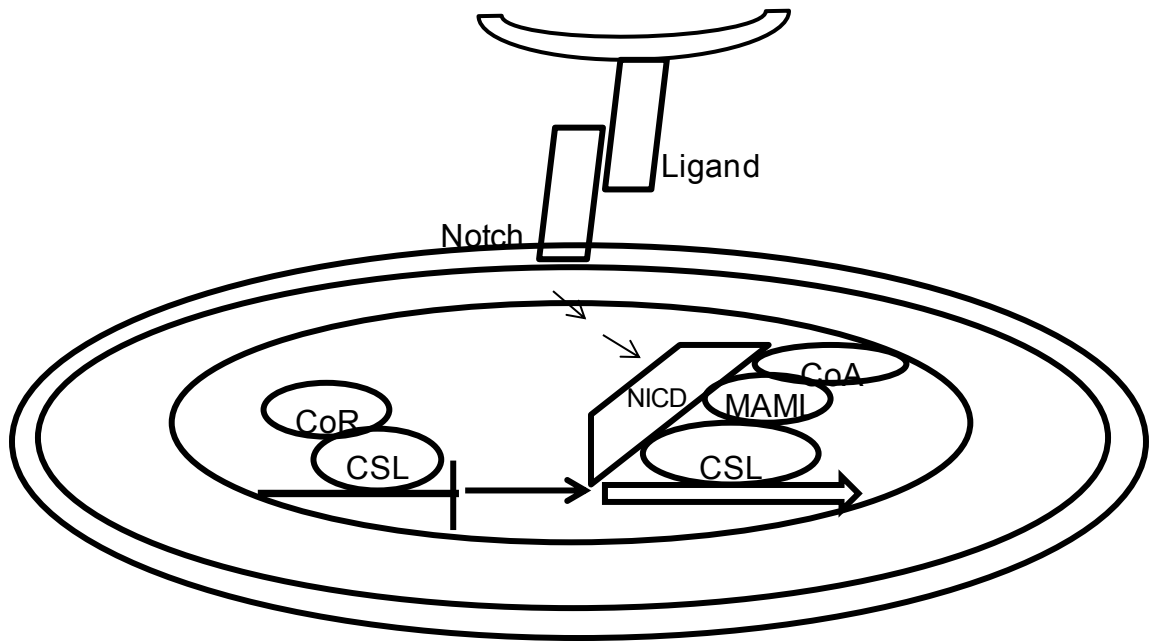
Figure 1.3: The Notch signaling pathway. Notch is activated by contacting ligand from a neighboring cell. Once activated, cleavage by ɣ-secretase occurs to free NICD to translocate to the nucleus. Within the nucleus NICD binds CSL which releases CoR. MAML then binds and co-activators are recruited to the complex to activate target genes[2]

Notch and Myogenesis

Over-expression of Notch signaling inhibits myogenesis in vertebrates[14, 20]. Notch signaling is a negative regulator of muscle differentiation via down-regulation of MyoD [27, 32]. The archetypical effect of Notch is to control cell fate decisions by inhibiting the differentiation of the cell expressing Notch receptor and promoting differentiation of the cell expressing the ligand[14]. Notch is context specific even in muscle as inhibition of Notch in young muscle impairs regeneration whereas forced activation of Notch enhances regeneration in old muscle[33]. The canonical target genes of NICD-CSL include proteins which belong to the Hes family of transcriptional repressors whose up-regulation negatively regulates tissue-specific transcription factors[34]. The target genes expressed in muscle upon Notch activation include the Hes and Hey genes whose protein products are involved in myogenesis [16, 29, 35].

Activation of Notch signaling increases proliferation of cells in injured mouse muscle [36]. This has been confirmed in other studies where over-expressing NICD caused increased proliferation and inhibiting Notch1 inhibited proliferation[14]. Numb is a protein that interacts with NICD to prevent its translocation into the nucleus and is also asymmetrically segregated in satellite cells during mitosis[36]. Numb positive cells express markers that force satellite cells down the myogenic lineage (Myf-5, Desmin) whereas Numb negative cells express Pax3 preventing their progression to the myogenic fate[14]. These results suggest that muscle injury activates Notch signaling which allows

myogenic precursor cells to proliferate by preventing their differentiation and cessation of Notch activity causes them to differentiate[14].

Premature myogenic differentiation and loss of progenitor cells has been seen in Delta1 mutant mice to cause muscle hypotrophy[37]. Mutant mice heterozygous for Notch ligand Delta 1 (Dll1) displayed accelerated differentiation after myoblast determination, as assessed by increases in MyoD, Myogenin and MHC expression in somites and a premature down-regulation of Myf5, the earliest MRF which specifies the first myoblasts from the dermomyotome[37]. By E12.5 MHC levels were reduced in mutant muscles derived from the hypaxial and epaxial lineages along with corresponding decreases of Pax3 and Pax7 expression[37]. This did not seem to be due to apoptosis, suggesting that the loss of satellite cells to participate in the generation of muscle led to the hypotrophic phenotype[37]. Similar results were seen in conditional knockouts of CSL mice[14]. These results suggest that attenuation of Notch signaling causes precocious differentiation of the Pax3+/7+ satellite cell pool[14].

Notch Interaction with Other Pathways

BMP signaling inhibits myogenesis[14]. BMPs belong to the TGFβ family of ligands[14]. Receptor binding by BMPs or TGFβs causes the phosphorylation of receptor SMADS (1, 2, and 3) which leads to activation of target genes as heterodimers with SMAD4[14]. C2C12 were treated with BMP4 during differentiation which blocked their differentiation and increased levels of Hes1 and Hey1 [38]. Addition of the ɣ-secretase inhibitor, L-685, 458 or transfection of

dominant-negative CSL restored differentiation and a 3 kb Hey1 promoter-reporter construct containing N1-ICD was activated by BMP4[38].

The insulin signaling pathway and the Notch pathway have been reported to interact via the FOXO proteins[14]. Mutant FOXO proteins which are constitutively active in the nucleus inhibit C2C12 differentiation and up-regulate Notch target genes, enhance NICD recruitment to those promoters and interact with CSL[14]. When Notch signaling was blocked differentiation proceeded to a measurable degree[14].

Notch and Ageing Muscle

Ageing muscle has a reduced capacity to regenerate itself and this association was shown in culture where satellite cells expressing CD34 and M-cadherin were unable to divide and thus generate myotubes. Old myoblasts contain high levels of TGFβ1 which inhibits their differentiation[16]. TGFβ acting via Smad3 induces the CDK inhibitors, p15, p16, p21, and p27[14]. Forced activation of Notch decreased their expression and caused old muscle to regenerate[14].

Notch and Quiescent Satellite Cells

CD34 is a marker of the quiescent adult satellite cell and Myf5 is the first marker seen upon commitment to myogenesis [39]. Numb has been shown to regulate Notch1 but not Notch3 during myogenesis [40]. A subpopulation of C2C12 cells express CD34 and Myf5 but do not express MyoD [39]. Upon induction of differentiation, the CD34+ cells do not differentiate into myotubes and do not express MyoD [39]. There is also a smaller population of cells that

are CD34-Myf5- which are suggested to maintain the CD34+ Myf5+ cells [39]. The CD34- cells in human and murine myoblast cell lines have been shown to express Notch1 which prevents their participation in differentiation [41]. Inhibiting Notch activation in these cells using a ɣ-secretase inhibitor (DAPT), or by over-expressing Numb led to enhanced myotube differentiation and hypertrophy[41]. Zebrafish embryos treated with DAPT also exhibited increased myoblast differentiation [41].

Alcoholic Myopathy

Alcohol abuse is a growing public health problem[42]. Someone who consumes who consumes more than 80 g of ethanol daily for more than 10 years is considered to be an alcoholic[42, 43]. Forty to sixty percent of chronic alcoholics suffer from reduced body weight, muscle weakness and locomotor difficulty independent of liver disease, neuropathy and malnutrition[42, 44, 45]. Alcoholic myopathy is identified by a reduction in the diameter of skeletal muscle fibers[46]. The fibers primarily affected are the fast-twitch, type II, which rely on anaerobic, glycolytic metabolism over the aerobic, oxidative type I fibers[46]. There is an inverse correlation between muscular strength and lifetime alcohol consumption[47]. Long-term alcohol feeding in mice causes atrophy in the gastrocnemius muscle (type II) and in addition haphazard fiber size and random multinucleated fibers are seen[48]. In rats, chronic alcohol feeding causes myopathy which is distinguished by reduced protein content in skeletal muscle and body weight compared to controls[42]. Measurement of fiber size in the rat demonstrates that the alcoholic myopathy presents as a reduction in fiber size

with minimal changes in fiber number [44]. Abstinence can dramatically reverse most of the myopathy but not always back to baseline values[44]. When chronic alcoholics abstain from alcohol, muscle strength is not fully recoverable, suggesting permanent changes in muscle function may have occurred[44].

Review of the mechanisms

Upon ingestion, alcohol permeates across the cell membranes into cells and can affect cellular function by interacting with cell membranes and proteins to affect signaling proteins[49]. Alcohol is primarily metabolized in the liver by alcohol dehydrogenase (ADH) and aldehyde dehydrogenase (ALDH2)[49]. The metabolism of alcohol releases toxic byproducts in the form of acetaldehyde which can cause tissue damage, formation of reactive oxygen species (ROS) and imbalances in the reduction-oxidation (redox) condition of liver cells[49]. Acetaldehyde is metabolized further to acetate mostly by ALDH2 to form acetate and NADH [49]. NADH gets oxidized in the mitochondria and acetate gets released into the blood and gets oxidized to CO_2 in skeletal muscle, heart and brain after which is gets metabolized to acetyl coA to participate in lipid and cholesterol biosynthesis[49]. Skeletal muscle barely has any ADH activity suggesting that most of its effects are mediated directly[50].

Ethanol reduces Protein Synthesis

Skeletal muscle mass is regulated by the balance between rates of synthesis and degradation and acute and sustained alcohol consumption impairs the rate of protein synthesis in general and more particularly myofibrillar protein synthesis[51]. Intraperitoneal administration of alcohol causes reductions of 30-

40% of protein synthesis in rats which can last for up to 24 hours[51]. Changes in ribosome number or efficiency of mRNA translation could decrease tissue protein synthesis[51]. Since 80% of muscle RNA is ribosomal, the alterations in total RNA content has been used to approximate the ribosome number[51]. In several studies where RNA content was measured, no significant change in RNA content of skeletal muscle was seen ~ 3 hours after acute alcohol exposure[51]. Efficiency of translation is measured by dividing the protein synthetic rate by total RNA content and provides a measure of how rapidly ribosmes are synthesizing protein[51]. After feeding rats a high dose of alcohol, the translational efficiency is decreased by ~ 40% in the gastrocnemius[51].

Ethanol causes Oxidative Stress

Other molecular mechanisms proposed to contribute to alcoholic myopathy include oxidative stress which may cause lipid peroxidation, muscle membrane changes and skeletal muscle apoptosis[44]. Type I muscle fibers have greater amounts of cytosolic and mitochondrial superoxide dismutase, catalase, glutathione peroxidase, and alpha-tocopherol (antioxidants) than type II muscle[46]. Liver damage can occur due to free radical damage caused by ethanol oxidation[46]. Depletion of mitochondrial DNA by alcohol in mouse skeletal muscle consistent with oxidative damage has been observed; the antioxidant α-tocopherol prevented the depletion[52]. Mitochondrial damage attenuates oxidation of fatty acids and increases lipid peroxidation, and in one study muscle mitochondrial damage was seen in 30% of the 57 alcoholics[44].

Apoptosis is not seen in skeletal muscle of rats exposed to acute or chronic alcohol [44]. In chronic alcoholics markers of apoptosis as assessed by levels of DNA fragmentation and TUNEL assays are increased and levels of BAX and BCL-2 (markers of protection from apoptosis) were reduced[44]. These results suggest that there are some limitations associated with the rat model in its capability to faithfully reflect the human situation.

Ethanol modulates the Notch Signaling Pathway

Ethanol has recently been shown to inhibit smooth muscle proliferation in vivo and in cell culture by regulating the Notch signaling pathway[53]. The researchers found that ligation injury induced Notch1 expression and that Notch1 mRNA and Notch1 intracellular domain protein levels were reduced in the presence of ethanol with no effect reported for Notch3 intracellular domain[53]. In human umbilical vein endothelial cells ethanol was shown to increase RBP-Jk reporter activity and Notch1 and Notch4 expression[54]. Recently it was shown that hepatic ischemia/reperfusion injury due to reactive oxygen species activates the Notch signaling pathway in cell culture and in vivo[55]. These findings suggest that ethanol modulates the Notch signaling pathway in multiple cell types in response to injury caused by reactive oxygen species in liver and perhaps in skeletal muscle.

Ethanol and Proliferation and Differentiation

Ethanol inhibits the proliferation of primary cultures of rat skeletal muscle cells[50]. It has been reported to cause a delay the differentiation of rat skeletal myoblasts in cell culture but is not reported to affect the completely differentiated

cells[50]. Liver regeneration is impaired by alcohol by inhibiting the proliferation of progenitor liver cells available to participate in the regeneration process[56]. Alcohol affects neuronal phenotype by interfering with neurotrophic signals important for differentiation[57]. Fetal alcohol syndrome is a consequence of exposure to excessive alcohol during development.

The C2C12 Murine Myogenic Cell Line

Generation, Description and Use

The original C2C12 cell line was derived in 1977 from myogenic cells isolated from two-month old C3H mice whose thigh muscle had been crushed with forceps 70 hours before isolation[25]. The myogenic cells were spindle-shaped similar to myoblasts isolated from newborn mice[25]. Cell fusion and myotube formation started on the third or fourth day in culture medium consisting of DMEM and 20% fetal calf serum[25].

The C2C12 cell line is derived from activated satellite cells [21, 58]. Cycling C2C12 cells are analogous to activated satellite cells present in the proximity of muscle fibers while the undifferentiated cells are comparable to quiescent satellite cells[7, 58]. When C2C12 were induced to differentiate in 1% fetal calf serum, myotubes appeared after 5 days and they were elongated, 100-600µm in length, 30-50µm thick and formed branches[58]. The MRFs are expressed during differentiation[58].

Since the C2C12 cell line encompasses the realm of myotube formation including quiescence, activation and differentiation, it provides a powerful system

to investigate multiple aspects involved in post-natal myogenesis such as regeneration, differentiation, myotube formation and the myotubes themselves.

Inhibition of the differentiation process of myoblasts is confirmed by seeing reductions in the levels of MRFs, the number of myonuclei, the size of myotubes and protein content of the myotubes which form[31, 59-62]. After differentiation has proceeded to the myotube stage, removal of the myotubes leaves the quiescent satellite cells attached to the culture dish, allowing the earliest progenitor cells that participate in the regeneration process to be studied[39, 41]. The entire C2C12 system can be recreated from a single cell[63].

Hypothesis

Muscle contains stem (satellite) cells that are essential to maintain homeostasis of muscle tissue. Upon injury satellite cells become activated, proliferate and differentiate into myoblasts. Myoblasts undergo fusion to form multinucleated myotubes. Myotubes subsequently merge with myofibers. Expression of the myogenic regulatory factors is essential for progression to terminal differentiation.

Alcoholic myopathy (muscle disease) manifests itself as a reduction in the diameter of muscle fibers. Upwards of 50% of chronic alcoholics suffer from alcohol induced muscle disease. Abstinence is the only cure but even then muscle strength does not always return to baseline levels. Alcohol has been shown to injure muscle and is incompletely metabolized in muscle suggesting that the direct effects of ethanol mediate the main effects of the myopathy. The role of ethanol on muscle stem cell differentiation remains poorly characterized.

I hypothesize that alcohol affects the muscle stem cell population to inhibit myoblast differentiation, and this contributes to the etiology of alcoholic muscle disease.

Specific Aims

The first goal of this project was to develop an assay capable of analyzing C2C12 myogenic cell differentiation into myotubes and to use that system to measure the effects of ethanol on that process. The second goal of this project was to measure the effects of ethanol on the transcriptional profile of differentiating C2C12 myogenic cells and to identify signaling pathways predicted to be affected by ethanol. The third goal of the project was to test whether the Notch signaling pathway was activated by ethanol during C2C12 myogenic cell differentiation and whether the quiescent satellite cells were affected by ethanol.

Chapter 2: Methods

Cell Culture

C2C12 mouse myoblasts were maintained in DMEM-High Glucose medium containing 20% FBS and 1% penicillin-streptomycin (P/S) (GM) at 37°C with 5% CO_2. To induce differentiation, once cells reached 70% confluence, the media was replaced with DMEM-High Glucose and 2% horse serum + 1% P/S (DM). For differentiation assays C2C12 cells were plated at a density of 10,000 cells/200ul/well in 96-well black tissue culture plates(BD Pharmingen) in GM. The following day (day zero) media was replaced with DM +/- compounds. Rapamycin (Sigma) was added at a final concentration of 100nM. Ethanol (PHARMCO-AAPER) was added at a final concentration of 100mM (0.6%) unless otherwise specified. The media +/- compounds was changed daily during the course of differentiation.

For RNA and protein isolation cells were cultured in $10cm^2$ culture dishes. To induce differentiation, when cells grew to 70% confluence in growth medium, the medium was replaced with differentiation medium.

Immunofluorescence Microscopy

C2C12 myoblasts that were differentiated in 96 well plates were fixed with 1% paraformaldehyde (in PBS) and then permeabilized and blocked with 2%FBS, 2%BSA and 0.2% Nonidet P40. Cells were probed with anti-TnT antibody (Hybridoma Bank (University of Iowa) (1:200) followed by FITC-anti-mouse antibody (Molecular Probes, Invitrogen) (1:1000). The cells were then counterstained with DAPI (in Glyercol:PBS). The stained cells were examined under an inverted fluorescence microscope (ImageXpress (Micro) (Molecular

Devices Corporation). Thirty-six non-overlapping images were recorded for each well using a digital CCD camera. Image analysis was performed using the the MetaXpress Count Nuclei and Cell Scoring Application Module programs that was custom adapted to assess myoblast differentiation. Please see **appendix** for Journal 8 (algorithm).

Cell Pellet Preparation for RNA and Protein Isolation

At time of harvest, cells were trypsinized, spun down and washed once with 10mls of ice-cold PBS and pellets were placed on dry ice and stored at -80C until further processing.

Denaturing RNA Gel Electrophoresis

200 ng of RNA was electophoresed on a 1.2% formaldehyde agarose gel containing ethidium bromide.

Quantitative RT-PCR

RNA was isolated from pellets using Qiagen RNeasy mini-kit with DNase digestion. RNA concentration and quality was assessed using a spectrophotometer. cDNA was synthesized from 2ug total RNA with SuperScript III Reverse Transcriptase (Invitrogen) using random hexamers. qPCR was performed on an ABI 7900 HT Fast Real Time PCR System using inventoried FAM or VIC labeled Taqman mouse primer/probes. Catalog numbers are listed in the **appendix**. Data was quantified using the standard curve method and normalized to B-Actin to obtain relative fold-change.

Microarray Expression Screen and Data Analysis

C2C12 cells were seeded on 10 cm^2 dishes in GM and once 70% confluent the medium was replaced with DM +/- 100mM Ethanol for upto 3 days. RNA was isolated each day using the RNeasy mini-kit (Qiagen). Three to four replicates were included for each condition. RNA was assessed for quality using the Agilent Bioanalyzer and submitted to the Yale Center for Genome Analysis for transcript profiling on Illumina Mouse Ref8v2.0 microarrays.

Raw expression values for all experimental arrays were processed at the Tufts Center for Neuroscience Research using Genome Studio (Illumina) and quantile normalization was performed using R. Probes that changed with ethanol ±1.22 fold relative to controls with a p-value of ≤ 0.05 were considered significant and used for further analysis through the use of Ingenuity Pathway Analysis (IPA) software (Ingenuity Systems; Redwood City, CA).

Ingenuity Pathway Analyses

The Functional Analysis identified the biological functions that were most significant to the data set. Molecules from the dataset that met the criteria for significance and were associated with biological functions in the Ingenuity Knowledge Base were considered for the analysis. Right-tailed Fisher's exact test was used to calculate a p-value determining the probability that each biological function assigned to that data set was due to chance alone[64]. The p-value that is determined by Fisher's Exact test result considers the number of genes in the pathway, the size of the pathway, expression values of genes in the

pathway, the number of genes in the dataset, and the total number of genes in the IPA database.

Canonical pathway analysis identifed the pathways from the IPA library of canonical pathways that were most significant to the data set. Molecules that met significance criteria and were associated with a canonical pathway in the Ingenuity Knowledge Base were considered for the analysis. The significance of the association between the data set and the canonical pathway was measured in two ways: 1) a ratio of the number of molecules from the data set that map to the pathway divided by the total number of molecules that map to the canonical pathway 2) Fisher's exact test was used to calculate a p-value determining the probability that the association between the genes in the dataset and the canonical pathway could be explained by chance alone[64].

For network generation, a data set containing gene identifiers and corresponding expression values was uploaded into the application. Each identifier was mapped to its corresponding object in the Ingenuity Knowledge Base. Molecules that met the criteria for significance were considered to be significantly regulated. These molecules, called Network Eligible molecules, were overlaid onto a global molecular network developed from information contained in the Ingenuity Knowledge Base. Networks of Network Eligible Molecules were then algorithmically generated based on their connectivity. The network score is the –log of the p-value[64]. In generation of overlapping networks, nodes represent entire networks and edges (relationships) represent the common genes between them[65].

The upstream regulator analysis is based on existing knowledge of anticipated effects between transcriptional regulators and their target genes stored in the Ingenuity database. For each potential transcriptional regulator two statistical quantities are calculated, 1) an overlap p-value which indicates the statsistical significance of genes in the dataset which are downstream of the transcription factor and 2) a regulation z-score which predicts the activation state of the transcription factor using gene expression patterns of the transcription factor and its downstream genes. Transcription factors with an absolute z-score ≥ 2 are predicted to be activated and predicted to be inhibited if the z-score ≤ -2[66].

Western Blotting

Total protein was extracted using RIPA lysis buffer + protease inhibitors and quantified using BCA Assay. Protein was denatured and run on 4-12% gradient gels under reducing conditions. Bands were transferred to PVDF membranes, blocked and probed with antibodies. Detection was done using ECL detection and Image Software was used to quantify the bands. Antibodies used included Notch1 (mN1A), a mouse monoclonal antibody raised against mouse Notch1 GST fusion protein (BD Pharmingen). The mouse monoclonal anti-α-tubulin clone DM 1A (Sigma) was used as a loading control.

Plasmid Constructs

The pHes1-luc-tr plasmid contains a 350bp fragment of the Hes1 promoter which is activated by NICD binding (H. Zhang (MCRI) and personal observations). The pCMV-Ren is a vector containing the renilla luciferase gene under a CMV

promoter (C. Yang (MGH). The MN1ICPD4v5 plasmid contains the mouse

Notch1- ICD in a pcDNA4V5 backbone (L. Liaw-MMCRI). pcDNA3 was used to

normalize for DNA amounts.

Reporter Assays

C2C12 cells were plated at a density of 10,000 cells/200ul/well in white 96-well

plates (Costar#3903). Transfections were performed the following day. DNA

(0.5-1ug) was diluted in sterile TE to give a final volume of 1-3ul. The

Lipofectamine LTX and PLUS (Invitrogen#15338-100) was diluted in Optimem

(Invitrogen) 1:10. This dilution was then used to make the various ratios of

lipid:DNA:PLUS for experiments in a final volume of 15-17ul. After a 30 minute

incubation, 75ul of media was removed from the wells of the plate and 20ul of

transfection mix was added per well. After a 4-24 hour incubation the media was

replaced with DM +/- compounds. Twenty-four hours later transgene expression

was assayed. Ethanol was used at a final concentration of 100mM. Luciferase

activities were determined as described by the manufacturer in a luminometer.

Relative Light Units (RLU) were determined by normalizing Firefly Luciferase

Activities to Renilla Luciferase values.

Isolation of Reserve Cells

C2C12 cells were cultured in GM until they reached confluence and the media

was replaced with DM for 7 days. C2C12 reserve cells were isolated using a

modified version of a short trypsinization (trypsin 0.1%/EDTA 0.1 mM, 2 minutes)

which is reported to remove all myotubes and leave only quiescent

undifferentiated reserve cells attached to the dish[41].

FACS Analysis

The reserve cells were detached from the dish using a 'non-protease' solution (CellDissociationFactor, Sigma) for 15 minutes. Viability was assessed by trypan blue and there were more than 90% viable cells. The cells were washed once in 8mls of PBS supplemented with 0.5% BSA and resuspended in PBS/BSA buffer. The cells were Fc blocked with mouse IgG and subsequently incubated with phycoerythrin (PE) - CD34 monoclonal antibody (clone RAM34, BD Biosciences) for 1 hour at 37ºC. As an immunoglobulin isotype control, cells in a separate tube were treated with PE Rat IgG2a, k antibody. Cells were analyzed and separated with FACS Calibur (BD Biosciences). Gating was implemented based on negative-control staining profiles followed by gating for immunoglobulin isotype controls.

Statistical Analyses

All results are expressed as the mean ± standard error of the mean (SEM). Each well was considered a biological replicate. Significance was determined either by two-tailed t-test, equal variance (Microsoft Excel) or for multiple comparisons by one-way ANOVA followed by the Tukey test for multiple comparisons using Prism 5.0 software (GraphPad Software; LaJolla, CA). A p value of 0.01 - 0.05 was considered significant (*), 0.001-0.01 was considered very significant (**) and a p-value < 0.001 was considered extremely significant (***) and indicated in graphs.

Chapter 3: The Effect of Ethanol on C2C12

Differentiation Assessed by High Content Screening

Figure Contributions:

I performed the experiments which generated the materials for the figures which are presented in this chapter.

Albert Tai (SCIID) wrote Journal 8 using Molecular Devices software which was used to measure C2C12 differentiation and take and store pictures of the wells.

I used Acuity software (Molecular Devices) to process and organize the data generated from Journal 8 into text files.

I analyzed the data in the text files using Microsoft Excel.

I contributed all the figures in this chapter.

Introduction

As mentioned earlier, alcoholic myopathy is characterized by a reduction in the diameter of muscle fibers which correlates with lifetime dose of alcohol. Muscle has the capability of regenerating itself after injury due to the presence of a population of quiescent satellite cells that upon activation, proliferate, differentiate into myoblasts and fuse to form myotubes and merge with myofibers. Alcohol has been shown to injure muscle tissue [67]. Ethanol was reported to inhibit the proliferation of rat satellite cells and delay the differentiation of rat skeletal myoblasts[50]. In work carried out by Garriga (2000) it was demonstrated that once the proliferative phase had ended, supplementation of the growth medium with alcohol altered the expression of creatine kinase isozymes[50]. This alteration in the absence of total decreased creatine kinase content was interpreted as resulting in a delay in differentiation (morphological changes were reported). On the whole the effect of ethanol on the murine activated satellite cell population during differentiation and the effects of ethanol on the resulting myotubes which form remains poorly explored.

The C2C12 murine myoblast cell line is derived from activated satellite cells[21]. When C2C12 cells are maintained in growth medium containing serum, they express high levels of MyoD, the myoblast commitment factor[63]. Upon transfer to low serum, levels of MyoD are down-regulated, expression of myogenin increases followed by induction of p21 and withdrawal from the cell cycle followed by the appearance of differentiated myocytes which then fuse into myotubes[1, 7, 18, 68]. The appearance of myotubes coincides with the

expression of cardiac Troponin T (TnT), a marker of regenerating myofibers[69, 70]. Myotube cultures derived from C2C12 also contain a population of quiescent stem cells [39]. These features make the C2C12 cell line an excellent model system to study regeneration events encompassing the events underlying the differentiation of myoblasts to myotubes and the formation of quiescent satellite cells.

When the C2C12 cells are exposed to low serum medium, some cells differentiate to form myotubes whereas others are resistant to differentiation and have been referred to as reserve cells[7]. Myoblast differentiation is generally analyzed by inspecting 100-150 myotubes or by assessing fusion competence by calculating the myogenic fusion index (MFI) which is derived by dividing the number of myonuclei by the total number of nuclei present per field of a microscope slide [31, 61, 62].

Observation of reductions in the MFI, length and diameter of myotubes and reductions in fluorescence (protein) content of myotubes generally suggest that the differentiation process is being inhibited [31, 59-62, 71]. However these analytical methods lack the ability to simultaneously take multiple morphological measurements of individual myotubes and myonuclei in an efficient manner, and to sample a large number of cells so as to improve statistical power and confidence level of the analysis. When I set out to measure the effects of ethanol on C2C12 differentiation the current technology had advanced to the point to allow one to perform precise high content measurement of single myotubes and reserve cells in a high throughput manner. Therefore a custom high content

immunocytochemical screening assay using microscopy and computer-aided analysis capable of measuring nearly every cell in a 96 well format was developed.

A typical well could contain more than 1000 myotubes and 20 000 reserve cells. Measurements taken on a cell by cell basis included the number, length, width, perimeter, area and integrated fluorescent intensity of myotubes stained for TnT. Measurements of nuclei number and area were also taken based on DAPI staining. The observation that during C2C12 differentiation the average nuclear area of a reserve cell was consistently larger than the nuclear area of a myonucleus suggested the possibility of an additional measurement to allow the discrimination of differentiated cells from non-differentiated cells. The ability of the system to detect inhibition of differentiation was tested by evaluating the effects of the C2C12 differentiation inhibitor, rapamycin[60, 71, 72] and my results are in concordance with the previously published findings that rapamycin reduces MFI and protein content of myotubes as assessed by fluorescence. Myotubes formed in response to ethanol were completely different from control myotubes according to all measured parameters. The average ethanolic myotube had a reduced diameter, length, perimeter, area, and TnT content. The ethanolic myotubes contained fewer nuclei compared to controls and displayed reduced MFI. Ethanol consistently increased the nuclear area of nuclei within myotubes as well as nuclei within the non-differentiated cells.

Ethanol did not appear to cause a delay in myotube formation as was previously reported. The converse situation was actually observed, more

myotubes formed during differentiation with ethanol while the number of reserve cells decreased.

To summarize, a high content screening assay was developed to measure ten cellular and nuclear parameters of C2C12 differentiation on a cell by cell basis. This assay: 1) demonstrated that the nuclear area varied between the non-differentiated cells and myonuclei, 2) was able to identify inhibition of differentiation by a known inhibitor and 3) showed that ethanol inhibits C2C12 differentiation.

Results

Description and Validation of the Journal

The programs available to measure a cell were able to identify a nucleus and an area surrounding it as representing the cell but were unable to consider that a cell could contain more than one nucleus such as a myotube. Therefore a specialized journal had to be written to accurately measure muscle cell differentiation. The manual selection of sites to count cells and nuclei would reduce precision and could potentially introduce a bias artifact that might confound the results of hypothesis testing. Therefore every possible site within the entire well was counted to increase precision and counteract confounding associations.

The journal underwent iterative validation and modification to yield the final version, Journal 8. The journal used the MetaXpress Count Nuclei algorithm to count the total number of nuclei (DAPI) and measure other nuclear parameters. The TnT+ cells were stained green (FITC) and those images were

thresholded. Green cells below a certain cutoff were excluded to avoid counting

artifacts. Each green cell (region) was assigned a region number. All

parameters relating to each region was measured. The regions were

superimposed on the DAPI image on which total number of nuclei had been

previously counted using the built-in nuclear count algorithm. The number of

nuclei was then counted within each region. Each region was assessed to make

sure it contained at least one nucleus before it was considered to be a cell. After

that step, the number of nuclei within each region was counted. Nuclear

parameters of nuclei within each cell region were measured. To make the

images available for manual review, the FITC and DAPI images for each site

were overlaid. Site/Image specific information i.e. number of cells, cell area and

number of myonuclei were written to each image. Some measurements were

written to the image and information specific to the regions was written on the

image and saved as jpeg images on the computer. Each cell was measured for

the following nuclear parameters, total number of nuclei, number of nuclei within

myotubes and nuclear area. The following cellular parameters were measured,

area, perimeter, length, breadth, and integrated intensity. Thirty-six pictures in

each well of a 96 well plate were taken. This encompassed almost the entire

well.

   Figure 3.1 shows the raw image data for the 36 sites on the DAPI image

(**Figure 3.1a**) and the FITC image (**Figure 3.1b**). **Figure 3.1c** shows a picture of

a site generated after analysis by the journal. There are a large number of cells

and nuclei in one well of a 96 well plate (**Figure 3.1a, b**) and counting all of them

A   **B**   **C**
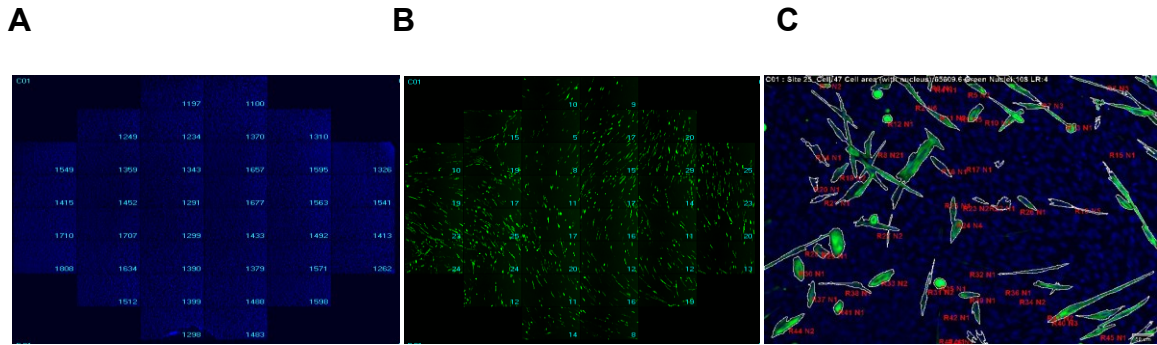
Figure 3.1: Analysis of C2C12 differentiation by journal. C2C12 cells were differentiated for 7 days. The cells were fixed and cells were immunostained for TnT and nuclei were counterstained with DAPI. **(A)** A typical well displaying all nuclei stained with DAPI in all 36 sites. **(B)** The same well stained for TnT with FITC staining. **(C)** A picture of a site after journal analysis depicting number of green cells, myotube area measurements, number of nuclei and a 50μm scale bar.
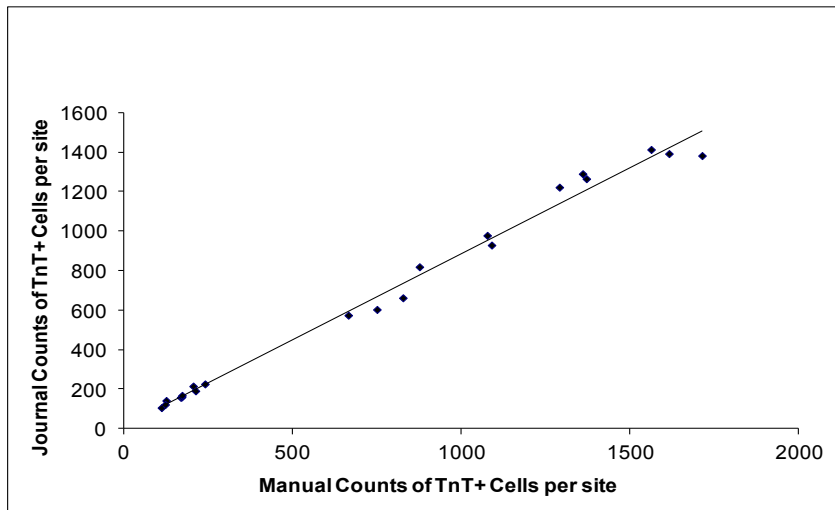
Figure 3.2: Manual counts and journal counts correlate with each other. 14 000 cells were counted in all 36 sites of 21 wells chosen at random in three 96 well plates. Correlation plot of custom algorithm counts versus manual counts. r^2=0.9901, 95% CI: 0.9875-0.9980, p-value ***, m=0.871.

manually would take an inordinate amount of time, therefore counting all cells in

multiple wells would be nearly impossible. Within the merged DAPI and FITC

image (**Figure 3.1c**), information displayed on the top of the image includes the

name of the well, the site number, the cell area, and the number of green nuclei

within the region. At the bottom of the image is a ruler indicating 50µm. As can

be noted from **Figure 3.1c**, some myotubes are stained so faintly they would

likely be missed by the human eye but are outlined by the journal. What is also

noticeable is that myotubes in various stages of the differentiation process are

visible. Some are in the early phases of terminal differentiation and contain one

nucleus whereas others are in later stages and display multiple nuclei. The

myotubes also display a complexity of shape. Surrounding each differentiated

TnT+ cell are numerous undifferentiated or reserve cells.

I evaluated the accuracy of the journal in recognizing TnT+ cells by

manually counting 14 000 cells present in 36 sites in 21 wells in three 96 well

plates and comparing my results to those from the algorithm. **Figure 3.2** depicts

the correlation plot of the custom algorithm counts versus manual counts. The

correlation was 0.99, the 95% confidence interval ranged from 0.9875 to 0.9980.

The p-value was < 0.001 and the slope was 0.871. These results indicate that

the journal is able to accurately recognize and count the number of multi-

nucleated myotubes which can possess a wide range of morphological

complexity e.g. branching versus non-branching.

Time Course of C2C12 Differentiation

A live cell-imaging time course of C2C12 differentiation was performed to understand the dynamics of differentiation and to identify a time point where 1) myotubes were still forming and 2) growing and 3) were of sufficient number and size to provide a wide range in which to test the effects of ethanol. The measurements from the individual cellular datum within a well were combined to generate average measurements per cell.

C2C12 cells were differentiated over a span of seven days and stained for TnT at various time points. Day 0 represents C2C12 myoblasts that were still in the growing phase i.e. maintained in growth medium. **Figure 3.3** depicts the course of C2C12 differentiation and the parameters chosen for evaluation. As mentioned in the introduction the parameters most often used by investigators who study myoblast differentiation include myonuclei number and measurements related to the myotube. The first TnT+ cells formed on day three of differentiation (**Figure 3.3a**). The TnT+ cells continued to form, fuse and grow on days five and seven of the time course (**Figure 3.3b, c**). **Figure 3.3d** depicts the effects of differentiation medium on the number of TnT- cells over time. The differentiation medium stimulates cell proliferation for two days which is akin to the proliferation events seen when satellite cells are activated. The number of TnT- cells increases from 10 000 cells on day 0 to ~ 50 000 on day 2 and then their numbers start tapering off on day 3 which coincides with the appearance of the first TnT+ cells (**Figure 3.3e**) and the TnT- cell numbers are reduced to ~ 30 000 on day 7.

A

B

C

D

E

F

G

H

I

J

K

49
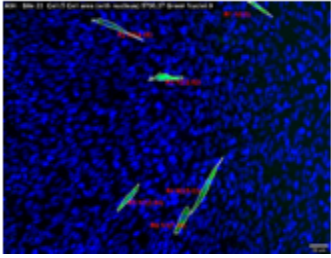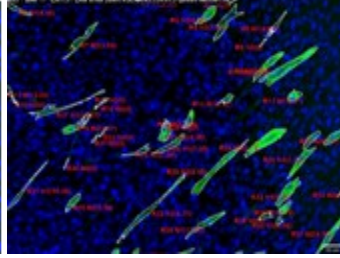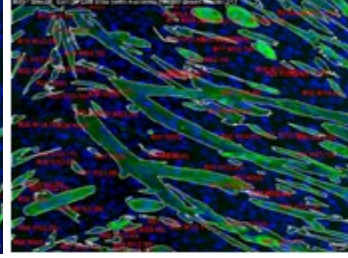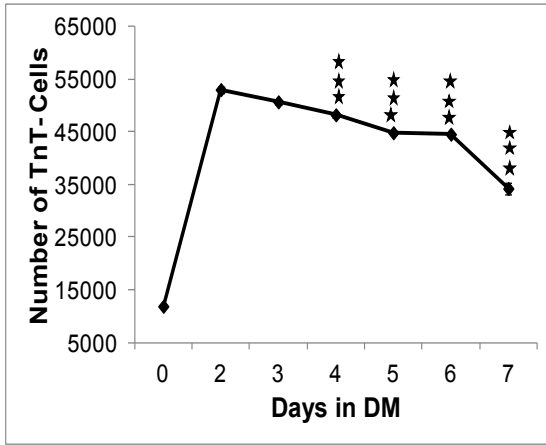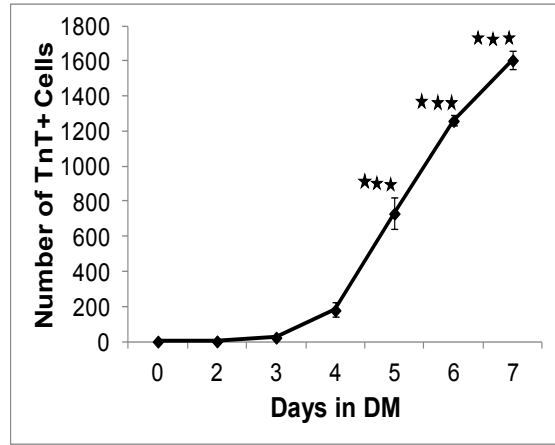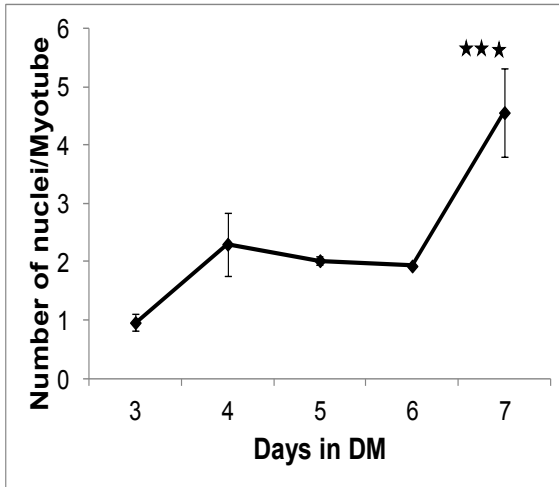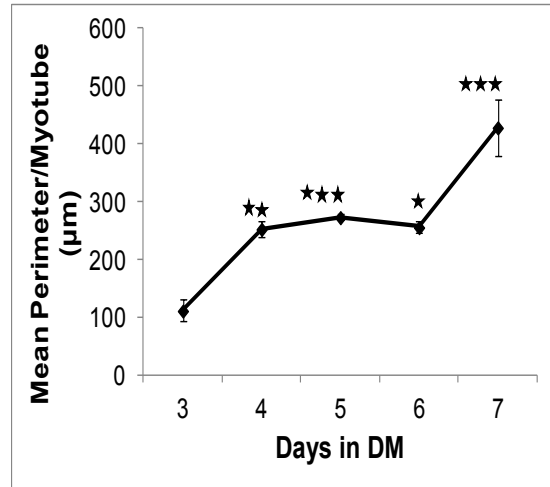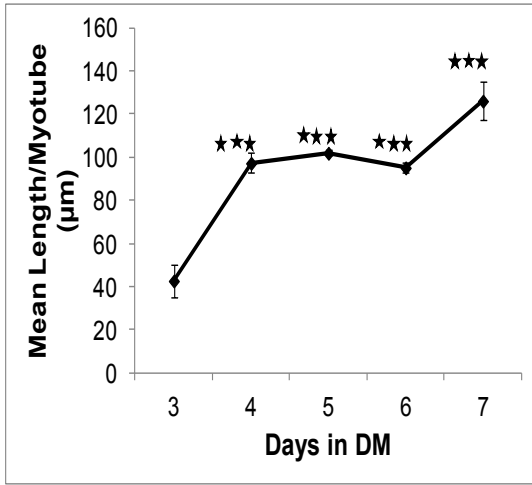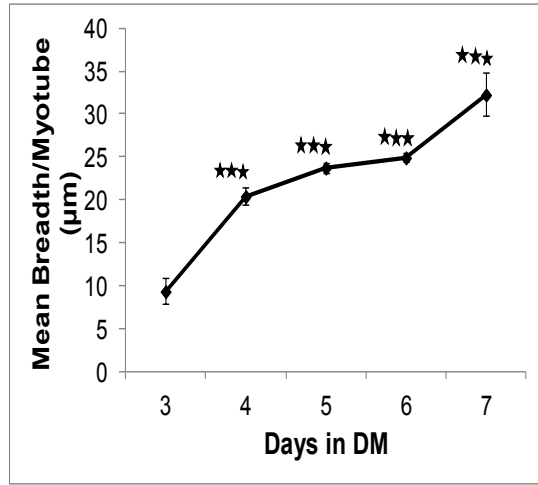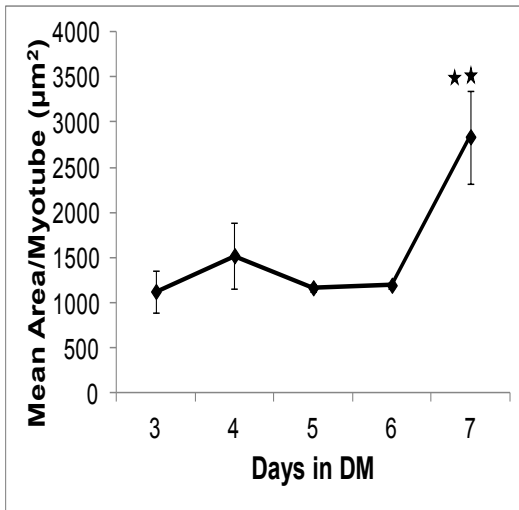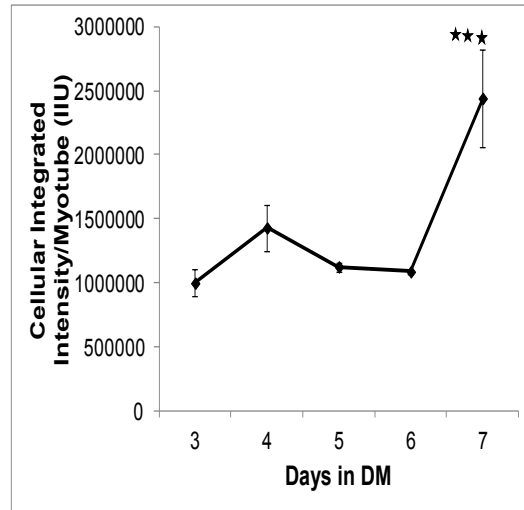
L
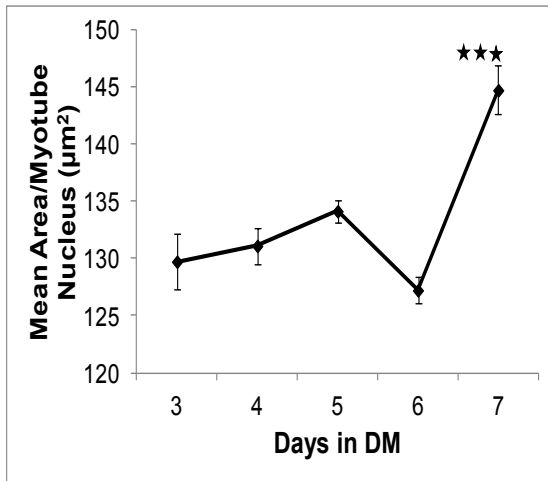
M
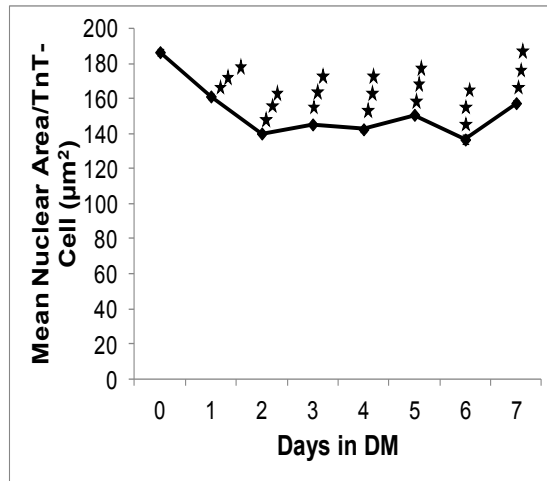
N
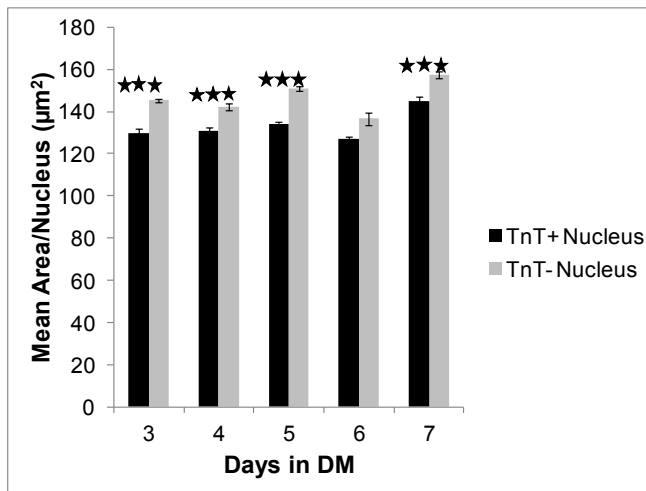
Figure 3.3: C2C12 cell differentiation is ongoing at 7 days. C2C12 cells were differentiated as previously described. **(A)** A typical well showing initial myotubes that form on day 3 **(B)** on day 5 **(C)** on day 7 **(D)** Number of TnT- cells, *p* vs. Day 2 **(E)** Number of TnT+ cells, *p* vs. Day 3 **(F)** Number of nuclei per myotube, *p* vs. Day 3 **(G)** Mean perimeter per myotube (μm), *p* vs. Day 3 **(H)** Mean length per myotube (μm), *p* vs. Day 3 **(I)** Mean Breadth per myotube (μm), *p* vs. Day 3 **(J)** Mean Area per Myotube (μm^2), *p* vs. Day 4 **(K)** Cellular integrated intensity per myotube (IIU), *p* vs. Day 4 **(L)** Mean area per myotube nucleus (μm^2), *p* vs. Day 3 **(M)** Mean nuclear area per TnT- nucleus (μm^2), *p* vs. Day 0. **(N)** Mean area per myotube nucleus and TnT- nucleus. Statistical analyses were performed by one-way ANOVA followed by Tukey's test for multiple comparisons. The averages are shown ± SEM (n=3-15). * *p*≤0.05, ** 0.001<*p*<0.01,*** *p*<0.001.

As differentiation progresses past day 3, TnT- cell numbers decrease as some of them are converted to TnT+ cells. The TnT+ cell number increases ~ 7-fold from day 3 to day 4. From day 4 to day 5 their cell number increases ~ 4-fold. From day 5 to day 6 there is a 1.7-fold increase in TnT+ cell number. On day 7 their numbers increase ~ 1.2 fold from day 6 to reach ~ 1600. This last increase in TnT+ cell number corresponds with a significant dip in TnT- cell number seen from day 6 to day 7 ($p<0.001$) (**Figure 3.3d**). A dip in TnT- cell number is seen from day 2 to day 3 which coincides with the initial appearance of TnT+ cells. Since this pattern repeats between days 6 and 7, it might suggest that on day 7 a group of TnT+ cells are being generated that are very similar to the TnT+ cells seen on day 3. **Figure 3.3d** shows that about 16 000 TnT- cells disappear between day 3 and day 7 but the magnitude of increase in TnT+ is 10-fold less showing that during differentiation there is a sub-population of cells within the reserve cell population which will undergo cell death if they do not differentiate.

Each TnT+ cell contains one nucleus on day three (**Figure 3.3f**). This number increases to two nuclei on day four due to fusion between the mono-nucleated TnT+ cells. Between days three and six, mono-nucleated TnT+ cells continue fusing with each other to form myotubes containing two nuclei. This data is consistent with myoblast fusion events captured by time-lapse microscopy and video. Between days six and seven a new round of fusion events occurs whereby the myotubes which mostly contain two nuclei fuse with each other to form myotubes which contain four nuclei. This suggests that the major myotube

fusion events occurs in a stepwise fashion whereby TnT+ cells preferentially fuse with similar TnT+ cells that contain a similar nuclear number. Mononucleated myocytes have been reported to fuse with myotubes that contain multiple nuclei [73].

The perimeter of the myotubes followed the same pattern seen for cell fusion (**figure 3.3g**). The mean perimeter of myotubes that formed on day 3 was ~ 100µm. Their size increased to ~ 250µm on day 4. Their size remained constant until day six when a burst of fusion occurred to yield myotubes that were ~ 430 µm on day 7.

The mean length per myotube (**figure 3.3h**) increased ~ 2.2-fold from ~43µm on day 3 to 97µm on day 4. There were some modest gains in length on day 5 (102µm) which disappeared on day six but once fusion occurred between days 6 and 7 the myotubes were ~ 126µm which is not two times more the length reached on day 4. This suggests that the length of the fusing TnT+ cells does not have to be equal for fusion events to occur between TnT+ cells.

The breadth of the myotubes (**figure 3.3i**) consistently increased on all days relative to day 3 ($p < 0.001$). On day 3 the mean breadth per myotube was ~ 9µm. On day 4 the width doubled to ~ 20 µm. On day 5 the breadth increased to ~23.8 µm. On day 6 the width increased incrementally by ~ one micron to reach ~ 25 µm. On day seven the mean breadth of the myotubes was ~32.3 µm. These results suggest that during differentiation there are modest but consistent gains in the breadth of the myotubes which form that are independent of fusion events.

The mean area per myotube was ~ 1000 μm^2 on day 3 (**figure 3.3j**). The myotube area did not change much until day 7 when the area more than doubled to ~ 2800 μm^2/myotube which seems to correlate with the occurrence of fusion events. The cellular integrated intensity/myotube (**figure 3.3k**) which represents the sum of pixel intensities within a myotube and is correlative for TnT protein content aligned well with results seen for area per myotube. On day 3 the integrated intensity per myotube was ~ $1X10^6$ IIU and on day 7 the intensity increased to ~ $2.5X10^6$ IIU.

The area per myotube nucleus (**figure 3.3l**) was ~ 130 μm^2 on day 3 and the area remained fairly constant until day 6 when a decrease in area was seen ($p > 0.05$) which seemed to occur in conjunction with fusion events. In general nuclear area correlates with levels of active gene transcription and cell size. Perhaps when fusion occurs, all the energies of the cells are focused on that event and the corresponding decrease in gene transcription seen in both nuclei may reflect silencing of unnecessary gene transcription. By day 7 the area per myonucleus increased to ~ 145 μm^2. This increase in size likely reflects the increased metabolic needs of the now larger myotube which is continuing to grow lengthwise and widthwise and this may be a marker of increased differentiation status.

The nuclear area of C2C12 myoblasts maintained in growth medium has been reported to be larger than the area of myonuclei[74]. The nuclear area per TnT- cells in growth medium (day 0) was ~ 186 μm^2 (**figure 3.3m**). After one day in DM the nuclear area decreased to ~ 161μm^2. After two days of culture in DM

the nuclear area decreased to ~ 140 µm^2. These results suggest that the new

cells that are generated when the growing myoblasts are transferred to

differentiation medium and undergo proliferation contain smaller nuclei than the

original myoblasts suggesting that these nuclei contain increased amounts of

heterochromatin compared to nuclei within growing myoblasts or that they are

smaller cells. The first and second day contains data from two types of cells,

those that will differentiate into TnT+ cells and TnT- cells that won't (reserve

cells). On day 3 the reserve cells show an increase in nuclear area (~ 145 µm^2)

compared to the average myotube nucleus (~ 130 µm^2) suggesting that the

nucleus within the myotube contains more heterochromatin than the nucleus in

the reserve cell. On day 4 there is not much change in nuclear area from day 3.

However on day 5 there is an increase in the nuclear area of the reserve cells to

~ 150 µm^2 suggesting the chromatin is adopting a more open configuration which

suggests active gene transcription. This active gene transcription may be

coincident with the initial stages of activating gene transcription that will convert

the TnT- cell into a TnT+ cell and this indicator may be a marker of the switch.

On day 6 the nuclear area of reserve cells decreases to ~ 136 µm^2. This dip is

somewhat similar to the dip seen between day 0 and day 2 and suggests the

generation of TnT+ cells is underway and on day 7 the nucleus of the reserve cell

increases to ~ 160 µm^2 which is not different from the size on day 1 (p>0.5) just

before the induction of differentiation. This suggests that the remaining reserve

cells are displaying increased gene transcription and are getting ready to

undergo a new round of TnT+ cell generation. As differentiation proceeds the

nuclei of the reserve cells seems to show dips which coincide with differentiation into TnT+ cells and then their nuclei grow larger suggesting that the longer they are in differentiation medium the larger they grow. This observation suggests that the nuclear area of the TnT- cell positively correlates with time suggesting that increased nuclear area may be a marker of increased differentiation. Since there is also a reduction in TnT- cells over time, this may suggest that within the set of TnT- cells that the subset that preferentially differentiates contains smaller nuclei representative of less committed cells and their nuclear area increases as they become activated to undergo cell differentiation. If this is the case then as differentiation proceeds the initial population of precursors that are generated on day 2 in the culture are the source of all the TnT+ cells which are being generated. These cells then become activated as evidenced by containing larger nuclei and then differentiate into TnT+ cells. Perhaps the cells with the larger nuclei represent a later differentiation step in the population of progenitor reserve cells.

The nuclear area of the TnT- cells was consistently larger than the nuclear area within the TnT+ cells during differentiation ($p<0.001$) (**figure 3.3n**). This finding suggests that myonuclei contain more heterochromatin compared to their non-differentiated counterparts indicating their chromatin is less plastic or open. The chromatin within the nuclei of the reserve cells seems to be more open suggesting that the reserve cells themselves may play an active role during differentiation. Since they are distinguishable from the nuclei within the myotubes this suggests that the differences in their areas may indicate a

difference between TnT- and TnT+ cells that can serve as a marker to differentiate them from each other .

Day 7 appeared to be an ideal point in which to investigate the effects of ethanol on differentiation for the following reasons. Day 7 provided a large number of myotubes, a wide range of values for all parameters in which to test the effects of ethanol. Furthermore statistical analyses were performed using one-way ANOVA to assess whether day 7 was different from day 0 or day 2 for TnT- cells or day 3 for TnT+ cells to assess whether the parameters were statistically different from the switch to differentiation (day 2) or the visible evidence of differentiation (day 3). Day 7 consistently yielded the time point at which all parameters differed from day 0 or day 2 or day 3 ($p < 0.0001$). These findings suggest that the time point that yields the largest dynamic range in which to study the effects of ethanol on C2C12 differentiation is on day 7.

The Effect of Ethanol on differentiating C2C12 Myoblasts

I compared the effects of ethanol and rapamycin to vehicle on multiple nuclear and cellular parameters during C2C12 differentiation using the high content imaging system. It has been reported that chronic alcoholics can possess blood alcohol concentrations of 100mM [50] so this dose was selected to test the effects of ethanol on differentiation. Rapamycin is an inhibitor of C2C12 differentiation [60, 72] and was tested to verify the imaging system could identify the effects of an inhibitor and to test what effects an inhibitor would have on the new parameters under study.

Since the high content screen yields results on multiple parameters and I was performing a t-test for each parameter, there was a possibility of increasing the chances of making a type I error i.e. a false positive error. To correct for significance effects contributed by false positives one can lower the acceptable level of significance to below 0.05. The Bonferroni correction yields a corrected p-value for multiple hypothesis testing and it is calculated by dividing 0.05 by the number of tests. In this case, the acceptable p-value for every test would be $0.05/12=4.17 \times 10^{-3}$. One danger of using the Bonferroni correction is that it is very stringent which then increases the chances of making a type II error i.e. a false negative error. To achieve a happy medium, the false discovery rate (FDR) is generally used to reduce the type I error and minimize the risk of missing significant biological effects. The steps one performs to use that correction are as follows – (1) the p-values from each t-test are ordered from smallest to largest and each test is then assigned a test number, *i,* with i=1 for the smallest p-value and in my case i=12 for the largest p-value – (2) an acceptable false positive rate (Q) is chosen, in this case 0.05. Individual adjusted p-values are then calculated for each *i* by using the formula (i/m)/Q where m=the number of tests. **Table 3.1** shows the adjusted p-values necessary to achieve to evaluate whether ethanol exerts any effects on C2C12 differentiation for the multiple parameters tested in the high content screen and the p-values for the effects of ethanol. All the adjusted p-values were less than what was calculated using the Bonferroni correction or the FDR for both rapamycin (data not shown) and for ethanol

Table 3.1: Ethanol alters the cellular and nuclear profile of C2C12 cells undergoing differentiation.

Parameter	Vehicle Mean	Vehicle SD	Ethanol Mean	Ethanol SD	P-Value	i	m	Q	(i/m)Q
Nuclear Area/TnT-Cell	140	7.37	164	8.81	9.91E-16	1	12	0.05	0.004
Mean Perimeter/Myotube	772	111	473	59.7	2.60E-15	2	12	0.05	0.008
TnT-Cell #/Well	41497	1395	34652	2298	2.72E-14	3	12	0.05	0.013
Mean Length/Myotube	178	11.3	147	13	3.45E-14	4	12	0.05	0.017
# nuclei/Myotube	6	1	4	1	1.69E-13	5	12	0.05	0.021
TnT+ Mean Breadth/Myotube	46.2	5.3	32.1	2.33	2.19E-12	6	12	0.05	0.025
Mean TnT+ Cell Area/TnT+ Cell	4612	982	2405	360	3.35E-12	7	12	0.05	0.029
Mean NucArea/Myotube Nucleus	133	3.77	140	3.25	1.99E-11	8	12	0.05	0.033
TnT+II/Myotube	3550397	555916	2491590	219876	3.89E-10	9	12	0.05	0.038
Total Number of Myonuclei/Well	7242	665	5484	1216	1.30E-07	10	12	0.05	0.042
TnT+Cell #/Well	1149	182	1506	152	4.01E-06	11	12	0.05	0.046
MFI	14.9	1.26	13.5	2.12	6.99E-03	12	12	0.05	0.050

Indicated parameters were measured after C2C12 cells were differentiated for 7 days. Student's t-tests comparing treated to control were performed followed by correction for multiple testing (FDR=0.05) (Bonferroni p=4.17E-03) (n=24)

suggesting that the imaging system can identify the effects of an inhibitor on C2C12 differentiation and the effects of ethanol on C2C12 differentiation.

Ethanol treatment produced smaller myotubes during differentiation (**figure 3.4a**) as evidenced by a ~ 40% reduction in myotube perimeter (**figure 3.4b**), a ~ 20% reduction in cell length (**figure 3.4c**) and a 30% reduction in myotube width compared with control treated cells (**figure 3.4d**). Ethanol treatment caused a 50% reduction in myotube area (**figure 3.4e**) and reduced the abundance of TnT by ~ 30% as measured by the per myotube integrated intensity (**figure 3.4f**). These findings suggest that ethanol causes smaller, shorter and thinner myotubes containing less TnT to form during differentiation. These findings were also seen with the myogenesis inhibitor, rapamycin suggesting that ethanol inhibits differentiation.

Interestingly while alcohol treated myotubes were smaller, there was a ~ 25% increase in the number of TnT+ cells that formed in response to ethanol treatment during C2C12 differentiation (**figure 3.4g**). There was a ~ 25% reduction in the total number of myonuclei per ethanol treated well compared to control wells (**figure 3.4h**). On a per myotube basis this translated to a 50% reduction in the number of nuclei per myotube (3 in alcohol treated cells versus 6 in control treated cells) (**figure 3.4i**).

Interestingly the myonuclei were on average 5% larger in the ethanol treated myotubes (**figure 3.4j**) and this situation was paralleled in the TnT- cells where the nuclei were on average ~ 16% larger (**figure 3.4l**). I previously saw (**figure 3.3l, m, n**) that as differentiation proceeds nuclear area of myonuclei and

A

Vehicle | Ethanol | Rapamycin

B

C

D

E
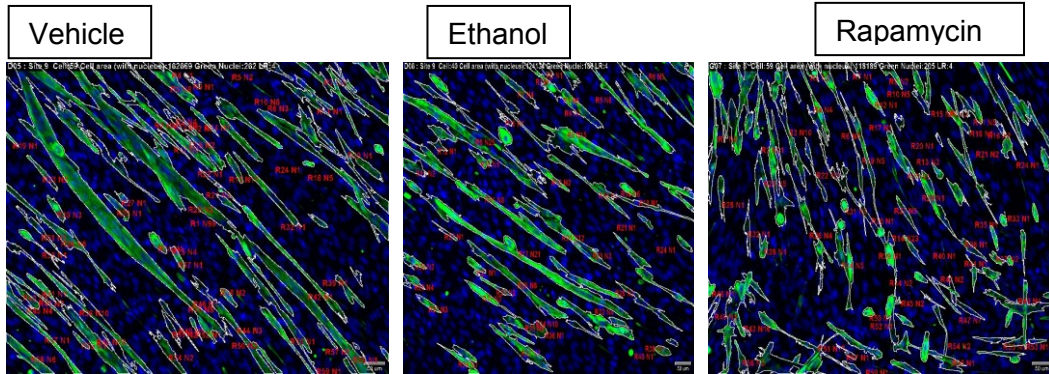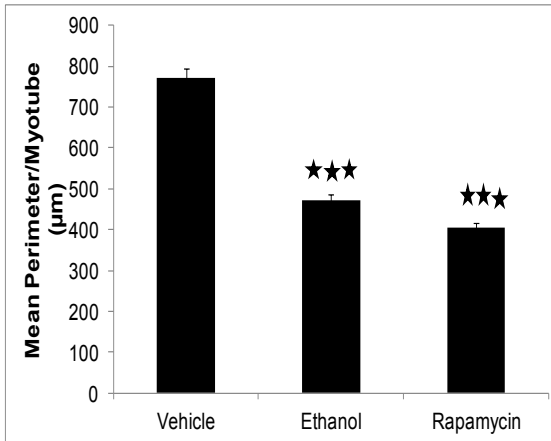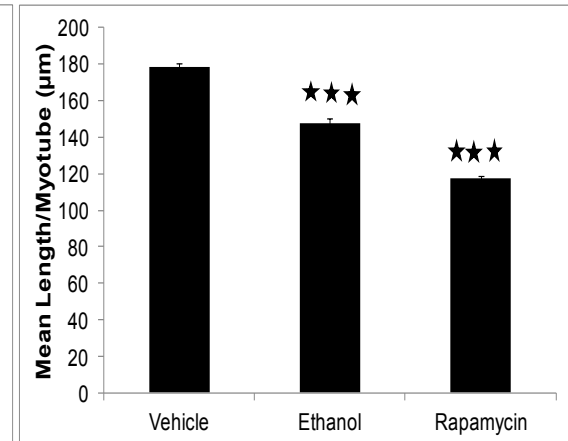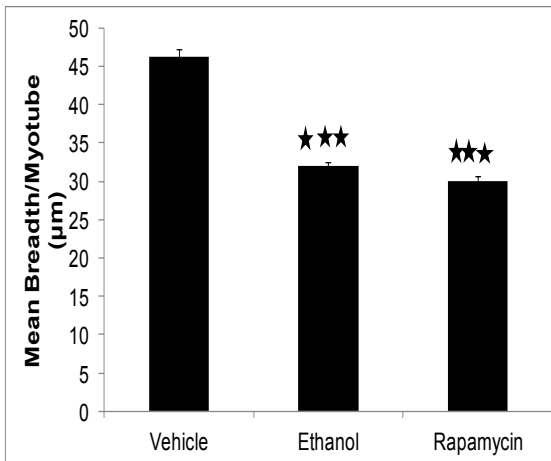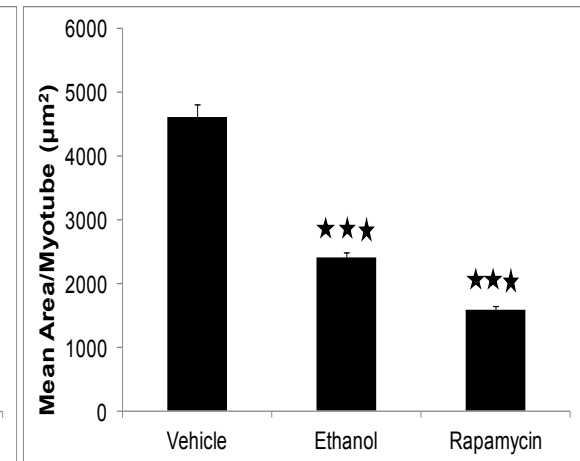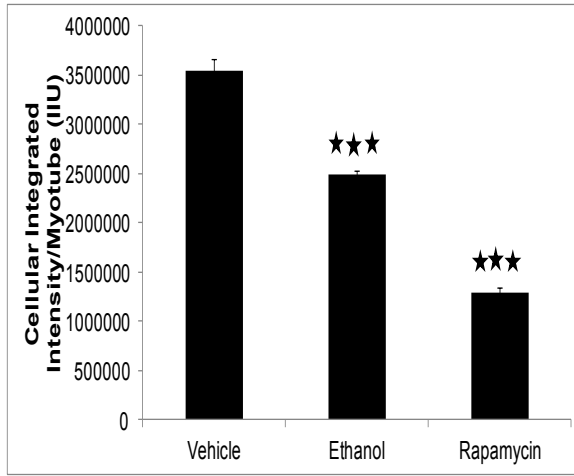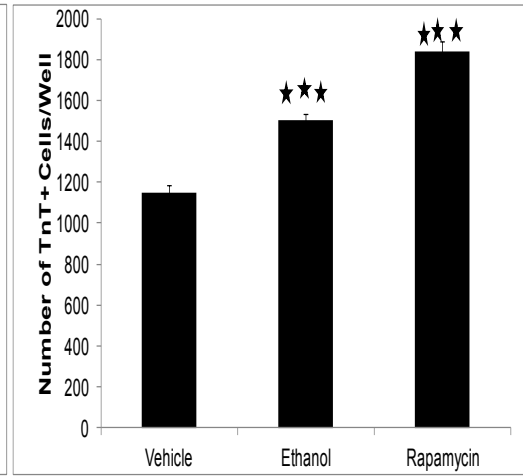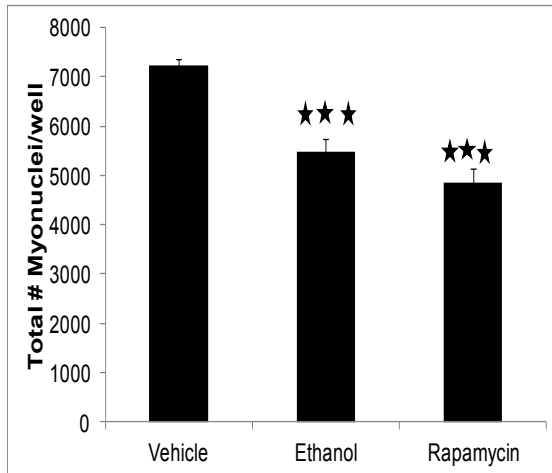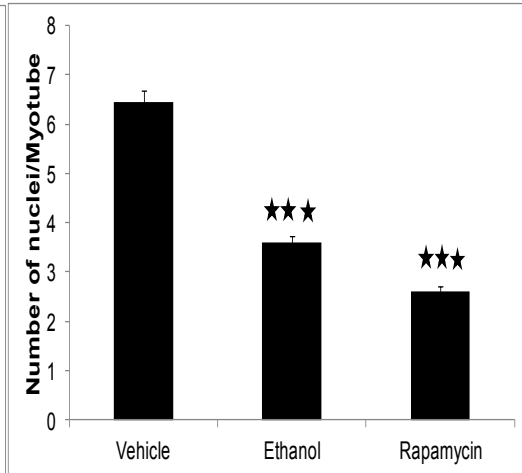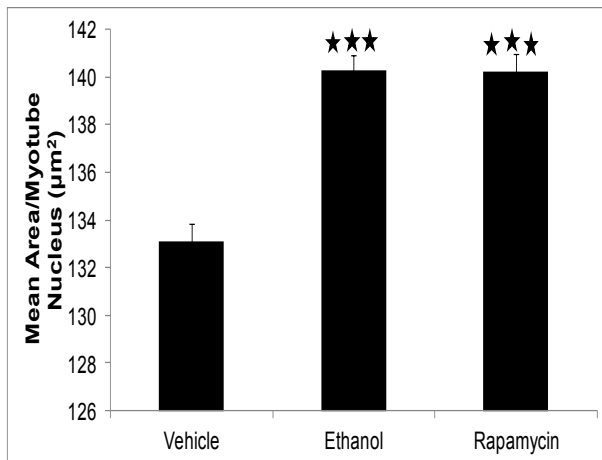
K
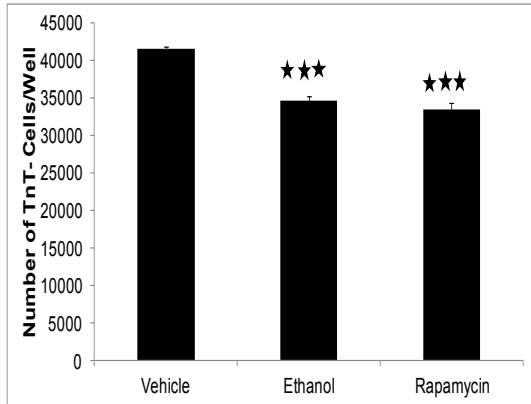
L
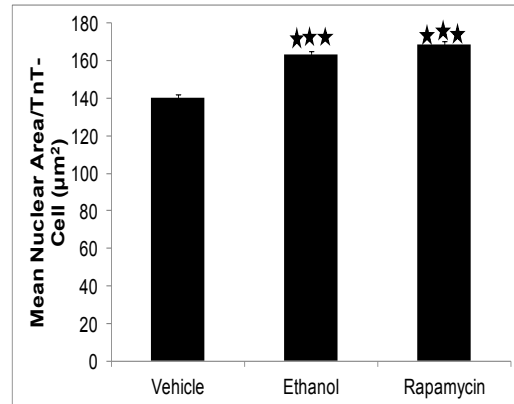
M
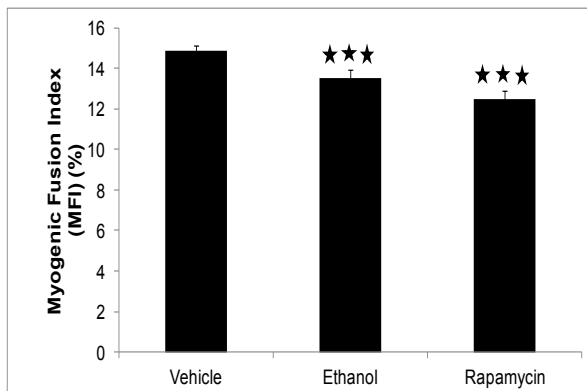
Figure 3.4: Ethanol inhibits C2C12 differentiation. C2C12 cells were differentiated in control medium or medium containing ethanol (100mM) or rapamycin (100nM) for 7 days (A) The cells were fixed and immunostained for Troponin T (TnT) and nuclei were counterstained with DAPI. (B) Myotube perimeter (µm) (C) Mean Length per Myotube (µm) (D) Mean Breadth per Myotube (µm) (E) Mean Area per Myotube (μm^2) (F) Cellular Integrated Intensity per Myotube (IIU) (G) Number of TnT+ cells per well (H) Total number of myonuclei per well (I) Number of nuclei/Myotube (J) Mean Area/Myotube Nucleus (μm^2) (K) Number of TnT- cells/well (L) Mean Nuclear Area/TnT- cell (μm^2) (M) MFI, Myogenic Fusion Index (MFI) (%). The averages are shown ± SEM (n=22-24), ***p<0.001 vs. Vehicle.

TnT- cells increases. The observation of the increase in nuclear area in all the cells might suggest that differentiation is being accelerated by alcohol. Since the nuclei are larger in the ethanol treated cells this is suggestive of increased active gene transcription in the ethanol treated cells compared to the control cells.

The myogenic fusion index is commonly used to measure myoblast differentiation and reductions correlate with inhibition of differentiation [61, 62]. The myogenic fusion index is calculated by dividing the number of myonuclei by the total number of nuclei. The myogenic fusion index (MFI) was decreased by ~15% in the ethanol treated cells (**figure 3.4m**). These results show that the high content screen was able to measure the effects of an inhibitor on C2C12 differentiation and that ethanol showed a similar profile to the myogenesis inhibitor, rapamycin on multiple parameters of C2C12 differentiation. Furthermore ethanol inhibited the myogenic fusion index which is a common measure used to assess inhibition of differentiation.

Discussion

A system of microscopy and computer-aided analysis was developed to measure the cellular and nuclear profile of C2C12 myogenic cell differentiation on a cell by cell basis within a well of a 96 well plate. The high-content screen was able to take measurements from over 1000 myotubes per well. Information from the high content screen revealed that C2C12 differentiation is a dynamic process with both differentiated and undifferentiated cells displaying altered phenotypes during differentiation.

The cells undergo a proliferative phase for two days in differentiation medium before displaying a differentiation phenotype on day 3. This phenomenon has been reported to be related to the cell cycle status of the individual myoblasts whereby cells that are in the G1 phase commit to differentiation whereas cells in other phases of the cell cycle will continue to progress until they reach the next G1 at which point they will commit to differentiate[75]. During C2C12 differentiation there was a decrease in the reserve (TnT-) cells over time and an increase in the TnT+ cells. This did not occur in a one-to-one ratio. This suggests additional subpopulations within the cell population which is resistant to differentiation exists. Within the reserve cell population there may exist specialized subpopulations of cells which might serve a similar purpose to glial cells in the nervous system i.e. provide support to support the culture. Perhaps some cells die to maintain homeostasis of the culture to prevent overcrowding. As differentiation progressed the major fusion events picked up by the high-content screen showed that fusion preferentially occurred between the TnT+ cells that contained similar nuclear number. This suggests that the high content screen can potentially identify discrete effects of molecules on these fusion events.

The high content screen revealed that the perimeter, area and integrated intensity of the TnT+ cells during C2C12 differentiation was measurable and increased over time.

The high content screen confirmed recent findings by Watanabe (2012) that the nuclear area of a growing C2C12 myoblast is larger than the nuclear

area of a myonucleus [74]. The authors report that the myonucleus is under greater force, and myonuclear movement is blocked, and there is reduced mobility of histone proteins which are indicators that chromatin plasticity decreases upon differentiation[74]. Embryonic stem cells have been reported to have a more open chromatin structure (increased plasticity) which decreases upon differentiation[76]. This suggests that nuclear area of myotubes can be used as a marker of differentiation.

Interestingly the high content screen revealed that although the nuclear area of reserve cells and TnT+ cells was reduced compared to the growing myoblasts, upon induction of differentiation the nuclear area in both cell types increased over time. In light of the recently reported findings, this might suggest that chromatin plasticity increases over time in all cells during differentiation.

However outside of reasons due to chromatin plasticity, the fact that the nuclear area in both cell types increases over time suggests that this phenotype may mark the advancing differentiation state. I also found that the area of the myonuclei was almost always consistently smaller than the nuclei of the reserve cells suggesting that the reserve cells possess a less differentiated phenotype compared to myonuclei.

The high-content screen demonstrated that the cellular and nuclear profiles were similarly altered whether a myogenesis inhibitor (rapamycin) or ethanol was administered to differentiating C2C12 cells. The major findings were that ethanol decreased the number of nuclei per myotube, the perimeter, area and integrated intensity of myotubes. Interestingly ethanol increased the number

of TnT+ cells while decreasing the number of TnT- cells. The decrease seen in the number of TnT- cells in the ethanol cultures during differentiation might suggest that ethanol is inhibiting the proliferation of a subpopulation of reserve cells. These hypotheses would need to be tested further.

Since there is an increase in the number of TnT+ cells and a decrease in the TnT- cells this may suggest that premature differentiation of a subset of the reserve cells is occurring. Premature differentiation of myoblasts into myotubes with concomitant decreases in proliferation has been observed by other researchers [36, 77]. During fetal mouse development when Notch signaling was attenuated the accelerated differentiation of progenitor cells occurred early in development, causing an increased number of muscle fibers to form compared to controls, but their numbers were depleted by embryonic day 12 and the fetuses displayed dramatic muscle hypotrophy[37]. My results support the phenomenon of premature differentiation of a subpopulation of reserve cells into myotubes. This would cause their eventual depletion of their numbers to inhibit differentiation as in seen in muscular dystrophy or the MyoD-/- mice[21].

Interestingly alcohol demonstrated a similar yet less severe phenotype compared to the effect of rapamycin on C2C12 differentiation. Rapamycin has been reported to inhibit C2C12 differentiation in part by blocking the terminal differentiation events of myoblast fusion [78]. An alternative explanation for the inhibition of differentiation by alcohol might be that myotubes are forming in the presence of alcohol but that they are blocked at the fusion stage and a result

contain smaller and fewer nuclei. This hypothesis would need to be tested further.

Using my approach, the most prominent effects of alcohol on C2C12 differentiation emerged. I measured the cellular and nuclear profile of C2C12 myogenic cells undergoing differentiation in the presence of ethanol and found that ethanol altered the nuclear and cellular landscape of C2C12 myogenic cells and inhibited their differentiation.

Chapter 4: The Effect of Ethanol on C2C12

Differentiation Assessed by Transcriptional Profiling

Figure Contributions:

I performed the experiments which generated the materials for the figures which are presented in this chapter.

Christopher Parkin (CNR) contributed **figure 4.4a-d.**

Christopher Parkin processed the raw fluorescence data from the microarrays using Genome Studio (Illumina) and the programming language and software environment R to generate text files which contained the expression data and the comparisons between the different conditions and their statistical significance.

I used Ingenuity Pathway Analysis software to process the microarray expression data and comparisons and to help me model, analyze and understand the data.

Figure 4.7 was generated using GENE-E software (Broad)

Figure 4.8 was generated using Ingenuity Pathway Systems software.

I contributed the remaining figures.

Introduction

Alcoholic myopathy results from long term use of alcohol. The development of this disease may be connected to gene expression changes which affect particular molecular signaling events leading to long term changes in muscle satellite cells as they become activated to proliferate and differentiate into myoblasts and subsequently into myotubes.

Ethanol exposure during pre-natal development leads to the fetal alcohol spectrum disorder (FASD) which in addition to causing defects on multiple organs also presents with impairments in muscle development[79]. A syndrome of fetal alcohol myopathy has been described in human newborns whereby the muscle biopsies displayed fiber hypotrophy, and a preponderance of fast twitch muscle (type II) fibers, and centrally located nuclei[80]. Centrally located myonuclei in fibers with small diameters are also defining features of newly regenerated myofibers [21, 81]. Ethanol has been reported to inhibit proliferation and differentiation during development, in addition ethanol has been reported to affect membrane-associated receptor signaling pathways, cause free radical damage and alter the binding of transcription factors[79].

Alterations in gene expression may lead to changes in molecular signaling pathways[82]. Gene expression profiling using microarrays allows one to concurrently measure the expression of thousands of genes in an unbiased fashion and identify clusters of genes with analogous function or regulation[82]. Furthermore, since microarray analysis is not focused on candidate genes, global gene networks and their connected biological pathways can be identified, and

this impartial examination of complicated biological events involved in the cellular response to ethanol may lead to novel hypotheses about mechanisms and treatment of diseases[82].

The effects of ethanol on differentiating satellite cells or myoblasts is poorly studied. Since skeletal muscle barely expresses alcohol dehydrogenase activity, the major effects of ethanol on muscle cells are likely exerted directly[50].

Myogenic differentiation follows a temporal series of orchestrated events characterized by the activation of quiescent cells, proliferation of activated satellite cells and myoblasts, cell cycle withdrawal, appearance of differentiated myocytes and cell fusion to form multinucleated myotubes[83]. The C2C12 myogenic cell line recapitulates the temporal process of myogenic differentiation. The process of myogenic commitment and activation of muscle-specific gene expression can be followed molecularly by measuring expression of the MRFs and the MEF2 family of factors [84]. MRFs are expressed sequentially whereby Myf5 and MyoD are expressed in dividing, determined cells and expression of myogenin is only induced during differentiation [84].

As mentioned previously, the inhibition of myogenic differentiation is confirmed at the cellular level by viewing reductions in the MFI and in reductions of myogenic regulatory factors (MRFs) at the transcriptional level[59, 85, 86].

I evaluated the effects of ethanol on the expression levels of three MRFS, MyoD, Myf5 and myogenin and on the levels of Mef2c during the first three days of culture in differentiation medium. I compared the gene expression profiles

71

between control and ethanol exposed C2C12 myogenic cells over a period of three days of culture in differentiation medium using high density Illumina microarrays and analyzed the data using Ingenuity Pathway Analysis (IPA) software[65].

I found that ethanol reduced levels of all MRFs and consistently reduced the levels of MyoD during differentiation. The microarray predicted that the muscular development pathway was associated with C2C12 differentiation (p<0.05). The qPCR values for MyoD and myogenin correlated with the microarray expression levels (p<0.01). Five additional genes from the microarray correlated with qPCR expression (p<0.0001).

Forty-six transcripts on the microarray were consistently altered by ethanol during all days of differentiation. Focused analysis on those transcripts which showed the most variation identified down-regulation in genes dependent on MyoD transcription (p=8.7X10^{-4}). Signaling pathways predicted to be consistently altered included calcium signaling, notch signaling, semaphorin signaling, CXCR4 signaling and chemokine signaling (p<0.05).

When the microarray was examined on a day by day basis, the p38, ILK, ERK/MAPK signaling and VEGF signaling pathways (p<0.05) which play roles in myogenic differentiation were predicted to be altered by ethanol. Multiple transcriptional regulators associated with differentiation including MyoD and myogenin were predicted to be altered by ethanol (p<0.05). Transcriptional regulators predicted to be activated by ethanol (z>2) included Notch and RBP-J (p<0.05). Notch signaling has been shown to inhibit myogenesis[14]. Network

analysis predicted the formation of a centralized network that via common transcripts connected to multiple networks. One of those transcripts whose up-regulation depends on MyoD acetylation [87] was down-regulated by ethanol on the microarray. Acetylation of MyoD is necessary for muscle regeneration in vivo and for myoblast differentiation in vitro[88]. The microarray predicted that molecular and cellular functions related to cell death, cell cycle and cellular growth and proliferation were altered in the ethanol treated cells ($p < 0.05$). On a cellular level I saw changes in cell number that trended towards the microarray predictions ($p < 0.05$).

To summarize, expression analysis of the effects of ethanol on levels of myogenic regulatory factors and on gene expression profiles of differentiating C2C12 cells 1) demonstrated that ethanol reduced the levels of MyoD, Myf5 and myogenin 2) predicted activation of Notch signaling by ethanol 3) predicted that multiple pathways related to myogenic differentiation were altered by ethanol and 4) predicted that MyoD levels and function were altered by ethanol. These results suggest that ethanol inhibits the differentiation of C2C12 myogenic cells primarily by causing the down-regulation of MyoD and by reducing the functionality of the protein.

Results and Discussion

Quality of Extracted RNA

Preservation of the natural state of RNA that is isolated from tissues or cells is vital for the acquisition of worthwhile data from downstream experiments such as gene expression profiling and quantitative real-time PCR (qRT-PCR)[89,

90]. When using a spectrophotometer A260/A280 and A260/A230 ratios greater than 1.8 are considered indicators of acceptable RNA quality [90]. Additionally RNA quality can be evaluated by denaturing agarose gel electrophoresis[90]. I evaluated the quality of isolated RNA by denaturing gel electorphoresis and measurement of A260/A280 and A260/A230 ratios (**figure 4.1, table 4.1**). Intact bands of 28S rRNA and 18S RNA were seen in a variety of samples derived from cells treated with or without ethanol and rapamycin (**figure 4.1**) in a discernible 2:1 ratio. There was no smearing which would be indicative of degradation. The A260/A280 ratios and A260/A230 ratios were higher than 1.8 except for one sample. It has been reported that PCR efficiency is independent of RNA quality so long as the amplicons lie in the range of 70-250 bp [89]. These results indicate that the current method of RNA extraction yields RNA that is of an acceptable quality for downstream applications of gene expression analysis.
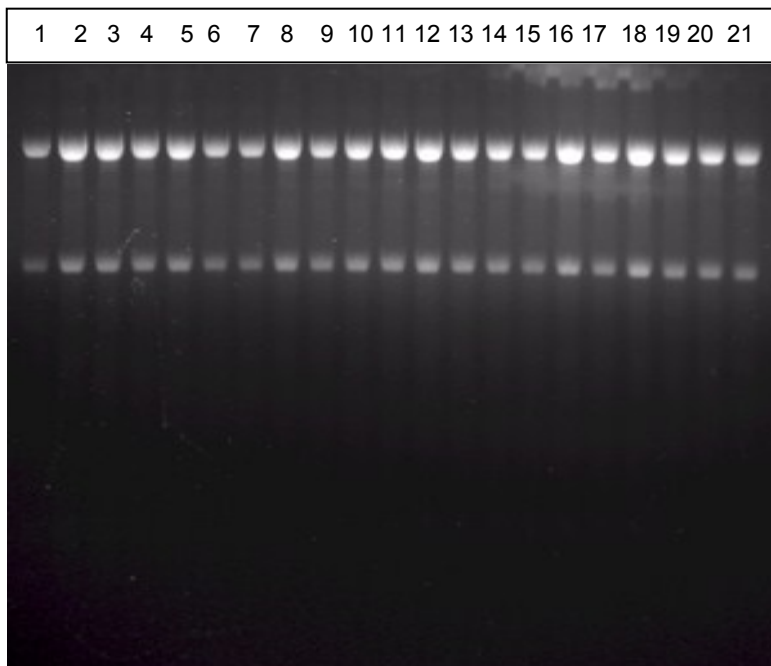
Figure 4.1: Quality of extracted RNA assessed by denaturing agarose gel electrophoresis. RNA was isolated from C2C12 cells and electrophoresed on formaldehyde agarose gel.

Table 4.1: RNA Quality assessed by A260/A280 and A260/A230 ratios measured in a spectrophotometer.

Sample Number	C2C12 Sample Name	A260/A280	A260/A230
1	Growth Medium	1.98	2.25
2	1 day DM_1	2.02	2.27
3	2 days DM	2.01	2.26
4	1 day DM_2	2.02	1.34
5	1 day DM 0.1% EtOH	2.02	2.28
6	1 day DM 0.3% EtOH	2.02	2.40
7	1 day DM 0.5% EtOH	2.01	2.32
8	1 day DM 0.7% EtOH	2.01	2.29
9	1 day DM 100nM Rapamycin	2.00	2.20
10	2 days DM	2.00	2.29
11	2 days DM 0.1% EtOH	2.03	2.37
12	2 days DM 0.3% EtOH	2.01	2.25
13	2 days DM 0.5% EtOH	2.02	2.19
14	2 days DM 0.7% EtOH	2.02	2.34
15	2 days DM Rapamycin	2.01	2.19
16	3 days DM	2.00	2.28
17	3 days DM 0.1% EtOH	2.02	2.35
18	3 days DM 0.3% EtOH	2.01	2.29
19	3 days DM 0.5% EtOH	2.00	2.23
20	3 days DM 0.7% EtOH	2.03	2.19
21	3 days DM Rapamycin	1.99	2.23

Selection of a reference gene for quantitative RT-PCR (qRT-PCR)

qPCR is a method to determine the quantity of a gene in a sample. It can detect few copies of a transcript with very high precision[91]. The accuracy of qRT-PCR depends on normalization of the target sequence to a housekeeping gene which is expressed at similar levels in control and treated samples [91, 92]. A variation in cycle threshold (Ct) of +/- 1 across all samples is considered acceptable[92]. I compared the Ct values of Beta-Actin and GAPDH from several samples of growing C2C12 cells and differentiating C2C12 cells in control medium and in the presence of ethanol over several days (**table 4.2**). Subtracting the largest Ct from the lowest Ct yielded a value of 0.89 for Beta-Actin and 1.61 for GAPDH. The variation in Ct over all samples is less than 1 for Beta-Actin which suggests that Beta-Actin is a suitable housekeeping gene.

Table 4.2: Beta-actin is an acceptable housekeeping gene

Sample	Ct of Beta-Actin	Ct of GAPDH
0 Day DM-1	19.02	18.77
0 Day DM-2	19.12	18.72
0 Day DM-3	19.44	**19.57**
1 Day DM-1	**18.83**	18.19
1 Day DM-2	19.63	19.01
1 Day DM-3	19.70	19.46
1 Day DM-1, 100mM EtOH	19.35	18.94
1 Day DM-2, 100mM EtOH	**19.73**	19.19
1 Day DM-3, 100mM EtOH	19.65	19.20
2 Days DM-1	19.31	**17.96**
2 Days DM-2	19.13	19.23
2 Days DM-3	19.62	19.46
2 Days DM-1, 100mM EtOH	19.02	18.31
2 Days DM-2, 100mM EtOH	19.43	18.80
2 Days DM-3, 100mM EtOH	19.68	19.07
3 Days DM-1	19.45	19.36
3 Days DM-2	19.57	18.89
3 Days DM-3	19.44	19.24
3 Days DM-1, 100mM EtOH	19.62	19.35
3 Days DM-2, 100mM EtOH	19.22	19.03
3 Days DM-3, 100mM EtOH	19.40	18.94
Largest Ct-Smallest Ct	**0.89**	**1.61**

Quantitative RT-PCR was performed on cDNA reverse-transcribed from RNA isolated from non-differentiating C2C12 cells or C2C12 cells differentiated over 1-3 days with or without ethanol. Ct values represent the number of cycles required for the fluorescent signal to pass the background.

The Effect of Ethanol on levels of MRFs and Mef2c

Expression of the MRFs and Mef2c relative to growth medium

Assessment of inhibition of differentiation is made by observing reductions in transcriptional levels of MRFs. Before evaluating the effect of ethanol on levels of the MRFs, I first compared the expression of Myf5, MyoD and myogenin during C2C12 differentiation relative to GM (**figure 4.2**) to establish baseline expression during differentiation. Myf5 is the earliest marker of myogenic commitment and is expressed on quiescent and activated satellite cells [39]. Levels of Myf5 were robust in growth medium and increased by ~ 10-15% upon induction of differentiation throughout the time course (**figure 4.2a**). This suggests that serum withdrawal either induces Myf5 expression in a population of cells that are initially Myf5- or a subpopulation of Myf5+ cells proliferate on the first day of differentiation.

Levels of MyoD have been reported to be down-regulated in a subpopulation of C2C12 cells undergoing differentiation and are referred to as reserve cells[7, 26, 93]. Yet using western blot analysis, protein levels of MyoD have been demonstrated to increase during C2C12 differentiation compared to GM[94, 95]. It has been shown that ~ 50% of C2C12 cells down-regulate MyoD in the nucleus 24 hours after induction of differentiation using immunocytochemical methods[7]. This discrepancy can be explained by the fact that western blot analysis measures MyoD protein which is present in the cytoplasm and the nucleus. I observed robust expression of MyoD in growth medium and ~ 50% reduction in levels of MyoD on days one and two in
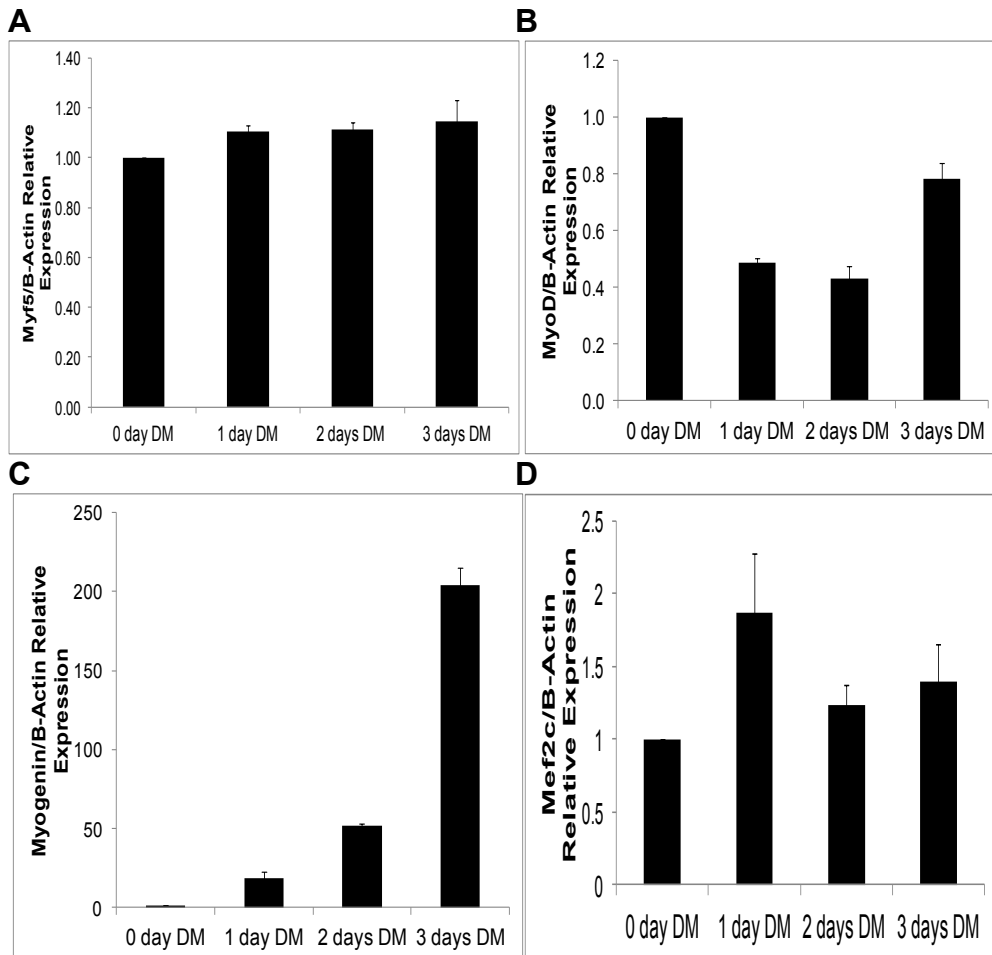
Figure 4.2: Levels of MRFs and Mef2c during C2C12 differentiation. C2C12 cells were induced to differentiate in DM for 3 days. **(A)** Myf5, **(B)** MyoD, **(C)** myogenin, **(D)** Mef2c mRNA levels were measured by qPCR every 24 hours. Data was quantified using the standard curve method and normalized to B-Actin to obtain relative fold-change to 0 day DM (GM) ± SEM. (n=3)

differentiation medium(**figure 4.2b**). My findings converge with the results reported for nuclear levels of MyoD. On day 3 levels of MyoD increase to ~ 80% relative to GM suggesting that this increase may be representative of two phenomena, one that some of the reserve cells start up-regulating MyoD and commit to differentiate as has been shown[7] and two, that MyoD expression is increased in the committed cells to activate genes which function in terminal differentiation.

Myogenin expression in C2C12 cells cultured in GM was negligible. Myogenin expression rapidly increased ~ 20-fold on day 1, more than doubled to ~ 50-fold on day 2 and quadrupled to ~ 200-fold on day 3 of differentiation (**figure 4.2c**). Western blotting reveals that myogenin expression is not seen in GM but is first evident 24 hours after culture in DM with levels increasing 24 hours later[68]. My results suggest that upon induction of differentiation by serum withdrawal, cells in the G1 phase of the cell cycle arrest and start expressing myogenin on day 1. On day 3 the myogenin levels increase as the MyoD levels increase. MyoD activates the myogenin promoter[12]. It is observed in differentiating C2C12 cells by using double-staining immunocytochemistry for MyoD and myogenin, that as the cells commit to differentiation by becoming MyoD+ this event is soon followed by those same cells becoming myogenin+[7]. My results follow these previous reported results.

The Mef2 proteins are not myogenic on their own, but they synergize with the MRFs to mediate expression of muscle-specific genes including contractile protein expression once myogenin has been expressed [12, 96]. Low levels of

Mef2c expression were observed in GM. Mef2C expression nearly doubled on day 1 in differentiation (**figure 4.2d**). Mef2c levels then decreased by ~ 60% on day 2 compared to day 1 and increased by ~ 20% on day 3 compared to day 2. These results show that Mef2c transcription increases as myogenin levels start increasing.

The Effect of Ethanol on the expression of the MRFs and Mef2c

I next looked at the effect of ethanol on the levels of the MRFs and Mef2c on differentiating C2C12 cells (**figure 4.3**). I found that ethanol reduced the levels of Myf5 by ~ 10% on day 1 ($p<0.001$) and levels of Myf5 remained reduced on the remaining days (**figure 4.3a**). MyoD levels were reduced by ~ 15% on day 1 ($p<0.01$), and reduced further by ~ 25% on days 2 and 3 ($p<0.001$) compared to controls (**figure 4.3b**). Myogenin levels were decreased by ~ 30% on day 1($p<0.01$) and increased slightly but were still reduced by ~ 20% on day 2 ($p<0.01$) and then increased by ~ 15% on day 3 ($p=0.05$) compared to controls (**figure 4.3c**). These results show that ethanol consistently reduces the transcriptional levels of the MRFs for two days during differentiation which indicates that the differentiation of C2C12 cells is impeded. Interestingly a trend of increasing myogenin levels was seen in the presence of decreased MyoD levels. As a MRF, myogenin can convert a variety of cell types to muscle cells
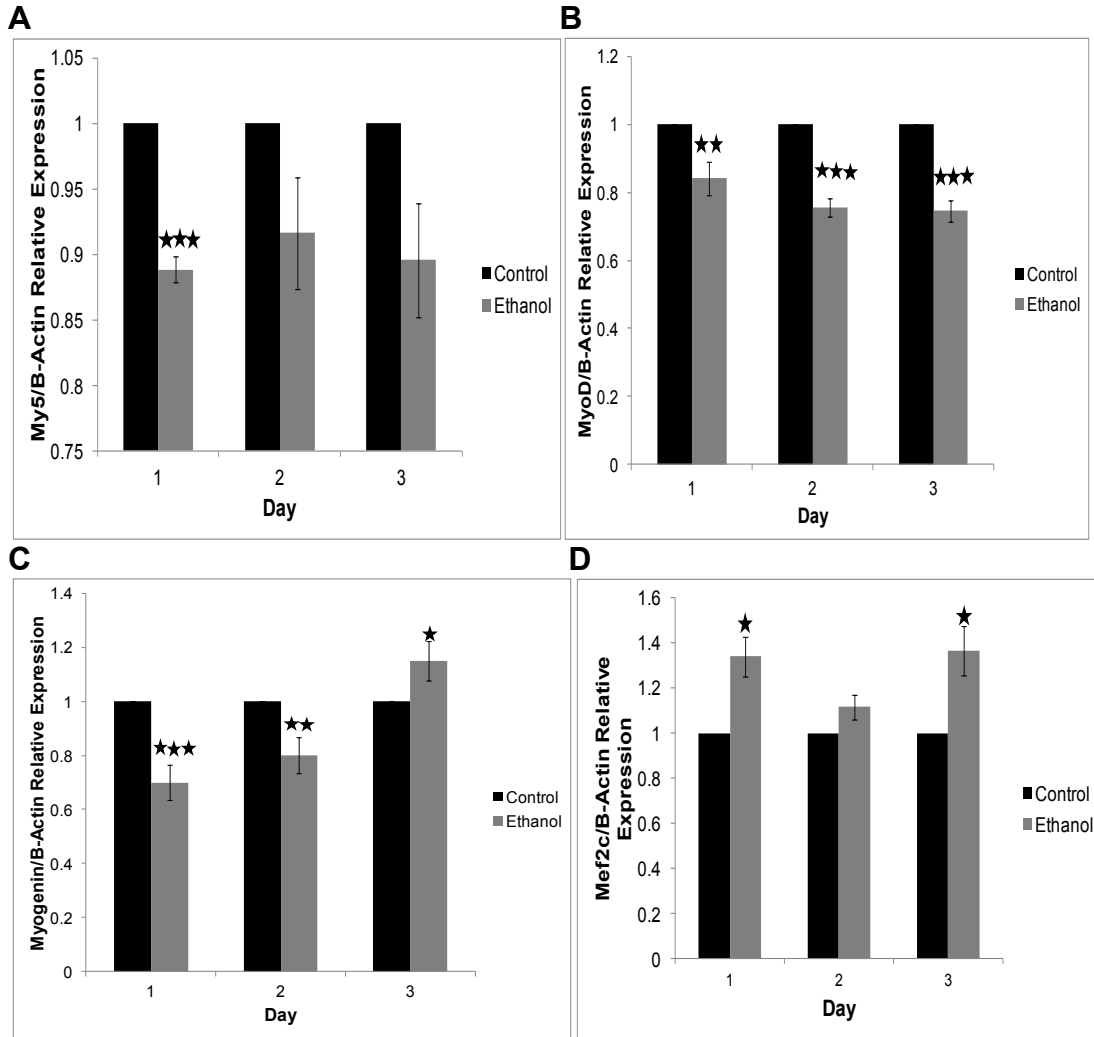
Figure 4.3: Ethanol reduces levels of MRFs and increases levels of Mef2c during differentiation. C2C12 cells were induced to differentiate in DM ± 100mM ethanol for 3 days. (A) Myf-5, (B) MyoD, (C) Myogenin, (D) Mef2c mRNA levels were measured by qPCR every 24 hours. Expression is relative to untreated controls ± SEM. *p≤0.05 (n=3-9).

but it is reported to be less efficient than MyoD in triggering the expression of some muscle specific genes[12]. After 72 hours of differentiation it has been reported that there is a small subset of C2C12 cells which express myogenin in the absence of MyoD[7]. Ethanol may be causing an increase in this same subset of cells as an adaptive response to complete the differentiation program in the presence of reduced MyoD protein and/or functionality. Levels of Mef2c were increased by ~ 35% on day 1($p \leq 0.05$), by ~ 10% on day 2 and by ~ 35% on day 3 ($p \leq 0.05$) compared to controls (**figure 4.3d**). Increased levels of Mef2c suggest that differentiation is being accelerated. It has been reported that myogenin and Mef2c can up-regulate each other's expression and induce the skeletal muscle program in P19 cells[97]. The finding that Mef2c levels are increased by ethanol suggests that this may be another compensatory mechanism in response to reduced MyoD activity during differentiation to up-regulate expression of myogenin and vice versa. The finding that both myogenin and Mef2c are increased on day 3 also suggests that structural protein genes are being activated earlier in the ethanol treated cells compared to controls. This might suggest that ethanol initially accelerates the differentiation of C2C12 cells. However since Myf5 and MyoD and for the most part, myogenin levels are reduced by ethanol, the continued presence of ethanol on C2C12 differentiation will eventually be inhibitory. Indeed knockdown of MyoD or Myf5 or myogenin by shRNA in differentiating C2C12 cells during the first 24 hours inhibits their differentiation as assessed by reductions seen in the MFI[98]. This underscores

the importance of MRF functionality early in the differentiation to complete the program.

Microarray analysis of the effects of ethanol on C2C12 differentiation

Tomczak (2003) describe studies of temporal expression profiling of C2C12 cells undergoing differentiation which demonstrate the expression patterns of well-known muscle specific genes suggesting the effectiveness of the time-series microarray approach to study the differentiation process of myoblasts[83]. Rajan (2012) performed temporal microarray analysis on C2C12 cells differentiating during the first 24 hours and identified 193 differentially expressed transcriptional regulators, and knockdown of over half of them inhibited differentiation as assessed by myogenic fusion index[98]. The reductions seen in the myogenic regulatory factors by ethanol during the first 3 days of differentiation suggests that ethanol is exerting its effects early in differentiation to inhibit the terminal events of myotube formation. It has been suggested that the process of C2C12 differentiation is mainly regulated at the transcriptional level since protein and transcript profiles have been found to correlate for more than 90% of genes identified by proteomics and compared to transcriptional profiling during C2C12 differentiation[98].

After observing the reductions in the myogenic regulatory factors by ethanol during C2C12 differentiation I examined the downstream signaling pathways that were being altered to inhibit differentiation. I performed gene expression profiling on C2C12 cells differentiating in the presence of ethanol over 3 days.

Microarray Design, Quality Control and Validation

Illumina arrays were chosen to perform transcriptional profiling. The Illumina gene expression profiling system is reported to detect mammalian poly(A+) mRNA with a specificity of 1:250,000, possess a limit of detection of 0.13 pM, and a range that extends over 3.2 logs and to be capable of detecting 1.3-fold differences with 95% confidence[99].

The microarray design chosen to study C2C12 cells undergoing differentiation consisted of 4 biological replicates in growth medium to serve as a reference set, 4 samples each in control DM and in DM containing 100mM ethanol on day 1, and 3 samples per group for the remaining 2 days. This gave a total of 24 arrays. The Illumina MouseRef-8v2.0 expression BeadChip array is derived from NCBI RefSeq database (build 36, release 22) and supplemented with probes derived from the Mouse Exonic Evidence Based Oligonucleotide (MEEBO) set as well as exemplar protein-coding sequences described in the RIKEN FANTOM2 database. The array targets 25,600 well-annotated RefSeq transcripts and over 19,100 unique genes.

To determine the focused effects of an agent on gene expression depends on limiting the number of confounding variables which might stimulate gene expression independently of the agent's effect[100, 101]. To ensure uniformity of array samples, 9 biological replicates of C2C12 cells undergoing differentiation, with, and without ethanol, and reference samples (63 samples total) were evaluated for the abundance of MyoD and myogenin. I also evaluated the samples for GAPDH abundance since I had observed that ethanol reduced

GAPDH levels early in differentiation which might suggest regulation of GAPDH by ethanol. It has recently been reported that ethanol increases levels of GAPDH to cause cellular damage in neuronal cells[102].

Samples were chosen to be included on the array if they passed three criteria for uniformity. The first was that the abundance of the gene of interest normalized to beta-actin in the sample had to be within one standard deviation of the mean. The second criterion was that the raw mRNA quantity of the sample before normalization to beta-actin had to be within one standard deviation of the average. The final test was visual inspection of the replicates for closeness of fit to each other on the x and y axes. Samples that passed all three criteria were chosen to undergo microarray analysis. Prior to microarray analysis the samples were evaluated for RNA quality by microcapillary electrophoresis with the Agilent Bioanalyzer [90]. A representative set of samples are shown in **figure 4.4a&b.** The 28S peak is twice the height of the 18S peak (**figure 4.4a**) and the virtual gel (**figure 4.4b**) depicts the same results. The RNA analysis algorithm also generates RNA Integrity Numbers (RIN), a score that measures the intactness of RNA samples and is based on total RNA ratio, height of the 18S peak, the fast area ratio and the height of the lower marker[90]. All samples had RNA Integrity Numbers (RIN) of 10 which is the highest score on the scale demonstrating that the RNA samples were intact. The raw data from the microarrays are depicted in the form of a box plot (**figure 4.4c**). Box plots are used to see the variation within an array and between arrays.
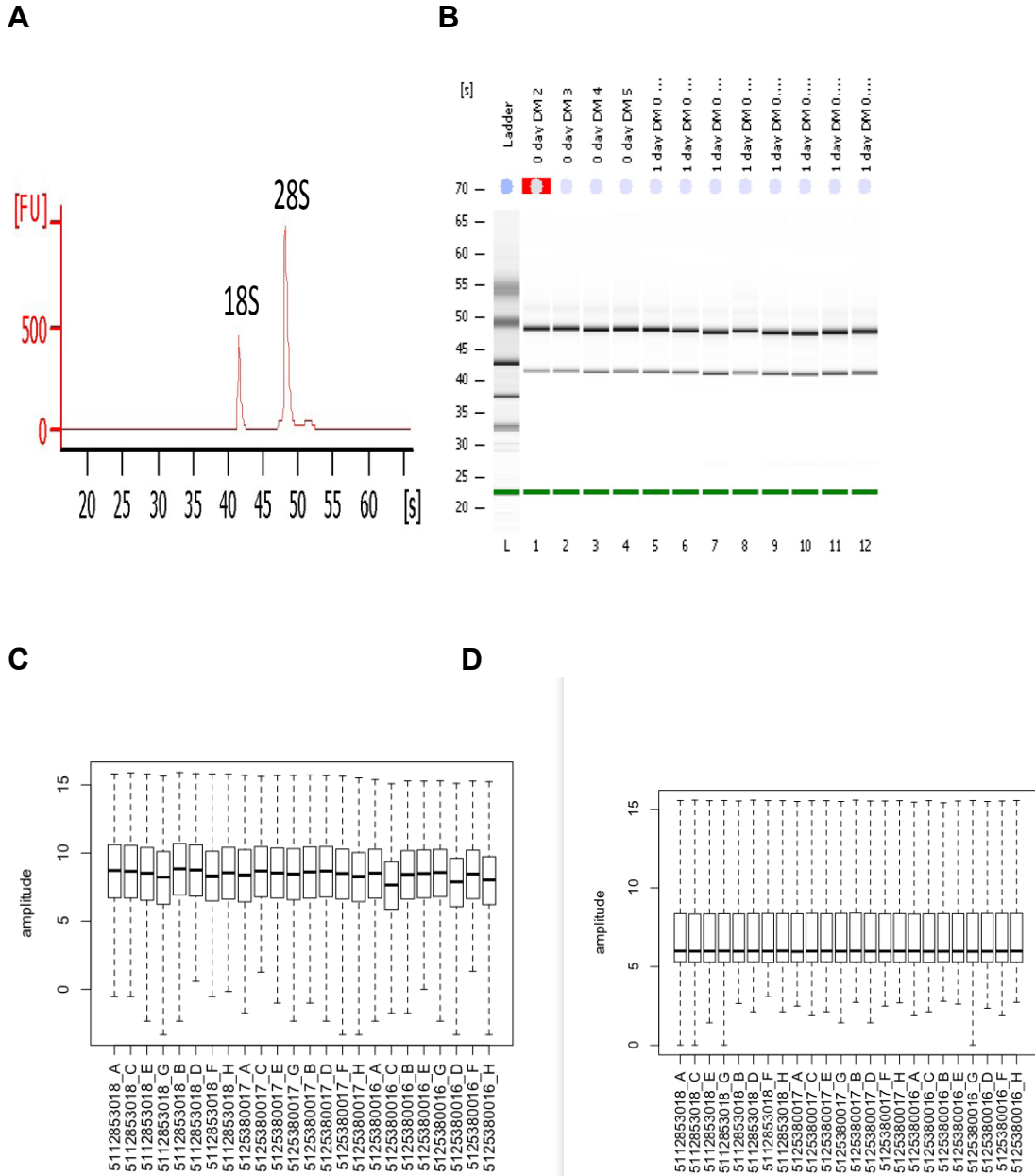
Figure 4.4: RNA quality and microarray data are acceptable. (A) A chromatogram of micro-capillary electrophoresis from an RNA sample depicting clearly visible 28S and 18S peaks. (B) Virtual gel generated from the electropherograms showing the 28S and 18S bands and a molecular sizing marker. Box Plot of microarray data showing the log-transformed signal intensities with the median depicted by a horizontal black line (C) before normalization (D) after quantile normalization to remove technical variation.

The median (depicted by the vertical line) shows that the signal intensities within and between the arrays are nearly equal and therefore display a normal distribution. The normalized data is shown in **figure 4.4d.** These data indicate that the quality of the RNA and the microarray data are excellent.

Next I confirmed that the expression between qPCR and microarray values for MyoD and myogenin correlated with each other throughout the time course (**figure 4.5**). The values correlated well showing a pearson r=0.84 (0.56, 0.92), p<0.0001 for MyoD and r=0.68 (0.31, 0.87), p=0.002 for myogenin. These results suggest that the array will be capable of identifying the differential gene signatures between control and ethanol treated cells during differentiation that correlate with reduced MyoD and myogenin expression.

I used Ingenuity Pathway Analysis (IPA) software to analyze the microarray results. I confirmed that the transcripts which were induced during C2C12 myoblast differentiation correlated with well-known muscle specific genes (**table 4.3**). The early events of quantity of muscle cells and myogenesis were significantly associated (0.001<p<0.007) with transcripts induced during the first day of C2C12 differentiation. On day 2 as the differentiation program progressed the induced transcripts during C2C12 differentiation correlated with transcripts associated with later events in muscular development such as aggregation of myoblasts and myofiber maturation (0.001<p<0.01). On day 3 transcripts associated with the even later events of muscle contraction were induced during C2C12 differentiation (0.01<p<0.04).

A
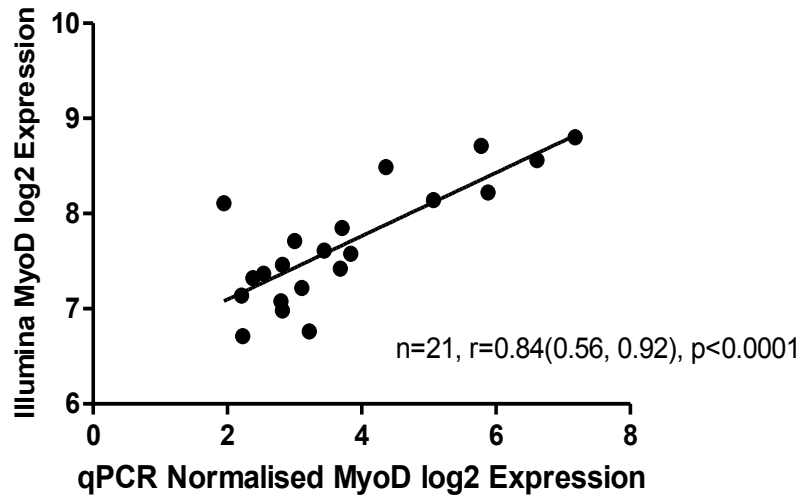
B
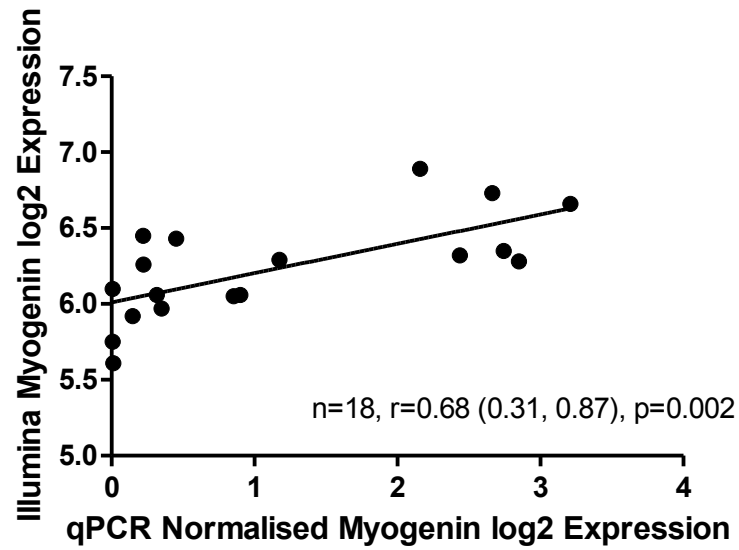
Figure 4.5: qPCR and microarray values correlate with each other. The log2 expression values for day 0-3 +/- EtOH between Illumina log2 values for (A) MyoD and (B) myogenin were correlated to qPCR beta-actin normalized values.

Table 4.3: The muscular development pathway is associated with transcripts induced during C2C12 differentiation

Day	Selected Functions	p-value range
1	Quantity of muscle cells, myogenesis	0.001-0.007
2	Aggregation of myoblasts and muscle cells, maturation of myofiber	0.001-0.01
3	Maturation of myofibers, quantity of skeletal muscle, contraction of skeletal muscle	0.01-0.04

Transcripts which were significantly changed (fold-change = ± 1.22, p≤0.05) during differentiation compared to growth medium were analyzed using Ingenuity Pathway Analysis (IPA) software and found to be significantly associated with the muscular development function containing functionally-characterized mammalian molecules.

These results demonstrate that the transcriptional profiles of differentiating C2C12 cells are well correlated with the expression of muscle specific genes suggesting that the effects of ethanol on differentiating C2C12 cells will be effectively identified by the microarray.

Focused Analysis of Ethanol regulated transcripts common to all days

There were 25, 697 probes on the array. 11, 574 - 11, 831 probes displayed an acceptable range of fluorescent intensity and so could be reliably detected. The number of probes which were consistently altered by ethanol administration during C2C12 differentiation and which showed a fold-change difference of ± 1.22, $p \leq 0.05$ ranged from 839-1473. These probes were entered into IPA to identify transcripts in common on all days. This analysis yielded 46 genes which displayed consistent performance on all days of differentiation, whose detection p-values I confirmed and whose sequences I confirmed by BLAST. I next confirmed by qPCR the expression of five genes present from this list that showed the most differential expression with ethanol on all days (**figure 4.6**). I found significant correlation for expression of the genes (Atf3, Mgp, Myl1, Hes1 and Hey1) by linear regression analysis ($r>0.07$, $p<0.0001$).

Hierarchical Clustering

I performed hierarchical clustering analysis of the 46 transcripts altered by ethanol treatment to find patterns in the data (**figure 4.7**). The transcripts on day 1 with and without ethanol clustered together. The transcripts on days 2 and 3 in DM clustered together and the transcripts which were affected by ethanol on
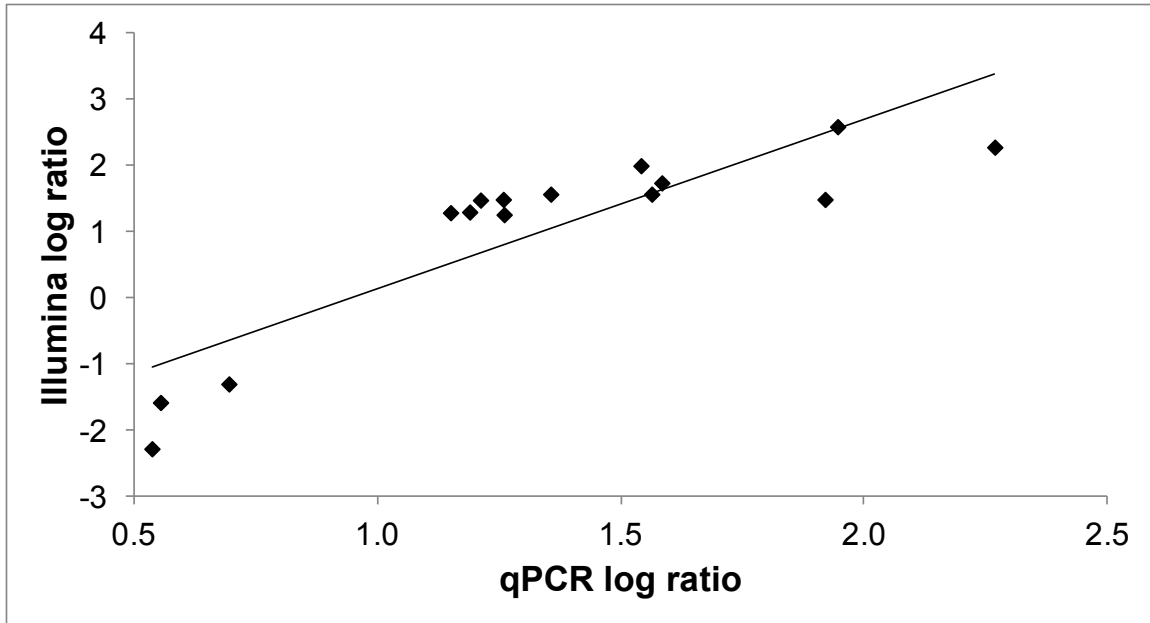
Figure 4.6: Microarray log2 fold differences correlate with qPCR log10 fold differences. Log ratios from the microarray compared with qPCR. Five genes (Atf3, Myl1, Hes-1, Hey-1 and Mgp) which showed ± 1.22 fold-change (p≤0.05) on the microarray were assayed by qPCR. Linear regression analysis yielded r>0.7, p<0.0001. Expression is relative to untreated controls (n=3).
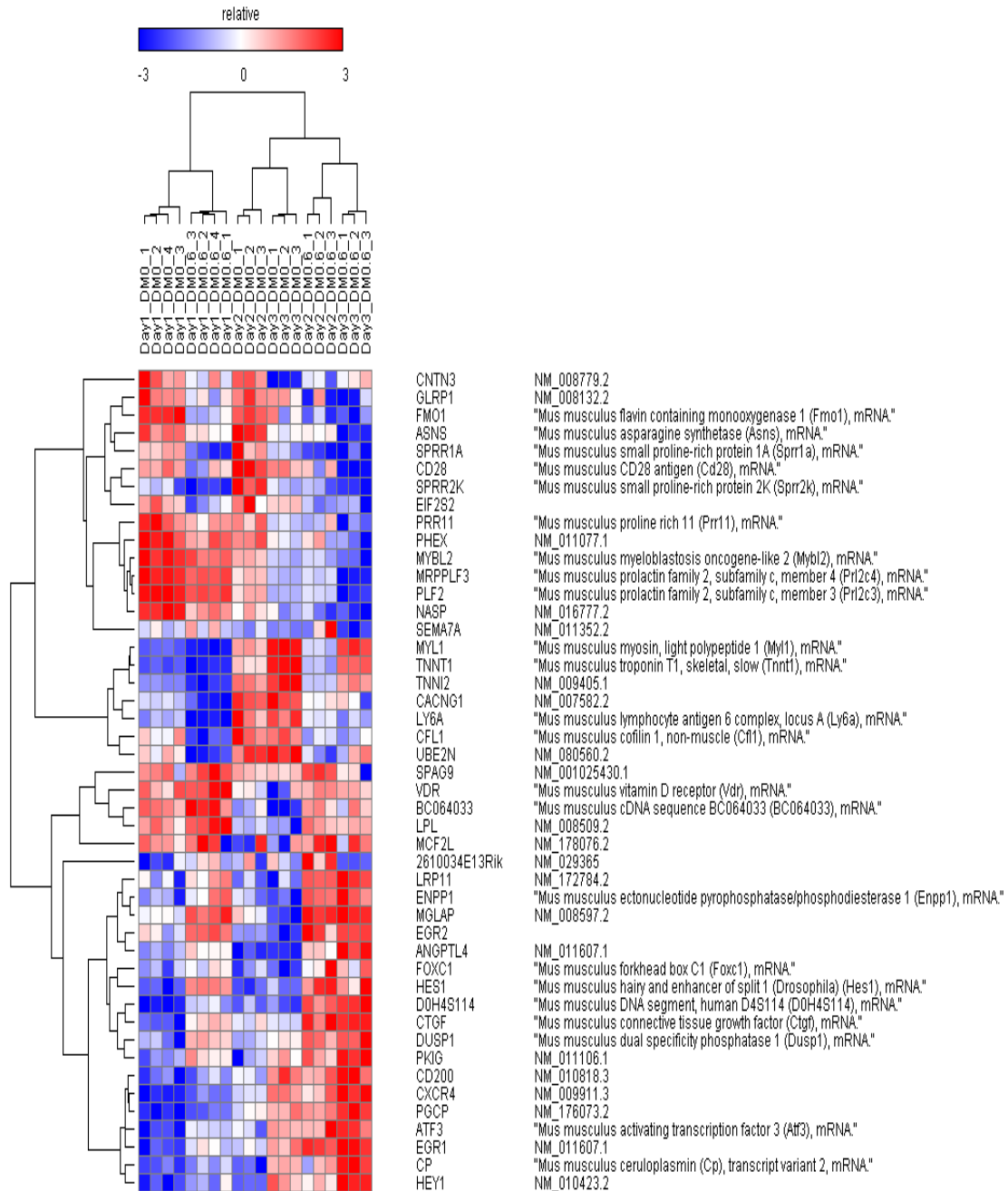
Figure 4.7: Transcriptional profile of ethanol on differentiating C2C12 Cells.
Expression values for the 46 transcripts which were identified to be differentially expressed between ethanol treated and control cells on all days of differentiation by IPA were inputted into GENE-E software (Broad) which used Spearman's rank correlation coefficient to cluster the transcripts.

days 2 and 3 clustered together. Although clustering can find major patterns in the data, it may not always correspond to changes on a phenotypic level[103]. Regardless, it was interesting to see that Myl1, Tnnt1 and Tnni2 clustered together. Bergstrom (2002) studied genes regulated by MyoD protein using expression arrays and reported that Tnni2 was increased in two sets of arrays, one where MyoD protein was induced using a MyoD-estrogen receptor hormone binding domain fusion protein stably expressed in MyoD-/-, Myf5-/- mouse embryonic fibroblasts and another in which intermediate protein synthesis of MyoD was prevented using cycloheximide[104]. De la Serna (2005) performed microarrays where mouse B22 cells were infected with MyoD producing retrovirus and also showed induction of Tnni2 transcript[105]. Di Padova (2007) performed microarrays where MyoD protein or its non-acetylatable version was induced in mouse embryonic fibroblasts (Myf5-/-, MyoD-/-) and found that Tnnt1 transcript was induced 56-fold by MyoD protein and in cells containing the non-acetylatable version, TnnT1 transcript was induced only 2.6-fold[106]. Muthuchamy (1992) reported the induction of Myl1 mRNA in rat myoblasts which transiently expressed exogenous MyoD1[107]. On each consecutive day in ethanol containing differentiation medium, the fold-change (FC) of Myl1 (-1.59 (p=1.75 X 10^{-5}); -2.29 (p=6.64 X 10^{-5}); -1.31 (p=0.01)), Tnnt1 (-1.32 (p=0.002); -1.78 (p=4.42 X 10^{-4}); -1.50 (p=4.27 X 10^{-4})) and Tnni2 (-1.50, (p=8.53X10^{-5}); -2.08 (p=4.19X10^{-5}); -1.66 (p=4.15 X 10^{-4})) was always lower compared to control medium over all three days (**figure 4.7**). These results suggest that

reduction of MyoD by ethanol may be the cause for the reductions seen in these transcripts.

Upstream Regulator Analysis

The 46 genes that were identified as being significantly differentially regulated by ethanol on all days of C2C12 differentiation were submitted into IPA to identify which MRF(s) could be mediating the observed effects. The upstream regulator analysis in IPA predicted that MyoD1 transcription factor was regulated by ethanol with a p-value of 8.7×10^{-4}.

Canonical Pathway Analysis

Pathway analysis has been suggested to do a satisfactory job of finding correlated sets of genes[108]. The canonical pathways in IPA are well-known metabolic and cell signaling pathways which have been curated and drawn by Ph.D. level scientists[65]. They are generated prior to data input, do not change upon data input and have directionality[65]. The source of the information contained in canonical pathways come from both specific and review journal articles, text books and KEGG ligand which contains knowledge on chemical substances and reactions important to life[65]. The canonical pathways predicted to be associated with ethanol during all days of C2C12 differentiation included calcium signaling ($p=1.25 \times 10^{-3}$), role of tissue factor in cancer ($p=2.98 \times 10^{-3}$), Notch signaling ($p=4.35 \times 10^{-3}$), semaphorin signaling in neurons ($p=8.02 \times 10^{-3}$), and CXCR4 signaling ($p=8.37 \times 10^{-3}$) (**table 4.4**). The ratio gives a representation of the percentage of genes in a pathway which are also present on an uploaded list, higher ratios represent pathways which have been affected

the most based on the genes in the IPA universe[65]. Up or down-regulation of a pathway is not predicted based on the significance or the ratio values, rather the function of the genes must be assessed to determine whether a pathway is up or down-regulated[65]. The pathway that displayed the highest ratio was Notch signaling with a value of 0.047 suggesting that of the pathways identified as being modulated by ethanol, Notch signaling is most affected during C2C12 differentiation. The fold-change (FC) of the Notch effectors on each day of differentiation, Hey-1(1.29 (p=0.008); (1.47 (p=0.002); 1.28 (p=0.02)) and Hes-1 (2.00 (p=4.94 X 10^{-7}); (2.27 (4.53 X 10^{-5}); 1.73 (p=0.003)) was increased by ethanol suggesting activation of the Notch signaling pathway. Activation of Notch signaling inhibits myogenesis and the differentiation of C2C12 cells [16].

Transcripts associated with calcium signaling pathway were reduced by ethanol. Three of the genes identified are markers of late differentiation and code for proteins involved in constructing the contractile apparatus[83] i.e. Myl1, Tnni2, Tnnt1 and one is an L-type calcium channel gene, Cacng1 ((days 1-3_FC-Ctrl-vs-EtOH: -1.46 (p=1.11 X 10^{-4}); -1.47 (p=0.002); -1.73 (p=0.003)) which is important for contraction and expressed late in differentiation[83]. Reducing intracellular calcium levels during C2C12 differentiation either by blocking L-type channels has been reported to inhibit the expression of myogenin, myosin heavy chain and myotube formation[109]. These results suggest that ethanol may interfere with calcium signaling to inhibit differentiation.

Table 4.4: Canonical pathways predicted to be altered by ethanol throughout C2C12 differentiation

Name	p-value	Ratio
Calcium Signaling	1.25E-03	4/207 (0.012)
Role of Tissue Factor in Cancer	2.98E-03	3/114 (0.026)
Notch Signaling	4.35E-03	2/43 (0.047)
Semaphorin Signaling in Neurons	8.02E-03	2/52 (0.038)
CXCR4 Signaling	8.37E-03	3/169 (0.018)

Microarray results were processed through IPA software to identify canonical pathways most significantly affected by ethanol. P-values represent the statistical association of differentially expressed genes in the dataset to all genes in the IPA universe and calculated using right-tailed Fisher's Exact Test. The ratio represents the number of molecules in the dataset in relation to molecules known to participate in the signaling pathway.

CXCR4 signaling was implicated as being regulated by ethanol during differentiation by the up-regulation of chemokine receptor 4, Cxcr4 (days 1-3_FC-Ctrl-vs-EtOH: 1.31 (p=0.001); 1.44 (p=0.02); 1.39 (p=0.003)), early growth response 1, Egr1(1.33 (p=7.22 X 10^{-4}); 1.44 (0.003); 1.24 (p=0.02)) and down-regulation of Myl1 (myosin light polypeptide 1). Activation of CXCR4 signaling inhibits C2C12 and primary myoblast differentiation [110-112]. Satellite cells express Cxcr4 on their surface and it has recently been shown that C2C12 cells express a functional CXCR4 receptor [110, 113]. Activation of CXCR4 signaling by administering its ligand, SDF-1 (CXCL12) to C2C12 cells has been shown to inhibit the differentiation of C2C12 cells by inhibiting MyoD protein, myogenin transcription and MHC expression[110]. Inhibiting the CXCR4 receptor with an antagonist, AMD3100, prevents SDF from inhibiting myogenic differentiation [110]. Blocking CXCR4 with an antagonist or siRNA at the start of differentiation decreased the myogenic fusion index in primary mouse myoblasts[111]. It has been reported that muscle regeneration is associated with re-expression of CXCR4 in the mdx mice[112]. These results suggest that up-regulation of CXCR4 by ethanol may be activating the CXCR4 signaling pathway to block the differentiation of C2C12 cells to allow the expansion of satellite cells. Later on during differentiation, endogenous levels of CXCR4 signaling may be necessary for proper fusion events.

Two independent studies performed in neurons and bone marrow cells demonstrated that activation of CXCR4 signaling increases transcription of Egr1[114, 115]. With regards to Myl1, activation of CXCR4 signaling by SDF has

been reported to increase the phosphorylation of myosin light chain and increase cell migration towards SDF-1 via Rho signaling[116]. Since I saw a reduction in Myl1 by ethanol this might suggest that CXCR4 signaling through Rho kinase is not the mechanism by which CXCR4 signaling may be regulated by ethanol or that Myl1 down-regulation might not be due to CXCR4 signaling but may instead be due to reduced calcium signaling.

The combined results from hierarchical clustering analysis, IPA upstream regulator analysis and canonical pathway analysis support and extend my previous findings that ethanol reduces MyoD transcript levels and strongly suggests that this decrease translates into a corresponding reduction in protein level and/or functionality to cause down-regulation and/or inefficient activation of MyoD targets to inhibit C2C12 differentiation.

Analysis of the effects of Ethanol on each day of differentiation

Since I had compressed the data from all three days to identify the major pathways which contribute to the inhibition of C2C12 differentiation throughout the time course, there was value to identify the major events affected by the MyoD and the other MRFs which were occurring on each day of differentiation in response to ethanol. Using IPA I analyzed the effects of ethanol on each day of differentiation. **Table 4.5** shows pathways within the top five canonical pathways from each day which play roles in myoblast differentiation and which are predicted to be regulated by ethanol.

Table 4.5: Canonical pathways predicted to be altered by ethanol on each day of differentiation.

Day	Signaling Pathway	p-value	Ratio
1	ILK	2.6E-04	17/193 (0.226)
1	P38 MAPK	5.34E-04	12/106 (0.113)
2	ERK/MAPK	7.7E-05	27/204 (0.132)
3	ILK	1.58E-06	27/193 (0.14)
3	VEGF	1.13E-05	16/99 (0.162)

ILK Signaling

On days 1 and 3 the ILK signaling pathway is significantly associated with ethanol with p-values of 2.6 X 10^{-4} and 1.58 X 10^{-6} respectively. Signaling via the integrins is necessary for myogenesis[117]. Over-expression of ILK blocks the differentiation of C2C12 cells by activating Erk whose down-regulation is necessary for expression of myogenin[118]. Over-expression of ILK has been reported to inhibit MyoD, myogenin, MHC and myotube fusion[118]. The role of ILK signaling has recently been confirmed to be important in myotube fusion since knockdown of Kindlin-2, a binding partner of β1-integrin inhibits the myotube fusion index in C2C12 cells and MHC but does not inhibit myogenin expression[119]. Since ILK signaling appears significantly associated with ethanol early in differentiation (day 1) and later in differentiation (day 3) this suggests that ethanol may be modulating ILK signaling to inhibit both early and terminal events that require the up-regulation of MyoD and myogenin during differentiation.

p38 Signaling

The p38 signaling pathway plays an important role in expression of muscle structural genes [12, 27]. p38 kinase phosphorylates the transactivation domain of Mef2 and its required for gene expression at the late phases of myogenesis[12].

On day 1 the p38 pathway was associated with regulation by ethanol with a p-value of 5.34 X 10^{-4} and a ratio of 0.109 (**table 4.5**). IPA uses a systems biology approach to make its predictions. **Figure 4.8** depicts a diagram of the

p38 MAPK Signaling
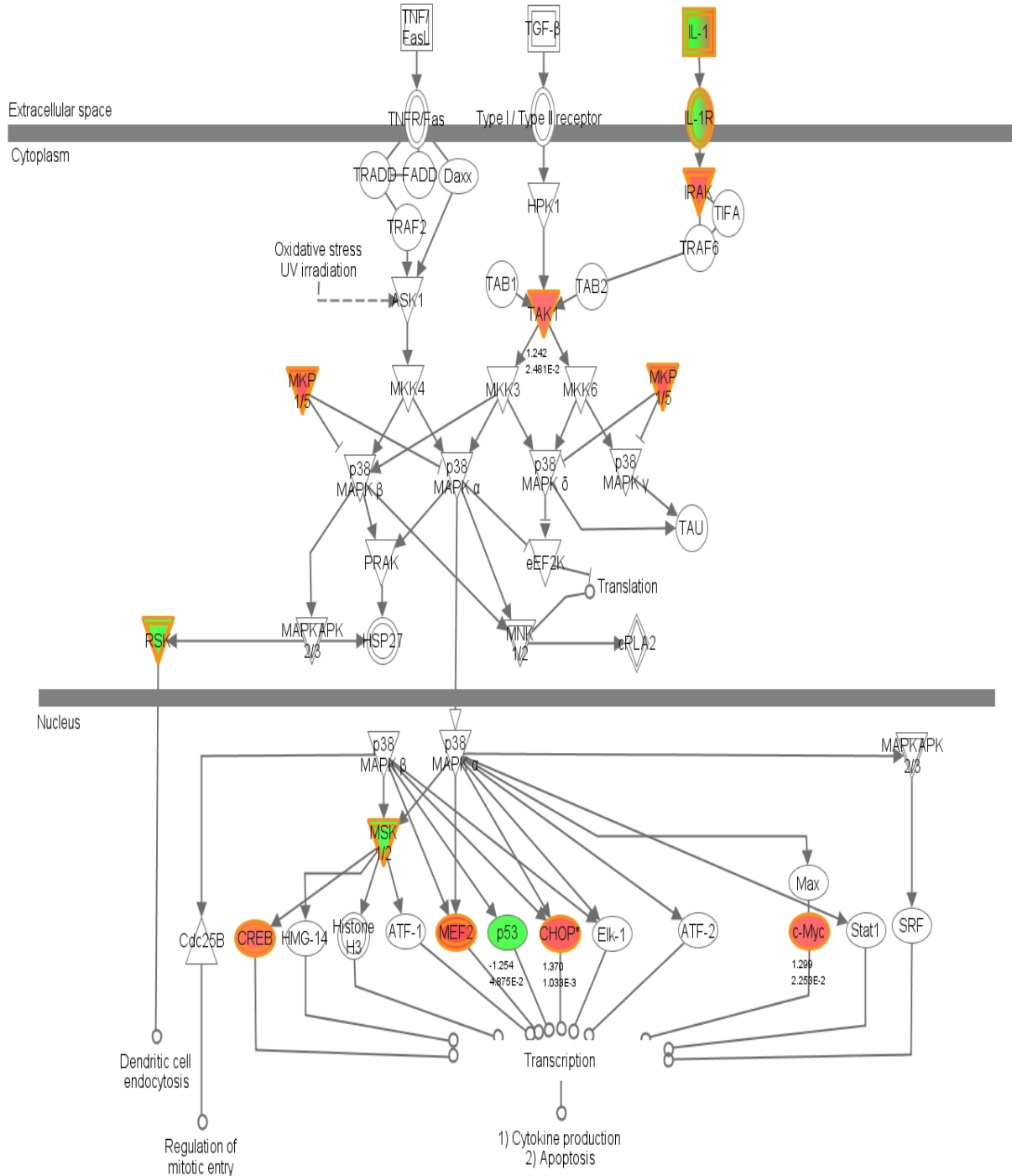
Figure 4.8: Ethanol modulation of the Ingenuity p38 Signaling canonical pathway on day 1 of differentiation. Ingenuity software overlaid fold-change values of ethanol/control from Day 1 DM onto a pre-derived pathway. Red= over-expressed gene in ethanol versus control, green = under-expressed.

canonical pathway drawn by IPA with the overlaid significant fold-change values from the dataset where available. Transcripts whose expression is increased by ethanol are colored red, and transcripts which show decreased expression in the presence of ethanol are colored green. Colored molecules which display no value represent a group of molecules where one member was present on the array, and the group is colored to represent that member's fold-change value. The results show that p38 signaling is modulated by ethanol in a context which is specific to myoblast differentiation and this information may yield novel hypotheses. Stepping back for a moment to look at the picture in its entirety suggests that ethanol activates p38 during C2C12 differentiation based on the increased number of red molecules. Activation of p38 signaling would be expected to accelerate differentiation.

The p38 pathway is necessary for the differentiation of C2C12 cells since myotube formation is inhibited when differentiating cells are treated with a p38 inhibitor or when differentiating C2C12 cells express a dominant-negative version of a p38 activator (MKK3)[94]. Inhibition of p38 signaling also causes significant decreases in MyoD and myogenin expression[94, 120]. The p38 pathway is also activated by cellular stresses and pro-inflammatory cytokines[121] which suggests that ethanol induced stress might activate the pathway. Therefore the identification of IL-1 signaling as potentially being increased by ethanol and thus leading to the activation of p38 signaling is a plausible event. However it has been reported that alcohol administration to growing C2C12 myocytes for 24 hours inhibits p38

phosphorylation and thus its activation[122]. The prediction by IPA that p38 is activated suggests that this is specific to ethanol during differentiation.

TAK1 kinase (TGF-β-activated kinase 1) is up-regulated by ethanol during differentiation. Inactivation of TAK1 by knockdown or a dominant negative form of TAK1 reduces proliferation of cells, reduces levels of Myf5, MyoD and myogenin and modestly reduces levels of Mef2d during differentiation[123]. TAK1 deficient MEFs do not differentiate in response to ectopically expressed MyoD but they can be rescued by over-expression of a constitutively active mutant of MAPK kinase 6 (MKK6) which activates p38 MAPK[123]. The importance of TAK1 for C2C12 differentiation was confirmed by knocking down TAK1 which decreased differentiation, and over-expression of TAK1 enhanced it[124]. This was assessed by observing increased levels of myogenin, MHC and TnT, and by the presence of increased number of myotubes containing 6+ nuclei as well as increased activation of p38MAPK[124]. In regenerating muscle TAK1 expression is increased along with levels of myogenin and MyoD[123]. Since the expression of TAK1 is increased by ethanol in differentiating C2C12 cells this may suggest activation of the p38 pathway but since MyoD and myogenin are reduced by ethanol (**figure 4.3b, c**) this effect may be independent of them. The software predicts that within the nucleus ethanol activation of p38α and β leads to induction of Mef2d transcription (fold-change = 1.53, p=2.77 X 10^{-4}). I saw an increase in another member of the Mef2 group, Mef2c (**figure 4.3d**) in response to ethanol. p38 directly phosphorylates Mef2c which is necessary for its transcriptional activity during differentiation and potentially for its own

transcription [121]. Mef2d was shown to be important together with MyoD to induce MyoD-late genes[121]. Constitutive activation of p38 signaling in C2C12 cells induces precocious differentiation by shifting expression of late-activated structural genes to earlier stages[120, 121]. Over-expression of the p38 activator in growing C2C12 cells causes higher levels of MyoD protein to be expressed compared to vector and earlier and stronger expression of myogenin and MHC[120]. Mef2 expression can also be activated by myogenin independently of MyoD[97] which might suggest that the increase seen in Mef2c is independent of p38 signaling. At any rate, activation of Mef2 transcription by ethanol could be shifting the expression of the structural genes earlier. Elevated Mef2c transcripts are detected in muscle from patients with myotonic dystrophy types I and II[125] so the significance of increased Mef2 transcription by ethanol during C2C12 differentiation needs to be investigated functionally and whether the mechanism for the increase in Mef2c is due to p38 signaling or due to myogenin.

The IPA pathway suggested that p53 down-regulation by ethanol is mediated by p38 MAPK β signaling. p53 mRNA levels are reduced 1.25-fold (p=0.05) by ethanol. Ethanol fed rats display no change in levels of p53 mRNA in their muscles[126]. p53 mRNA and protein levels have been reported to increase during C2C12 differentiation and interfering with the wild-type protein by transfecting a dominant-negative version inhibits their differentiation into myotubes[127, 128]. Transducing TP53 or Rb genes in p53-/- myoblasts has been reported to rescue differentiation by restoring MyoD activity[128]. These results suggest that the p53 down-regulation by ethanol may be associated with

inhibition of differentiation but this would need to be tested and whether this effect is mediated through p38.

CHOP (Stress-Induced C/EBP Homology Protein) was up-regulated by ethanol during differentiation with a fold-change increase of 1.37 (p=1.03 X 10^{-3}). This was predicted to be mediated by p38 MAPK α signaling. CHOP has been reported to down-regulate MyoD in the reserve cells within C2C12 cultures and prevent their premature differentiation[93]. Knocking down CHOP with shRNA in C2C12 cells induced earlier and stronger expression of myogenin and MHC and the myotubes which formed contained more nuclei[93]. The converse experiment of retrovirally transducing CHOP in C2C12 cells led to reductions in myogenin and MHC and the myotubes which formed contained fewer nuclei[93]. C2C12 cells which express CHOP do not express MyoD or myogenin[93]. The increased levels of CHOP by ethanol may correlate with reduced levels of MyoD. Ethanol may be increasing the number of reserve cells on day 1 of differentiation which are expressing higher levels of CHOP and lower levels of MyoD.

c-myc was up-regulated 1.3 fold by ethanol (p=0.02) and this increase was predicted to be mediated via p38 signaling. c-myc mRNA has been reported to be increased in muscle from female rats fed chronically with ethanol[126]. c-myc mRNA is down-regulated during C2C12 differentiation[70, 129]. Transforming C2C12 cells with c-myc and shifting them to low serum medium was shown to cause cell death of some cells but those which escaped death were able to differentiate into myotubes containing one nucleus, and they demonstrated a fusion defect[130]. Pending further investigation, the increase seen in c-myc

mRNA might suggest that C2C12 differentiation is inhibited by the loss of uncommitted cells (Myf5- or MyoD-) by cell death or by a fusion defect caused by up-regulation of c-myc.

VEGF Signaling

IPA predicted that ethanol altered signaling through VEGF receptors during C2C12 differentiation in part by decreasing signaling to cause reductions in expression of downstream targets important in cell survival and in part by increasing signaling to increase expression of a down-stream target to increase cell proliferation. During myogenesis, stimulation of VEGF signaling during C2C12 differentiation is reported to increase differentiation and promote myotube hypertrophy presumably through an autocrine mechanism [63]. MyoD was shown to physically interact with the VEGF promoter using the technique of chromatin immunoprecipitation and expression of a dominant-negative version of MyoD in C2C12 cells reduced isoform expression of VEGF[63]. Inhibiting VEGF signaling during C2C12 differentiation reduced MRF expression, blocked myogenic differentiation and caused myotube hypotrophy[63]. These results suggest that the down-regulation of MyoD by ethanol may be modulating VEGF signaling to inhibit differentiation.

To summarize, I was able to identify that canonical pathways important in differentiation are predicted to be affected by ethanol. Over-expression and/or abrogation of these pathways have been shown to cause down-regulation of MyoD and/or myogenin and to inhibit myoblast differentiation. My results show

that the down-regulation of MyoD and myogenin by ethanol is translatable to alterations in signaling pathways which may inhibit C2C12 differentiation.

Upstream Regulator Analysis

The IPA upstream regulator analysis makes predictions on which transcription factors could be causing the expression changes seen in the dataset by assigning a z-score[66]. This analysis is based on knowledge mined from the literature between target genes and upstream regulators stored within the Ingenuity database[66]. When the direction of change is compatible with the literature across most of the genes then the upstream regulator is predicted to be activated or inhibited[66]. If there is no clear pattern, there is no z-score and no prediction. The analysis also assigns an overlap p-value that finds instances of statistically significant overlap between an upstream regulator and a list of targets whose levels are changed in the experimental condition[66]. **Table 4.6** shows selected transcriptional regulators predicted to be associated with ethanol during C2C12 differentiation. MyoD1 was associated with ethanol on all three days with p-values ranging from 8.31×10^{-5} to 3.65×10^{-8}. The regulation z score trended towards inhibition of MyoD1 by ethanol on day 3. MyoD activates its own transcription [131, 132] therefore direct ethanol inhibition of MyoD itself may inhibit MyoD and its targets. Since this inhibitory effect is most evident on day 3, this suggests that the initial down-regulation of MyoD on day 1 leads to increasing reduction of MyoD protein/functionality on day 2 which leads to even more decrease in MyoD protein/functionality on day 3. On day 3, of differentiation myogenin is associated with ethanol ($p = 7.5 \times 10^{-3}$) with a.

Table 4.6: Transcriptional regulators predicted to be associated with transcripts perturbed by ethanol.

Day	Fold Change	Transcription Regulator	Predicted	Regulation z-score	p-value of overlap
1	-1.22	MYOD1		-0.11	8.31×10^{-5}
2		MYOD1		-0.19	3.65×10^{-8}
3	-1.52	MYOD1		-1.20	1.53×10^{-7}
3	1.36	MYOG		1.33	7.50×10^{-3}
1		PAX3			3.22×10^{-2}
2		PAX3		1.32	1.51×10^{-3}
3		PAX3		-1.07	2.17×10^{-6}
2		PAX7		0.63	2.58×10^{-3}
1		Notch		1.92	1.14×10^{-1}
2		Notch	Activated	2.35	3.65×10^{-3}
3		Notch		0.50	1.12×10^{-2}
1		NOTCH1		1.94	1.88×10^{-2}
2		NOTCH1		1.51	1.15×10^{-5}
3	-1.40	NOTCH1		0.18	5.82×10^{-5}
2		NOTCH3		-0.67	2.19×10^{-2}
3	-1.22	NOTCH4		1.43	1.48×10^{-3}
1		MAML1			3.25×10^{-2}
3		MAML1			4.39×10^{-3}
1		RBPJ		1.926	4.37×10^{-2}
2		RBPJ	Activated	2.031	2.36×10^{-1}
3		RBPJ		0.649	2.58×10^{-3}

Microarray results were processed through IPA software to identify transcription factors significantly affected by ethanol. P-values represent the statistical association of differentially expressed genes in the dataset to all genes in the IPA universe and calculated using right-tailed Fisher's Exact Test. A regulation z-score is predicted to be significantly activated if ≥2 and inhibited if ≤ 2.

prediction trending towards activation. This suggests that myogenin activation

compensates for MyoD inhibition during ethanol mediated C2C12 differentiation

Pax3 was associated with ethanol on all three days with p-values ranging from

3.22×10^{-2} to 2.17×10^{-6}. On day 2, Pax3 was predicted to be slightly activated

by ethanol and predicted to be slightly inhibited by ethanol on day 3. Over-

expression of Pax3 inhibits C2C12 differentiation, and prevents MyoD induced

differentiation but does not prevent myogenin induced differentiation in fibroblasts

cultured in low serum[133]. Retroviral transduction of Pax3 into C2C12 cells

increased cell proliferation and delayed differentiation but differentiation still

proceeded to the myotube stage[134]. However the myotubes

were thinner than in controls[134]. Pax3 over-expression led to increased

numbers of MyoD expressing cells but there was no increase in the

transcriptional levels of MyoD suggesting increased protein stability was involved

[134]. The expression of a dominant-negative version of Pax3 inhibited Myf5,

MyoD and myogenin and prevented C2C12 differentiation in low serum[134].

However the reserve cells did not express Pax3 but did express Pax7[134]. It

has been suggested that Pax3 expression may be transiently increased not only

to allow cells to proliferate and expand the satellite cell pool in response to injury

but also to cause satellite cell commitment to differentiation but that

differentiation only proceeds once the inhibitory Pax3 signal is alleviated[134].

Pax3 is important in embryonic development for the migration of myogenic

precursor cells into limb buds and for stimulating proliferation which expands the

pool of myogenic progenitor cells [36]. The role of Pax3 in adult regenerative

myogenesis is still being delineated however it does seem to be important for commitment to myogenic lineage since mesenchymal stem cells which over-express Pax3 differentiate towards the myogenic lineage[135]. These results suggest that Pax3 activation by ethanol may repress MyoD driven differentiation and promote myogenin driven differentiation. This may cause an increase in the proportion of myotubes which have not or do not express MyoD and instead express myogenin. Myotubes formed primarily through myogenin expression may display an altered phenotype/functionality compared to myotubes formed primarily through MyoD.

Pax7 is associated with ethanol on day 2, p = 2.58×10^{-3} with a regulation z-score trending towards activation by ethanol. A subpopulation of reserve cells within cultures of differentiating C2C12 cells have been shown to express Pax7, and not express myogenin and escape differentiation[136]. Over-expression of Pax7 and MyoD in 101T1/2 cells represses their myogenic conversion as scored by myogenin expression[136]. Within differentiating and differentiated cultures of C2C12 cells, down-regulation of MyoD has been observed in cells which over-express Pax7[136]. However another study found that retroviral expression of Pax7 in Pax7 null C2C12 cells increased the number of cells expressing MyoD but these cells were unable to differentiate into normal myotubes[137]. These conflicting studies converge on one point, namely that over-expression of Pax7 inhibits C2C12 differentiation and reduces MyoD functionality.

It may be that Pax7 is activated by ethanol on day 2 which represses MyoD driven differentiation and that Pax7 activation may signal that ethanol is causing expansion of the satellite cell pool.

Notch was predicted to be activated on day 2 by ethanol with a z score = 2.35 and an overlap p value = 3.65×10^{-3}. Notch1 was significantly associated with alcohol on all 3 days with p-values ranging from 1.88×10^{-2} to 5.82×10^{-5}. Notch 1 trended towards activation on days 1 and 2. On day 3 Notch was still associated but not predicted to be activated and on day 3 the Notch1 transcript was down-regulated by ethanol on day 3 by 1.4-fold (p=0.008). Notch3 was associated with ethanol, p = 0.02 and Notch 4 was associated with ethanol, p = 0.001 and its transcript was down-regulated 1.22 fold (p=0.03) and trended towards activation. MAML was associated with ethanol on days 1 (p=0.03) and 3 (p=0.004). RBPJ was predicted to be activated by ethanol on day 2 with a z-score of 2.03 and associated with ethanol on days 1 (p=4.37×10^{-2}) and on day 3 (p=0.003) with trends seen towards activation on day 2. Notch signaling inhibits MyoD transcription [18, 138] therefore activation of Notch signaling may inhibit MyoD and differentiation. Since activation of Notch-1 has been reported to cause myogenic progenitor cells which express Pax3 to proliferate, ethanol may be causing expansion of the satellite cell pool [36].

The results from the upstream regulator analysis suggest that the strongest inhibitory action which causes the strongest down-regulation of MyoD seen on day 3 occurs on day 2. One hypothesis which could tie these results together is that ethanol activates Notch signaling which inhibits MyoD

transcription and transient activation of Pax3 further represses MyoD. Notch

signaling and Pax3 activation would also cause expansion of the satellite cell

pool. On day 3 of differentiation MyoD levels are still decreased, but myogenin

levels and Mef2c levels are increased which suggests that differentiation is no

longer primarily mediated by MyoD but is mediated mostly by myogenin. Since

myogenin driven differentiation is reported to not be as effective as MyoD driven

differentiation this may contribute to ethanol's inhibitory effects on C2C12

differentiation.

Network Analysis

IPA generates networks of interconnected genes which may represent

significant biological function[139]. Focus genes within the dataset that interact

with molecules within the Ingenuity database are identified as network eligible

molecules and these become seeds to generate networks[137]. The first step in

generating a network is to rank the focus genes by interconnectivity with the best

connected getting the highest rank[139]. This focus gene is removed from the

list and becomes the seed to generate a network[139]. The remaining focus

genes are added to the seed gene to generate a network containing up to 35

molecules and molecules from the Ingenuity database are used to specifically

connect two or more smaller networks by merging them into a larger one[139].

The networks are scored based on the number of network eligible molecules they

contain, the higher the score the lower the probability of finding the network

eligible molecules in a given network randomly[65]. Network analysis is very

different from canonical pathway analysis in that networks are generated de novo

based on input data, do not have directionality and contain molecules that

operate in several pathways[65].

Networks formed on each day of differentiation with ethanol treatment. On

day 3, an overlapping network formed where each node contained a network and

the relationships were drawn by presence of the common genes between them

(**figure 4.9**). I subjected the list of these overlapping genes to analysis by IPA.

Pax3 was predicted to be a significantly associated upstream regulator (p=0.01).

The central network was composed of genes which function in lipid metabolism,

small molecule biochemistry and cell morphology. This network connected to the

network which contained genes involved in cellular movement, skeletal and

muscular system development and function and cardiovascular system

development and function via FMO1 (fold-change -1.46, p=0.02). di Padova

(2007) performed gene expression microarrays in Myf-/-, MyoD-/- MEFs that

were transduced with wild-type MyoD or a non-acetylatable version of MyoD at

various time points[87]. FMO1 was strongly induced after 24 hours in wild-type

and expression was reduced ~ 50% compared to the non-acetylatable version
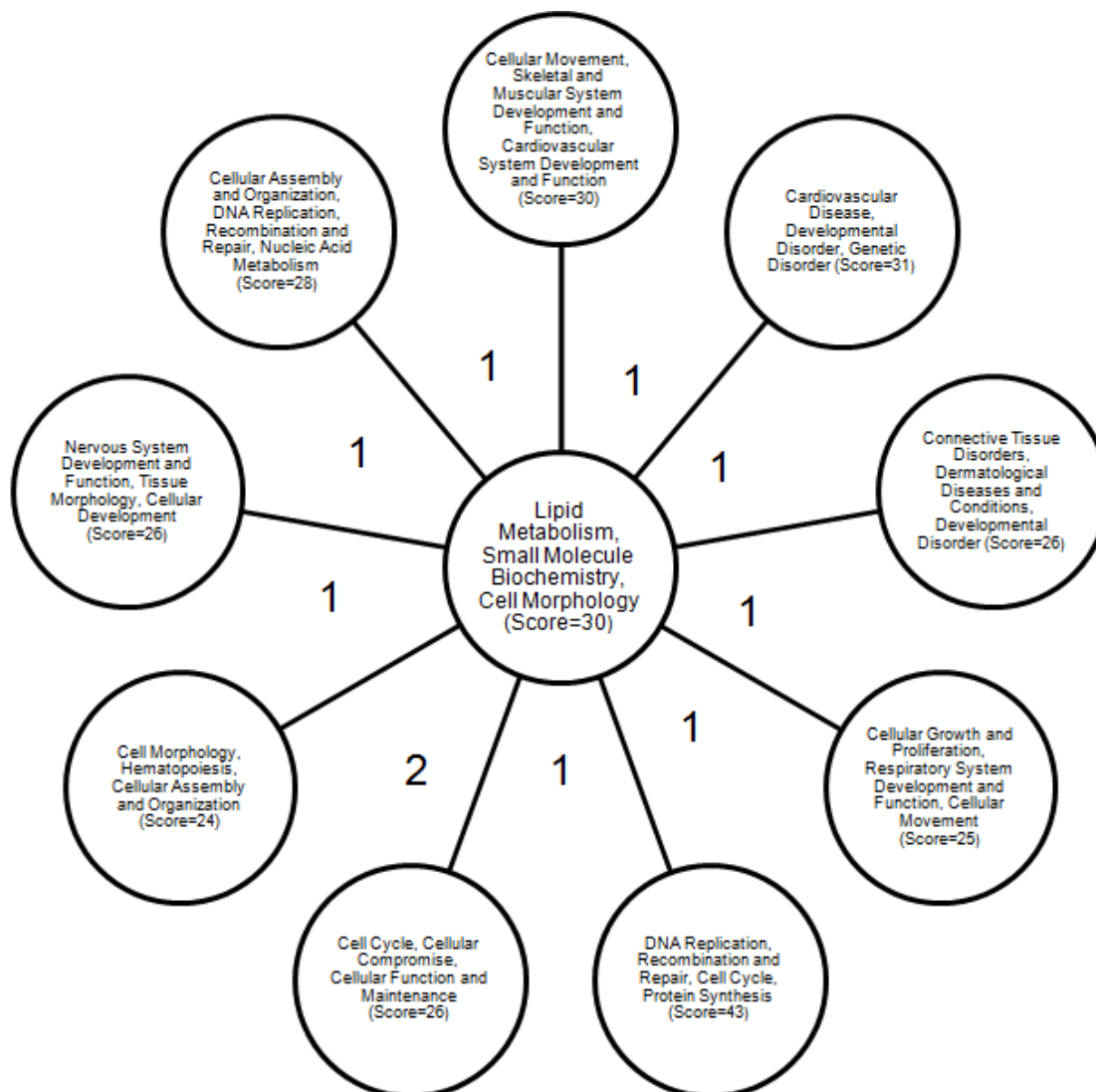
Figure 4.9: Overlapping gene networks predict reduced acetylation of MyoD by ethanol. Networks were formed from the focus genes that were differentially expressed in ethanol containing cultures on the 3rd day of differentiation using IPA. Networks were connected by genes common to both networks. The numbers represent the number of common genes. Within the bubbles are the network names which contain the top biological functions that the molecules operate in. The network scores, shown in parentheses are based on the probability of finding network eligible molecules in the network using Fisher's exact test. The network score = $-\log_{10}$ (p-value).

(Geoprofile code: GDS2854/1417429_at/Fmo1/Mus musculus)[87].   Chen

(2006) performed microarrays on C2C12 cells differentiating over 6 days and

FMO1 transcript was strongly induced in the differentiated cultures (Geoprofile

code: GDS2412/1417429_at/Fmo1/Mus musculus)[140].   These results suggest

that MyoD acetylation is impaired in C2C12 cells undergoing differentiation in the

presence of ethanol. MyoD targets might be refractory to full activation which

might contribute to impaired differentiation of C2C12 cells.

Observed Biological Trends and Biological Trend Prediction by IPA

IPA predicts the effects of gene expression changes in the dataset on

biological processes based on expected causal effects derived from the literature

and compiled in the Ingenuity database[65]. I had previously analyzed the

effects of different ethanol doses on the number of TnT- cells and TnT+ cells

during the first three days of C2C12 differentiation. If the array could predict the

cellular effects I observed then that would not only be a good validation of the

array's predictions for hypothesis generation, but also it would imply that the

array would have a high probability of identifying the factor(s) that is/are

modulated by ethanol causing inhibition of C2C12 differentiation. **Figure 4.10**

shows the effects of ethanol administration during C2C12 differentiation on the

number of TnT- and TnT+ cells on days 2 and 3. The number of TnT- cells

increases at all doses of ethanol on day 2 compared to controls. This reaches

significance at a dose of 0.5% (82mM) ($p<0.001$) (**figure 4.10a**). On days 3 and

4 the number of TnT- cells (reserve cells) decreases at doses $\geq$ 0.3% (50mM)

($p<0.001$) (**figure 4.10b, c**).
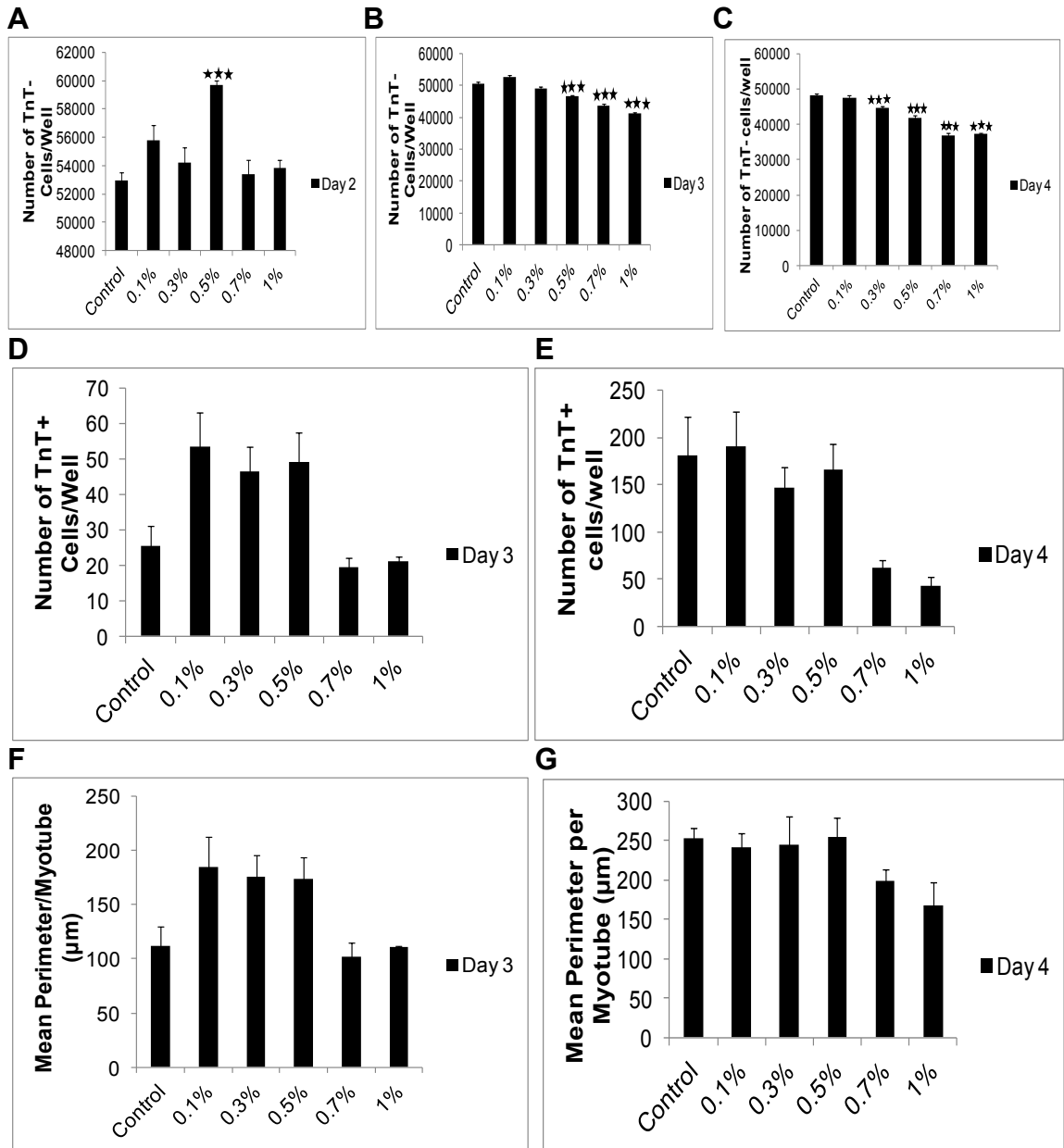
Figure 4.10: The effect of ethanol on differentiating C2C12 cells. C2C12 cells were differentiated in the presence of ethanol as indicated (%). **(A)** Number of TnT-cells on day 2 **(B)** on day 3, **(C)** on day 4 **(D)** Number of TnT+ cells on day 3, p≤ 0.05 by one-way ANOVA **(E)** on day 4 **(F)** Mean perimeter per myotube on day 3, p≤ 0.05 **(G)** on day 4. The averages are shown ± SEM (n=3-15), ***p<0.001 vs. Control by one-way ANOVA followed by Tukey's test for multiple comparisons. 0.1%=17mM, 0.3%=50mM, 0.5%=82mM, 0.7%=115mM, 1%=180mM

These results suggest that ethanol initially promotes the proliferation of C2C12 myogenic cells during differentiation but that this proliferative effect is absent on day 3.

On day 3 the groups of TnT+ cell number are significantly different by one-way ANOVA ($p \leq 0.05$) but not when they are compared to each other after correction for multiple comparison testing (**figure 4.10d**). However at doses of 0.1% (17mM) to 0.3% (50mM) there is a trend of ethanol increasing the number of TnT+ cells compared to controls. At doses $\geq 0.7\%$ (115mM) ethanol tends to decrease the number of TnT+ cells.

On day 4 the number of TnT+ cells does not vary by one-way ANOVA between control and alcohol treated cells ($p > 0.05$) (**figure 4.10e**). However there is a trend towards decrease of TnT+ cells at 0.3% (50mM) and 0.5% (82mM) ethanol with more noticeable decreases seen at 0.7% (115mM) and 1% (180mM) ethanol. The perimeter of the TnT+ cells in the different groups are significantly different by one-way ANOVA on day 3 ($p \leq 0.05$) but no groups are significantly different from each other ($p > 0.05$) (**figure 4.10f**). However the TnT+ cells do display an increased perimeter at doses between 0.1% (17mM) and 0.5% (82mM) ethanol. At 0.7% (115mM) and 1% (180mM) the perimeter is very similar to that of controls. On day 4 the perimeter of the TnT+ cells are almost indistinguishable between control and ethanol ($p > 0.05$) but slight decreases are seen at 0.7% (115mM) and 1% (180mM) ethanol(**figure 4.10g**). These data suggest that ethanol causes more cells to differentiate faster compared to controls which results in an increased number of TnT+ cells on day 3 compared

to controls and furthermore the perimeter of the cells which differentiate in the presence of ethanol are larger (**figure 4.10f**). This might suggest that ethanol is providing a differentiation advantage. However this differentiation advantage disappears on day 4. The control cells septuple their TnT+ cell number to ~ 175 on day 4 from ~ 25 on day 3 whereas with ethanol treated cells at a dose of 17mM less than half of that increase is seen, the TnT+ cell number triples from ~ 55 cells on day 3 to ~ 175 cells on day 4. The corresponding perimeter of the cells between control and alcohol on day 4 are virtually identical abrogating any advantage by ethanol during differentiation (**figure 4.10g**).

To summarize, these data suggest that ethanol initially promotes the proliferation and differentiation of C2C12 myogenic cells but over time, ethanol has an anti-proliferative effect and decreases the rate of differentiation thus impeding the process.

Tables **4.7-4.9** display selected molecular and cellular functions that are significantly associated with 0.6% (100Mm) ethanol on all days of differentiation. These include functions within the categories of cellular growth and proliferation, cell death and cellular development. Within cellular growth and proliferation (**table 4.7**) the growth of cells was significantly associated with ethanol on all days with p-values ranging from 3.69×10^{-5} to 5.48×10^{-10}. The growth of cells was predicted to be decreased on day 3 with a z-score of -2.22. Proliferation of hematopoietic cells was associated with ethanol on day 1 with a p-value = 0.01and a z-score which suggested an increase in the function. The general category of proliferation of cells is significantly

Table 4.7: Functions associated within the category of cellular growth and proliferation significantly associated with ethanol during C2C12 differentiation.

Day	Functions Annotation	p-value	Bias corrected z-score	Prediction	Number of Molecules
1	Growth of cells	3.69E-05	-0.411		110
2	Growth of cells	5.48E-10	-1.457		197
3	Growth of cells	8.44E-07	-2.221	Decreased	158
2	Proliferation of cells	2.60E-07	1.369		243
3	Proliferation of cells	1.80E-09	-0.541		221
1	Proliferation of granulosa cells	3.16E-03	2.354	Increased	5
1	Proliferation of T lymphocytes	1.62E-02	2.177	Increased	29
2	Proliferation of connective tissue cells	2.22E-03	2.447	Increased	43
2	Proliferation of mesenchymal cells	2.27E-03	2.085	Increased	10
3	Proliferation of muscle cells	1.73E-03	0.623		26

Microarray results were processed through IPA software to identify high-level biological functions significantly associated with 0.6% (100mM) ethanol. P-values represent the statistical association of differentially expressed genes in the dataset to all genes in the IPA universe and calculated using right-tailed Fisher's Exact Test. A regulation z-score is predicted to significantly increase the function if ≥2 and

Table 4.8: Functions associated within the category of cell death significantly associated with ethanol during C2C12 differentiation.

Day	Functions Annotation	p-value	Bias corrected z- score	Prediction	Number of Molecules
1	Cell death	2.66E-06	-0.482		185
2	Cell death	6.49E-08	1.419		303
3	Cell death	1.25E-09	0.323		271
1	Apoptosis	2.85E-06	-0.364		148
2	Apoptosis	3.43E-07	0.846		237
3	Apoptosis	7.49E-09	0.679		212
2	Cell death of muscle cells	7.52E-05	0.41		36
2	Cell death of hematopoietic progenitor cells	8.37E-05	2.048	Increased	28
2	Cell death of hematopoietic cells	1.09E-04	2.225	Increased	29
2	Cell death of fibroblast cell lines	4.52E-03	2.514	Increased	43
2	Anoikis	4.56E-03	-2.259	Decreased	13
2	Apoptosis of embryonic stem cells	4.61E-04	-1.118		8
2	Apoptosis of muscle cells	6.42E-04	0.651		27
2	Apoptosis of stem cells	1.24E-03	-1.329		9
2	Cell death of stem cells	2.27E-03	-1.013		10
2	Regeneration of muscle cells	3.35E-03			3
2	Cell death of T lymphocytes	3.37E-03	1.103		31
3	Cell death of muscle cell lines	8.77E-07	-0.159		14
3	Apoptosis of muscle cell lines	6.68E-06	-0.092		12
3	Self-renewal of hematopoietic progenitor cells	1.48E-03	-0.458		5

Microarray results were processed through IPA software to identify high-level biological functions significantly associated with 0.6% (100mM) ethanol. P-values represent the statistical association of differentially expressed genes in the dataset to all genes in the IPA universe and calculated using right-tailed Fisher's Exact Test. A regulation z-score is predicted to significantly increase the function if ≥2 and decreased if ≤ 2.

Table 4.9: Functions associated within the category of cellular development significantly associated with ethanol during C2C12 differentiation.

Day	Functions Annotation	p-value	Bias corrected z- score	Prediction	Number of Molecules
2	Differentiation	9.36E-10	1.24		198
3	Differentiation	5.94E-08	-0.496		163
2	Differentiation of cells	4.19E-09	1.491		185
3	Differentiation of cells	2.47E-07	-0.228		152
2	Development of hematopoietic progenitor cells	1.66E-04	1.249		23
2	Development of hematopoietic cells	1.34E-04	1.252		24
2	Growth of muscle cells	2.44E-03	0.328		12
2	Regeneration of muscle cells	3.35E-03			3
2	Differentiation of hematopoietic cells	4.16E-03	1.51		27
2	Growth of hematopoietic progenitor cells	4.08E-03	0.604		13
2	Differentiation of hematopoietic progenitor cells	4.58E-03	1.252		26
2	Development of muscle cells	4.56E-03	-1.264		13
3	Differentiation of myoblasts	8.63E-04	0.258		12
3	Myogenesis of cells	1.69E-03	-1.797		9
3	Maturation of cells	1.76E-03	-2.384	Decreased	35
3	Differentiation of muscle cells	2.22E-03	0.297		22
3	Differentiation of skeletal muscle satellite cells	2.61E-03			3
3	Differentiation of muscle cell lines	2.98E-03	-0.377		14
3	Gametogenesis	3.13E-03	2.221	Increased	28

Microarray results were processed through IPA software to identify high-level biological functions significantly associated with 0.6% (100mM) ethanol. P-values represent the statistical association of differentially expressed genes in the dataset to all genes in the IPA universe and calculated using right-tailed Fisher's Exact Test. A regulation z-score is predicted to significantly increase the function if ≥2 and decreased if ≤ 2.

associated with ethanol on day 2 ($p = 2.6 \times 10^{-7}$) and on day 3 ($p = 1.8 \times 10^{-9}$) with the z-score trending towards increase (z=1.37) on day 2 and a slight trend towards decrease on day 3 (z = - 0.5). Significant associations are seen for ethanol increasing the proliferation of mesenchymal and granulosa cells (z>2, p~ 2×10^{-3}). Ethanol is predicted to slightly increase the number of muscle cells, $p = 1.73 \times 10^{-3}$, z=0.62. This might suggest that ethanol causes the proliferation of progenitor cells within the culture which causes them to transdifferentiate into other cell types. This hypothesis would need to be investigated further.

Cell death is significantly associated with ethanol on all days (day 1 ($p = 2.66 \times 10^{-6}$), day 2 ($p = 6.49 \times 10^{-8}$), day 3 ($p = 1.25 \times 10^{-9}$). The z-scores suggest that ethanol trends towards decreasing cell death on day 1 (z= -0.49) and towards increasing it on day 2 (z=1.42) and a slight trend towards increase is seen on day 3 (z=0.32). On day 2 ethanol is associated with cell death of muscle cells ($p = 7.52 \times 10^{-5}$) and apoptosis of muscle cells ($p = 6.42 \times 10^{-4}$) with trends seen towards increase for both cell death (z=0.41) and apoptosis (z=0.65). On day 3 cell death of muscle cell lines ($p = 8.77 \times 10^{-7}$) and apoptosis of muscle cell lines ($p = 6.68 \times 10^{-6}$) are significantly associated with alcohol. Cell death of hematopoietic progenitor cells is predicted to be increased on day 2 ($p = 8.37 \times 10^{-5}$), z=2.048. Conversely, cell death of stem cells ($p = 2.27 \times 10^{-3}$, z=-1.01) and apoptosis of stem cells ($p = 1.24 \times 10^{-3}$, z= - 1.33) trend towards a prediction of decreased death of progenitor cells. These latter results support the cellular findings of decreased cell number of TnT- cells on day 2 (**figure 4.10b, c**).

In summary, the results on cell death suggest that less differentiated cells are more vulnerable to the effects of ethanol in comparison to their more differentiated counterparts as has already been suggested[50].

Differentiation was associated with ethanol on days 2 ($p=9.36 \times 10^{-10}$, $z=1.24$) and 3 ($p=5.94 \times 10^{-8}$, $z= -0.5$) (**table 4.9**). Development of muscle cells ($p=4.56 \times 10^{-3}$, $z=-1.26$) trended towards a decrease on day 2 whereas differentiation of hematopoietic progenitor cells trended towards an increase ($p=4.58 \times 10^{-3}$, $z=1.25$) which could suggest that precocious differentiation of progenitor cells is a reason for the observed increase of TnT+ cells by ethanol on day 3. On day 3, differentiation of myoblasts ($p=8.63 \times 10^{-4}$, $z=0.26$), and myogenesis of cells ($p=1.69 \times 10^{-3}$, $z=-1.8$) is associated with ethanol. Differentiation trended towards an increase but myogenesis trended towards a decrease. The myogenesis function includes more markers that function in the commitment of cells compared to the differentiation function therefore ethanol may decrease the commitment to differentiation. Maturation of cells ($p=1.76 \times 10^{-3}$, $z=-2.38$) is associated with ethanol and predicted to decrease. These results suggest that the push towards differentiation is increased by ethanol on day 2 which leads to the increase of the number of TnT+ cells seen on day 3. (**figure 4.10d**). On day 3 differentiation tends to decrease compared to control cells (**figure 4.10e** and this prediction is validated by the microarray ($p=2.98 \times 10^{-3}$, $z = -0.38$). The function of gametogenesis was predicted to increase on day 3 ($z=2.21$, $p=3.13 \times 10^{-3}$). It has been reported that C2C12 cells can trans-differentiate into sperm-like cells in the presence of retinoic acid[141].

Ethanol may cause the dedifferentiation of a subpopulation of C2C12 myogenic cells but this hypothesis would need to be investigated further.

To summarize, the predictions from IPA for biological functions were borne out at the cellular level which shows that working backwards from the end results (microarray) to the initial data (reduced expression of MRFs) will suggest the primary factor(s) that ethanol modulates to inhibit C2C12 differentiation.

Conclusions

Ethanol reduces levels of the MRFs during C2C12 differentiation. Unbiased analysis by IPA on the transcriptional profile of C2C12 cells differentiating in the presence of ethanol identified transcriptional effects consistent with down-regulation of MRFs.

The data that I have presented show that the MRFs, MyoD, myogenin and Myf5 are inhibited by ethanol during differentiation. Microarray analysis of differentiating C2C12 cells exposed to ethanol show that the MRF which 1) consistently displays the most significant association with differentially regulated transcripts by ethanol, 2) is involved in canonical pathways predicted to be modulated by ethanol, 3) is the most prominent of the upstream regulators predicted to be associated with network formation by ethanol is MyoD. The effects of ethanol on the differentiation of C2C12 cells appear to be exerted through MyoD.

Chapter 5: The Role of Ethanol on the Notch Signaling

Pathway during C2C12 Differentiation

Figure Contributions:

I performed the experiments which generated the materials for the figures which are presented in this chapter.

I contributed all the figures in this chapter.

Introduction

The highly conserved Notch signaling pathway is crucial for skeletal muscle regeneration[14]. Alcohol activation of Notch signaling inhibits MyoD induced C2C12 differentiation [16, 18, 19, 138] while at the same time, it is important for the maintenance of quiescent cells. Inhibition of Notch signaling in the mouse C2.7 myoblast cell line promotes their differentiation into large myotubes [41].

The canonical Notch signaling pathway involves interaction between the Notch receptor and ligand bearing cell to cause release of the Notch intracellular domain (NICD) into the nucleus where it interacts with the DNA binding protein CSL (CBF1, Su(H), RBP-J) to activate gene transcription of targets[16, 35]. The primary target genes of NICD-CSL include the HES and HERP family of bHLH transcriptional repressors whose up-regulation negatively regulates tissue-specific transcription factors[34].

Ethanol has been reported to regulate Notch signaling in a variety of cell types. In a mouse model of alcoholic pancreatitis, ethanol inhibited regeneration after injury and impaired expression of the critical Notch effector, Hes-1[142]. Administration of a ɣ-secretase inhibitor promotes the differentiation of embryonic pancreatic precursor cells[143]. Ethanol is reported to impair placentation by de-regulating Notch signaling [106]. Alcohol hypersensitivity has been reported in mice which are deficient for the neural gene (neuralized) that affects Notch signaling [144]. Ethanol inhibits the proliferation of smooth muscle cells by decreasing Notch1 signaling [53]. In endothelial cells alcohol stimulates

angiogenesis via increased Notch 1 signaling[54]. In an in vitro model for second-trimester cerebral cortical neuroepithelium ethanol does not induce cell death but induces proliferation while depleting neural epithelial stem-cell populations which signifies that ethanol induces the premature differentiation of stem to blast cells[145]. Knock-down of ethanol sensitive micro-RNAs in this system increased Jagged-1 (Notch receptor ligand) mRNA levels and ethanol was found to increase Jagged-1 transcript [145].

These studies clearly demonstrate that Notch signaling occurs in a context dependent manner and that ethanol modulates Notch signaling in a variety of cell types to impair numerous processes including differentiation and regeneration. The effect of ethanol on Notch signaling in differentiating and reserve C2C12 cells is unknown.

I found that ethanol activated Notch signaling during C2C12 differentiation and increased levels of the Notch effectors, Hes-1 and Hey-1. Blocking Notch activation abrogated the ethanol induced increase in Hes-1 expression, increased levels of MyoD and partially restored differentiation. Ethanol reduced Notch 1 transcript, Notch1-ICD protein levels and the number of quiescent CD34-cells which are reported to express Notch1[41]. These results suggest that ethanol modulates Notch signaling which inhibits the terminal differentiation of C2C12 myocytes and inhibits expansion of quiescent reserve cells.

Results

Ethanol activates Notch Signaling during C2C12 Differentiation

Canonical targets of Notch signaling include Hes-1 and Hey-1 (CHF2, Hrt1, Hesr-1, HERP2) which was identified as a Notch effector and repressor of C2C12 terminal myogenic differentiation [146]. Up-regulation of Hes-1 (**figure 5.1a**) by ethanol was observed on all days with a 2.27 fold-change increase seen on day 2 ($p<0.001$) and a 1.58 fold-change increase on day 3 ($0.001 \leq p \leq 0.01$) of differentiation compared to controls. The magnitude of Hey-1 (**figure 5.1b**) increase by ethanol was ~ 1.20 fold on all days which reached significance on day 2, $p<0.001$ compared to controls. These results show that ethanol increases levels of the Notch effectors, Hes-1 and Hey-1 during the first 3 days of differentiation with maximal levels seen on the second day of differentiation.

To evaluate whether alcohol activates Notch-dependent transcription during the first 24 hours of C2C12 differentiation I tested whether alcohol could activate a luciferase reporter plasmid containing the Hes-1 proximal promoter which contains a consensus binding sequence for the Notch-ICD. I confirmed that the Hes-1 proximal reporter is activated by Notch signaling as has been previously described [147]. Ethanol increased the Hes-1 proximal promoter ~ 1.3 fold ($p \leq 0.05$) (**figure 5.1c**) which is within the range of ethanol induction of Hes-1 and Hey-1 transcript after 24 hours (**figure 5.1a**). These results show that ethanol activates Notch signaling during C2C12 differentiation.
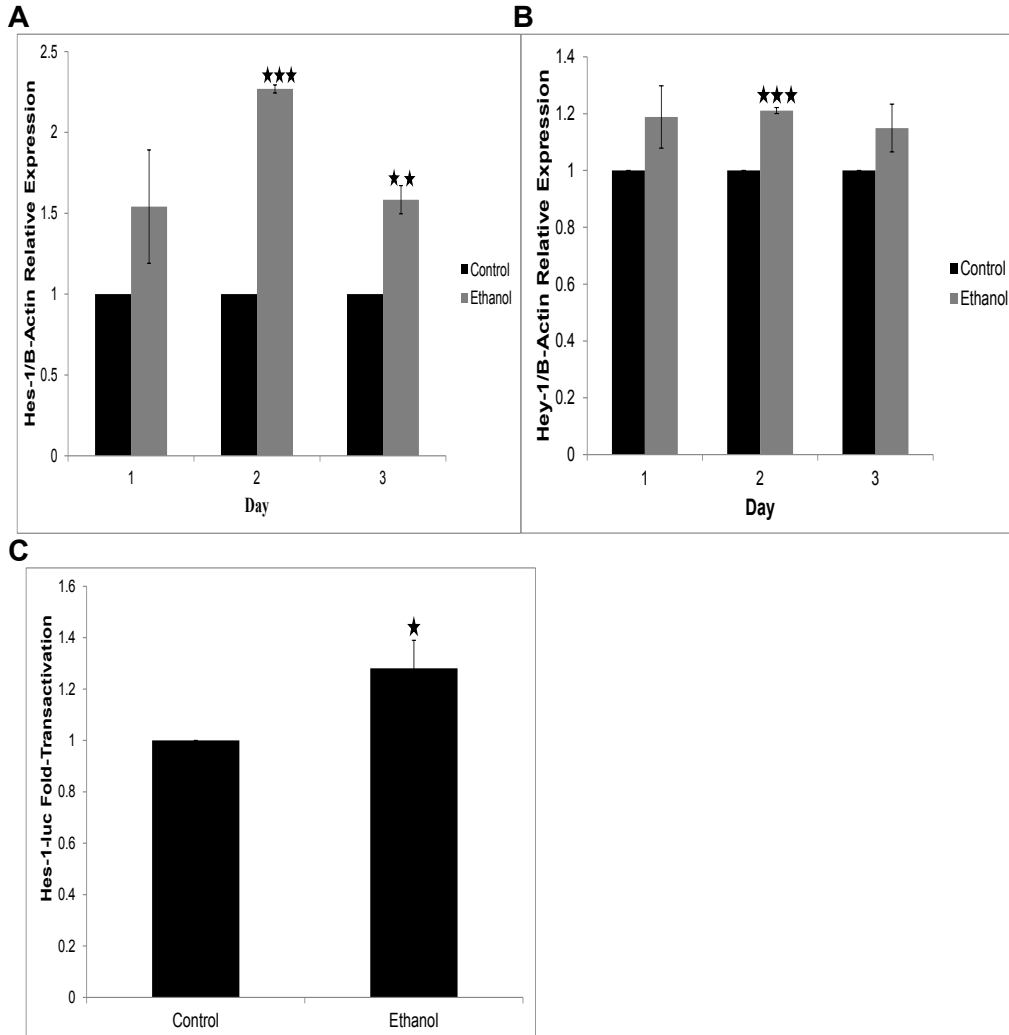
Figure 5.1: The Notch signaling pathway is activated by ethanol during C2C12 differentiation. C2C12 cells were induced to differentiate in DM± 100mM ethanol for 1-3 days. **(A)** Hes-1, **(B)** Hey-1 mRNA levels were measured by qPCR every 24 hours. Data was quantified using the standard curve method and normalized to B-Actin to obtain relative fold-change to untreated controls ± SEM (n=3), 2-tailed Student's t-test was performed. **(C)** C2C12 cells were transiently transfected with (350bp)-Hes-1-luc in growth medium (DMEM with 20% FBS). ~ 4-24 hours post transfection media was changed to DM ± ethanol for 24 hours. Individual samples were normalized for transfection efficiency (pCMV-Ren). Expression is relative to untreated controls ± SEM(n=3), 1-tailed Student's t-test was performed.

To confirm that the increase in Hes-1 expression by ethanol was mediated through Notch signaling, I differentiated C2C12 cells in the presence of ethanol and the ɣ-secretase inhibitor (GSI), L-685,458, which prevents the final cleavage of the Notch receptor and therefore the release of the intracellular domain[38]. The effect of L-685, 458 on Hes-1 levels caused an approximately 40% decrease compared to controls (**figure 5.2a**). This would be expected if low-level endogenous Notch signaling is blocked. Hes-1 expression was increased by ethanol (**figure 5.2a**) and the addition of L-685, 458 effectively abrogated the increase in Hes-1 expression by ethanol (p<0.001) to levels seen with L-685, 458 which confirms that the induction of Hes-1 by alcohol is mediated via activation of Notch signaling.

Activation of Notch signaling or over-expression of Notch target genes inhibits MyoD expression [138, 148]. MyoD expression is down-regulated by ethanol during C2C12 differentiation (**figure 5.2b**) so I tested whether activated Notch signaling contributes to the ethanol induced decrease seen in MyoD. L-685, 458 increased MyoD levels by ~ 12% compared to vehicle, which is expected if low-level Notch mediated repression of MyoD is relieved. Ethanol reduced levels of MyoD by ~ 30% and the addition of L-685, 458 partially restored levels of MyoD by ~ 14% (p=0.02) which shows that alcohol induced Notch activation plays a role in reducing the levels of MyoD.

A

B
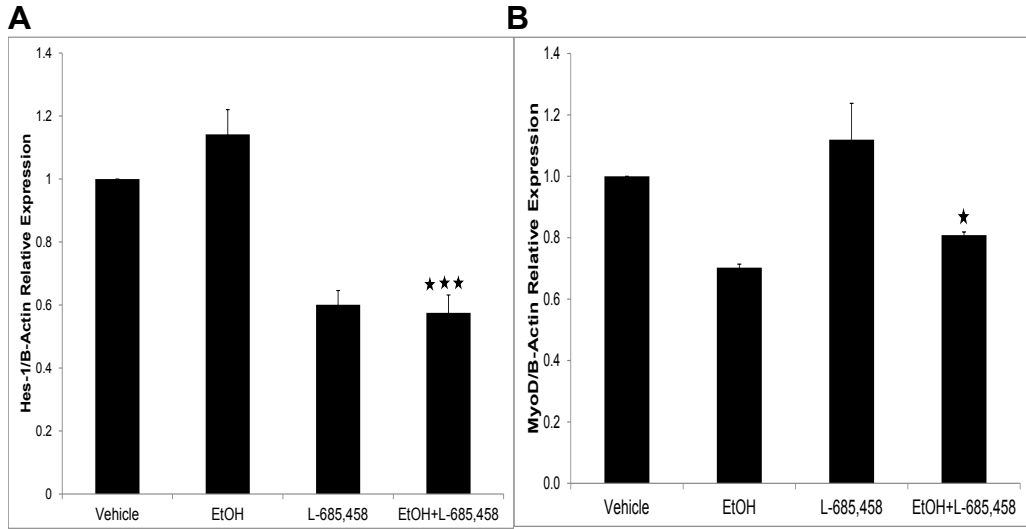
Figure 5.2: **Inhibition of Notch signaling curbs ethanol induced changes in Notch target genes during C2C12 differentiation**. C2C12 cells were induced to differentiate in DM ± 100mM ethanol ± 1uM L-685, 458 for 2 days. Hes-1 (n=4) and MyoD (n=2) mRNA levels were measured by qPCR. Expression is relative to untreated controls ± SEM, p<0.05 versus Ethanol.

These results confirm that alcohol activates the Notch pathway during

C2C12 differentiation. Inhibition of low-level Notch signaling with a GSI in C2C12

cells differentiating in the presence of ethanol abrogated the expression of the

canonical Notch effector, Hes-1, and partially rescued the ethanol induced down-

regulation of MyoD. These results suggest that inhibition of differentiation by

ethanol may be partially relieved by blocking Notch signaling.

Blocking ethanol induced Notch activation improves C2C12 differentiation

Since Notch signaling inhibits C2C12 differentiation[16], I tested whether

inhibiting ethanol induced Notch activation would improve C2C12 differentiation.

C2C12 myoblasts were treated with vehicle, alcohol, L-685, 458, or alcohol + L-

685, 458 during differentiation (**table 5.1, 5.2, figure 5.3**) over 7 days.

 Administration of L-685, 458 to differentiating C2C12 cells increased the

number of differentiated TnT+ cells by ~ 30% (**table 5.1, figure 5.3g**). My results

confirm previous reports [38] that L-685, 458 increases the number of myotubes

which form during C2C12 differentiation. L-685, 458 enhanced differentiation as

indicated by the ~ 35% increase in the MFI (p=2.19 X 10^{-14}) compared to vehicle

(**figure 5.3a**). The number of TnT- cells (reserve cells) decreased by ~ 15%

(**figure 5.3h**) (p=5.20 X 10^{-13}) which is expected since previous reports have

demonstrated that ɣ-secretase inhibitors inhibit satellite cell proliferation and self-

renewal[149]. These data suggest that some Notch expressing cells which do

not differentiate in vehicle are able to differentiate in the presence of L-685, 458.

Table 5.1: L-685, 458 alters the cellular and nuclear profile of differentiating C2C12 Cells

Parameter	Vehicle Mean	Vehicle SD	L-685, 458 Mean	L-685, 458 SD	P-Value	(i/m)Q
MFI	9.05	1.17	12.3	1.12	2.19E-14	0.004
TnT- Cell #/Well	42407	1646	36237	1745	5.20E-13	0.008
TnT+Cell #/Well	1247	87.2	1586	92.9	1.21E-11	0.013
Total Number of Myonuclei/Well	4218	540	5082	539	4.75E-09	0.017
Mean Length/Myotube	147.00	6.56	131.00	8.98	1.78E-08	0.021
Mean Perimeter/Myotube	502.00	46.3	431.00	43.5	2.45E-08	0.025
Mean NucArea/Myotube Nucleus	126	1.86	128	1.69	9.85E-08	0.029
Nuclear Area/TnT-Cell	132	3.57	137.0	3.34	2.78E-06	0.033
TnT+ Mean Breadth/Myotube	37.4	3.00	32.5	3.13	3.80E-06	0.038
TnT+II/Myotube	2405647	219061	2233376	220901	0.001	0.042
Mean TnT+ Cell Area/TnT+ Cell	2453	356	2285	320	0.032	0.046
# nuclei/Myotube	3.38	0.39	3.22	0.41	0.058	0.050

C2C12 cells were differentiated for 7 days in DM ± L-685, 458. The cells were fixed and cells were immunostained for TnT, nuclei were counterstained with DAPI and indicated parameters were measured (see Methods). Student's t-tests comparing treated to control were performed followed by correction for multiple testing (FDR=0.05). The averages are shown ± SEM (n=24).

Ethanol
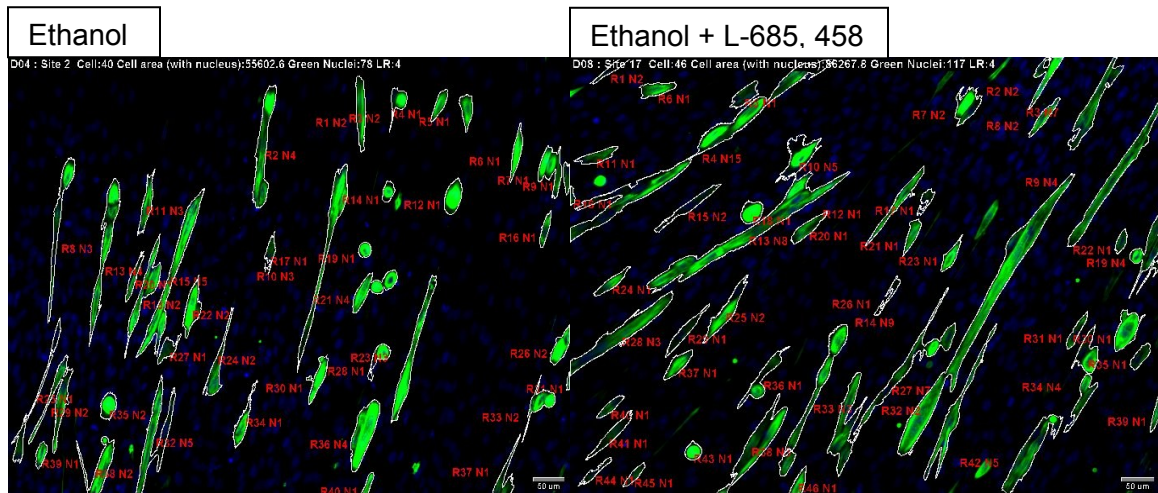
Ethanol + L-685, 458

Table 5.2: L-685, 458 alters the cellular and nuclear profile of ethanol driven C2C12 differentiation.

Parameter	Ethanol Mean	Ethanol SD	EtOH+L-685,458 Mean	EtOH+L-685,458 SD	P-Value	(i/m)Q	Interaction
TnT- Cell #/Well	36559	2209	31280	2489	7.11E-13	0.004	ns
MFI	7.58	0.99	9.89	0.96	7.55E-09	0.008	*
TnT+II/Myotube	1547729	127179	1763886	108089	1.89E-08	0.013	***
TnT+ Mean Breadth/Myotube	26.3	3.46	29.3	2.66	4.23E-05	0.017	***
# nuclei/Myotube	2.09	0.23	2.35	0.25	8.72E-05	0.021	*
Mean TnT+ Cell Area/TnT+ Cell	1433	302	1661	269	1.59E-04	0.025	***
Total Number of Myonuclei/Well	3003	483	3426	369	0.001	0.029	**
Mean Perimeter/Myotube	307	38.5	324.0	31.6	0.032	0.033	***
Mean NucArea/Myotube Nucleus	126.6	3.01	127.7	2.35	0.049	0.038	**
Nuclear Area/TnT-Cell	140	8.90	143	6.74	0.053	0.042	ns
TnT+Cell #/Well	1439	164	1462	139	0.49	0.046	***
Mean Length/Myotube	107	7.29	106	5.27	0.51	0.050	***

Indicated parameters were measured after C2C12 cells were differentiated for 7 days in DM containing EtOH (100mM) ± L-685, 458 (1uM). Student's t-tests comparing treated to control were performed fol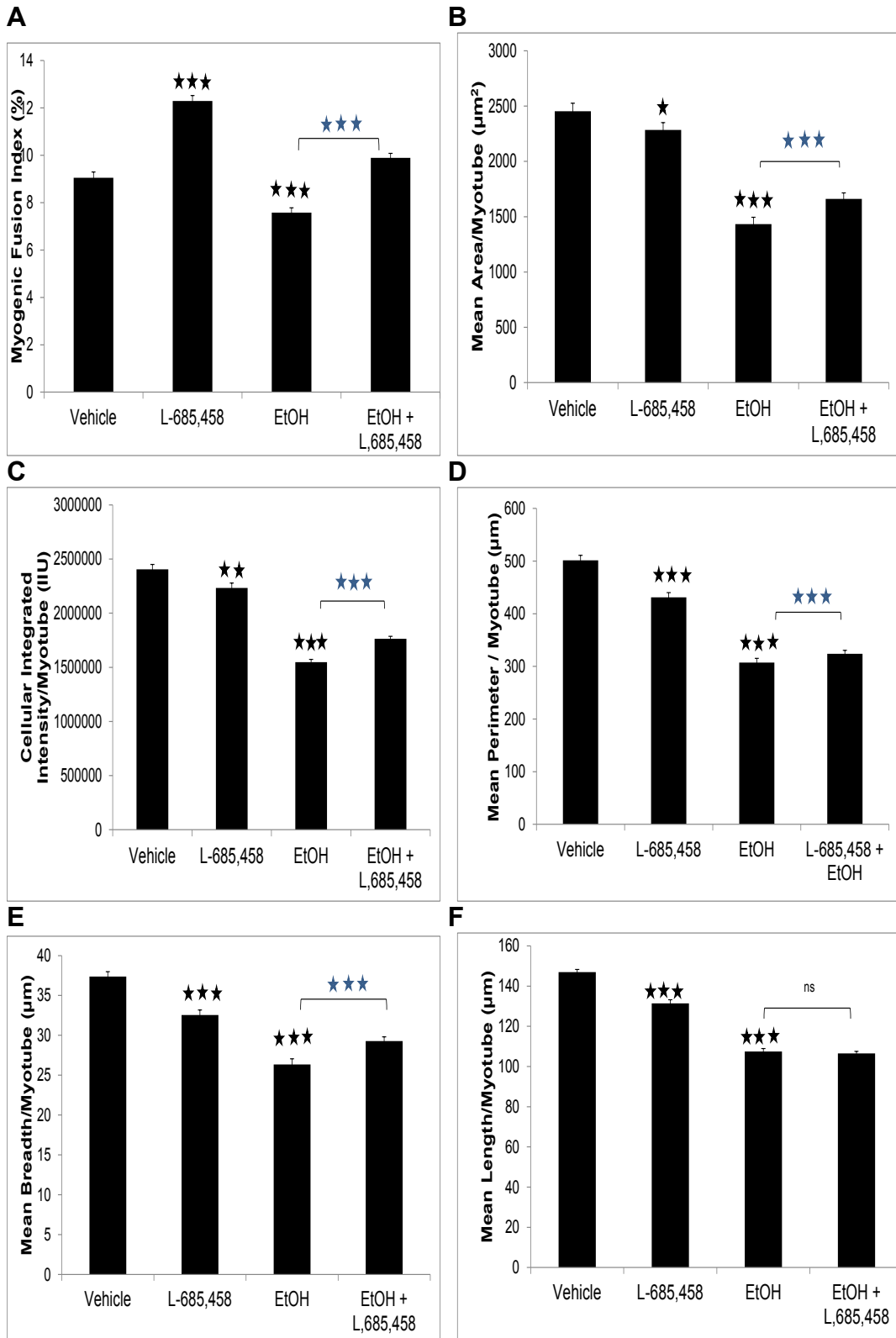lowed by correction for multiple testing (FDR=0.05), (n=24). Images depict a site from an ethanol treated well and a site from an ethanol + L-685, 458 treated well.
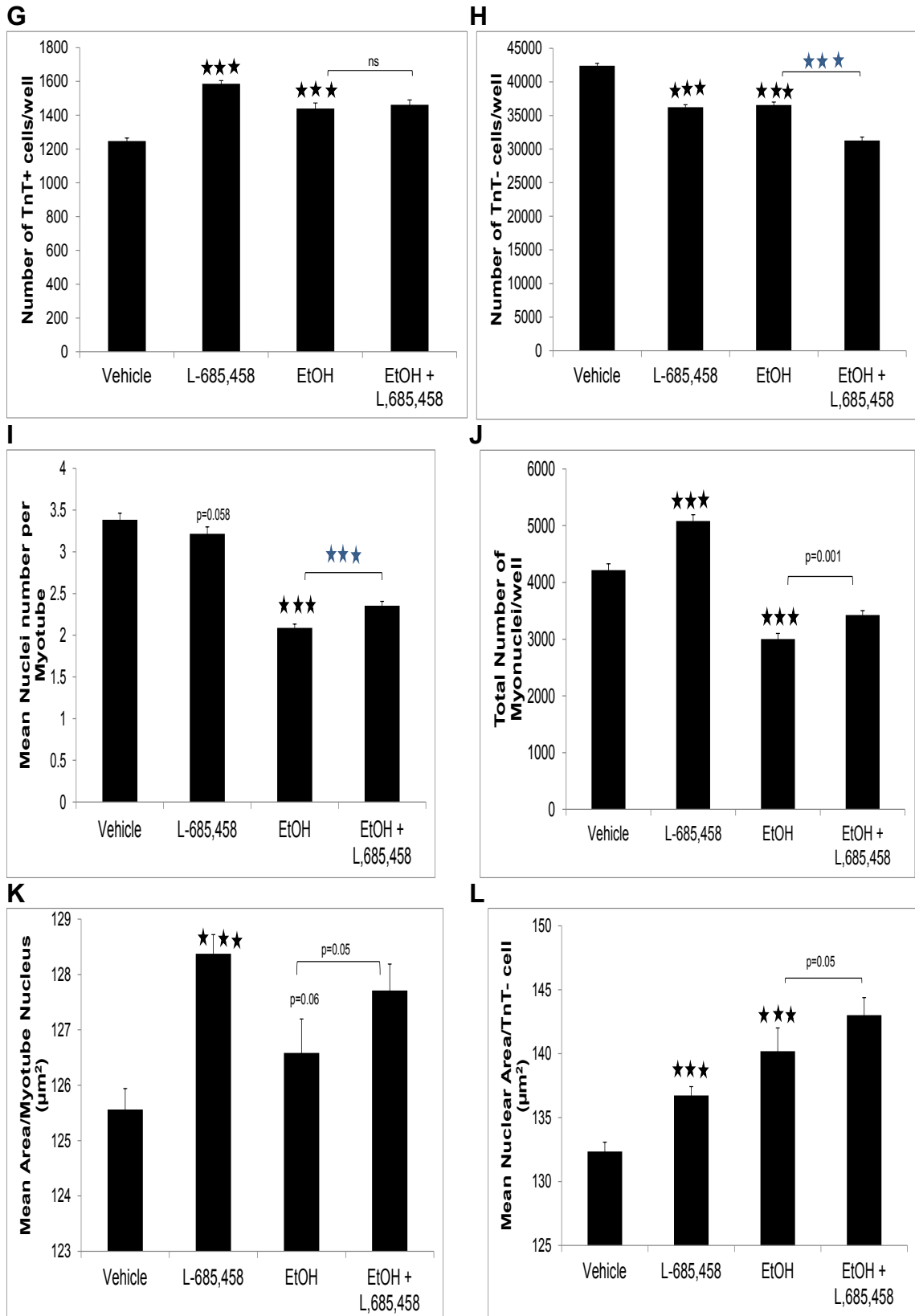
Figure 5.3: Blocking ethanol induced Notch activation ameliorates C2C12 differentiation. Confluent C2C12 myoblasts were induced to differentiate for 7 days in DM containing either vehicle, ethanol (100mM); L-685,458 (1uM) or ethanol + L-685,458. (A) Myogenic Fusion Index (MFI) (%) (Repeated Measures (RM) two-way ANOVA of Vehicle-Ethanol or L-685, 458-$F_{1,46}$=6.6, p=0.01 for interaction), FDR post-hoc * p≤0.05. (B) Mean Area per Myotube (μm^2) (RM two-way ANOVA $F_{1,46}$=16.1, p=0.0002 for interaction). (C) Cellular Integrated Intensity per Myotube (IIU) (RM two-way ANOVA $F_{1,46}$= 59.1, p<0.0001 for interaction). (D) Mean myotube perimeter (μm) (RM two-way ANOVA Ethanol $F_{1,46}$ = 47.1, p < 0.001 for interaction). (E) Mean Breadth per Myotube (μm) (RM two-way ANOVA $F_{1,46}$=62.1, p<0.0001 for interaction). (F) Length per Myotube (μm) (two-way ANOVA $F_{1,46}$=12.6, p<0.0001 for interaction). (G) Number of TnT+ cells per well (RM two-way ANOVA $F_{1,46}$=46.9, p<0.0001 for interaction). (H) Number of TnT- cells/well (RM two-way ANOVA $F_{1, 46}$=2.47, p=0.12 for interaction). (I) Number of nuclei/Myotube (RM two-way ANOVA $F_{1,46}$= 13.7, p=0.0006 for interaction). (J) Total number of myonuclei per well (RM two-way ANOVA $F_{1,46}$=7.56, p=0.0085 for interaction). (K) Mean Area/Myotube Nucleus (μm^2) (RM two-way ANOVA $F_{1,42}$= 10.4, p=0.0018 for interaction). (L) Mean Nuclear Area/TnT- cell (μm^2) (one-way ANOVA $F_{3,23}$= 5.2, p<0.0001). The averages are shown ± SEM (n=22-24), *p≤0.05.

The myotubes which formed in the presence of L-685, 458 contained on average ~ 5% fewer nuclei (p=0.058, ns) (**figure 5.3i**) and exhibited ~ 7% decrease in TnT+ content as assessed by the area (p=0.03) and integrated intensity per myotube (p=0.001) (**figure 5.3b, c**). The area per TnT- and TnT+ nucleus increased by ~ 3% compared to vehicle (p=2.78 X 10^{-6}, 9.85 X 10^{-8} respectively) (**figure 5.3k, l**). The length, breadth and perimeter of the myotubes which formed in the presence of L-685, 458 were smaller by ~ 13% compared to vehicle (p=1.78 X 10^{-8}, 3.80 X 10^{-6}, 2.45 X 10^{-8} respectively). The average myotube which formed in the presence of L-685, 458 contained more nuclei, was less dense, and was shorter and thinner than its vehicle treated counterpart. This myotube phenotype resembles newly regenerated myofibers which have smaller diameters.

I then analyzed the effects of L-685, 458 on C2C12 cells differentiating in the presence of ethanol and tested for interaction using two-way ANOVA followed by multiple comparison testing (**table 5.2, figure 5.3**). Finding a significant interaction would further support that a biological effect of alcohol is in part mediated by activation of the Notch pathway.

The MFI increased by 30% (p=7.55 X 10^{-9}) in the presence of ethanol and L-685, 458 compared to ethanol alone (**figure 5.3a**) and exhibited a significant interaction effect (p=0.01). Blocking Notch pathway activation during ethanol driven C2C12 differentiation restored the myogenic fusion index (MFI) to 9.89%, (SD=0.19) which was slightly higher than the levels which are seen in vehicle

treated cells, MFI=9.05% (SD=1.17) (**figure 5.3a**). The MFI serves as a measure of differentiation. A reduction in the MFI indicates that differentiation is inhibited and restoration of the MFI is akin to restoring differentiation[38, 59-61, 86]. Therefore blocking ethanol induced Notch activation restored C2C12 differentiation.

I measured the cellular and nuclear profile of the myotubes and reserve cells to characterize and determine the extent of rescue. The combined effect of ethanol and L-685, 458 on differentiating C2C12 cells decreased the number of TnT- cells by ~ 15% compared to ethanol alone (p=7.11 X 10^{-13}) and the interaction was slightly non-significant (p=0.12) (**figure 5.3h**). Each compound on its own decreased reserve cell number by ~ 15% compared to vehicle and the combined effect of both compounds caused TnT- cell number to decrease to ~ 30% of vehicle. This indicates that an independent and additive effect is occurring in TnT- cells which suggests that ethanol decreases reserve cell number independently of Notch activation.

A significant interaction effect was seen for the two compounds on TnT+ cell number (p<0.001), and this translated into a negligible effect on TnT+ cell number (1.5% increase, p=0.49) compared to ethanol alone (**figure 5.3g**). Since both compounds on their own increase TnT+ cell number by ~ 17% during differentiation compared to vehicle, these results suggest that for TnT+ cells, the effects of ethanol and L-685, 458 cancelled each other.

The addition of GSI to C2C12 cells differentiating in the presence of ethanol compared to cells differentiating in the presence of ethanol alone

improved nearly all cellular parameters of the myotubes that formed and significant interaction effects between the two compounds was observed. The integrated fluorescent intensity per myotube which represents protein content improved by ~ 14% (p=1.89 X 10^{-8}, interaction p < 0.001) (**figure 5.3c**). Myotube area correlated with integrated intensity and increased by ~ 16% (p=1.59 X 10^{-4}, interaction p<0.001) (**figure 5.3b**). Myotube width increased by ~ 11% (p=4.23 X 10^{-5}, interaction p<0.001) (**figure 5.3e**), length did not change (p=0.51) but the interaction was significant (p < 0.001) (**figure 5.3f**), and the perimeter increased by ~ 5% (p=0.03), interaction p < 0.001 (**figure 5.3d**). The number of nuclei per myotube increased by ~ 13% (p=8.72 X 10^{-5}), interaction p ≤ 0.05 (**figure 5.3i**). These results show that the amount of rescue compared to vehicle is modest which suggests that inhibition of Notch signaling is not sufficient to abrogate the effects of ethanol on C2C12 differentiation.

The effect of both compounds on myotube nuclear area (**figure 5.3k**) and TnT- nuclear area (**figure 5.3l**) was not significant after correcting for multple comparisons (p=0.05 for both). The interaction was significant for myonuclear area (0.001<p<0.01) but not for TnT- nuclear area (p=0.37) confirming that ethanol induced activation of Notch signaling affects myotubes.

The only parameter in the dually treated cells that exceeded levels seen in vehicle was an increase in TnT+ cell number. The other parameter that was different between the two groups was the decrease in reserve cell number in cells treated with ethanol and GSI compared to vehicle. These results suggest that the pool of differentiation committed cells is increased in the dually treated

cells due to blockage of endogenous Notch signaling by GSI. The effect of increasing the number of cells committed to differentiation would also increase fusion events which would explain the improvements seen in myotube protein content, morphology and myonuclear number to restore some of the effects of inhibition of C2C12 differentiation by ethanol.

Ethanol reduces N1-ICD levels and the CD34- reserve cell population during C2C12 differentiation

Signaling through Notch1 is important to maintain the satellite cell pool in postnatal myogenesis. Activation of Notch1 has been reported to promote the self-renewal of satellite cells and blocking Notch1 causes commitment of progenitor cells to the myoblast lineage and the differentiation of reserve cells in C2.7 myoblasts [36, 41, 138]. Activation of the Notch ligand, Delta-1 is reported to activate Notch 1 signaling and to inhibit C2C12 differentiation [16, 19].

Therefore I compared the levels of Notch1 on the microarray and the levels of Notch1-ICD (N1-ICD) by western blotting between control and ethanol treated C2C12 cells during the first three days of differentiation.

During C2C12 differentiation, compared to GM, Notch1 mRNA levels increased on day 1, (FC=1.27, p=0.055); did not change on day 2 (FC= - 1.01, p=0.92); and increased again on day3, (FC=1.29, p=0.035). This suggests that the induction of differentiation by serum withdrawal causes an increase in the number of Notch1 expressing cells on day 1 to increase the satellite cell pool. On day 2 the levels of Notch1 expressing cells are the same as in GM suggesting that the Notch1 expression is down-regulated. On day 3 the levels of

Notch1 start increasing again which may reflect renewal of the satellite cell pool.

In ethanol treated cells, Notch1 levels remained constant compared to controls

on day 1, (FC= - 1.01, p=0.93) suggesting no effect of ethanol. On day 2, Notch1

levels were still fairly constant, (FC= - 1.06, p=0.63) but on day 3 Notch1 levels

decreased significantly (FC= - 1.40, p=0.008) suggesting that ethanol reduces

the number of Notch1 expressing cells during differentiation and perhaps inhibits

self-renewal of the satellite cell pool.

I measured the effect of ethanol on levels of N1-ICD during the first 3 days

of differentiation. N1-ICD protein levels were constant the first two days of

C2C12 differentiation and decreased to nearly undetectable levels on day 3 (data

not shown). Ethanol did not affect N1-ICD protein levels on the first day of

differentiation (data not shown) but decreased the level of N1-ICD protein by ~

50% (p=0.03) after two days (**figure 5.4**). These data show that ethanol

decreases the number of cells that express N1-ICD or the levels of N1-ICD per

cell. The presence of the GSI, DAPT or L-685, 458 during C2C12 differentiation

did not change the levels of N1-ICD protein (p = 0.20) compared to vehicle which

is expected since blocking the
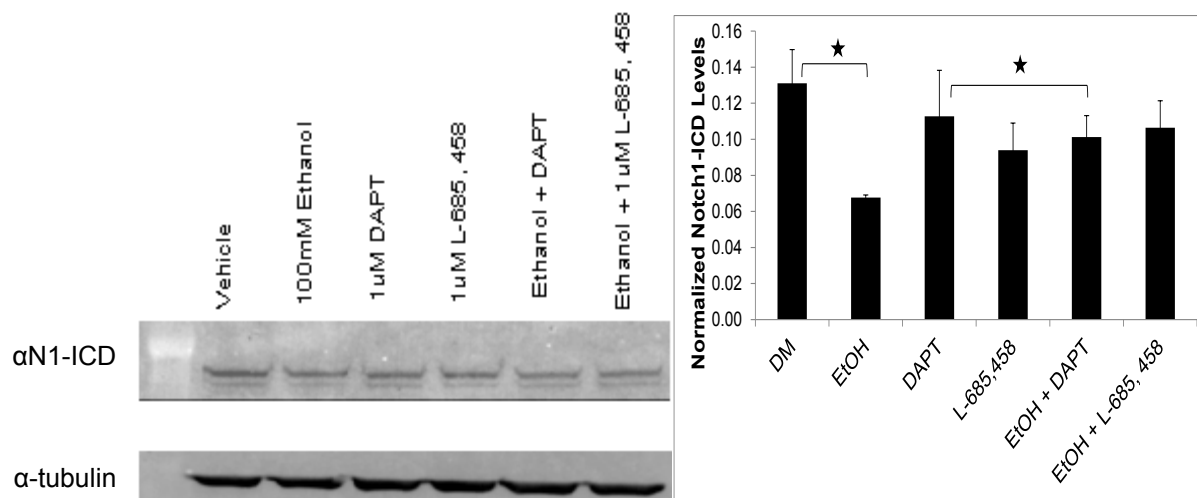
Figure 5.4: Ethanol decreases Notch1-ICD protein in differentiating C2C12 cells.
C2C12 cells were differentiated in DM ± 100mM EtOH ± 1uM DAPT ± L-685, 458 for
2 days. Protein was extracted from cells and 50ug of total protein was used for
western blot analysis. Blots were probed with anti-Notch1-ICD mouse monoclonal
antibody(top) and anti-α-tubulin mouse monoclonal antibody (bottom). Bands were
visualized using chemiluminescence, quantified and analyzed by Image Software.
The α-tubulin band was used as the loading control. The averages are shown ± SEM,
$p \leq 0.05$ (n=3).

final Notch cleavage event should not result in any change in endogenous N1-ICD levels. Co-administration of DAPT or L-685, 458 and ethanol during C2C12 differentiation increased N1-ICD levels by ~ 50% which shows that there is restoration of some Notch1 expressing cells or levels of protein in Notch1 expressing cells. This was accompanied by a non-significant interaction effect by 2-way ANOVA (p=0.20). These data suggest that ethanol does not interfere with Notch1 expressing cells at the site of γ-secretase cleavage.

Finally I examined the effect of ethanol on Notch1 expressing reserve cells which contribute to the maintenance of the satellite cell pool[41]. It has been reported that within the reserve cells of the C2.7 mouse myoblast cell line, there is a population of CD34- cells which express Notch1 and blocking Notch signaling with DAPT or the Notch inhibitor, Numb, causes them to fuse into myotubes[41]. I examined the population of CD34-/+ cells within the C2C12 cell line 7 days after culture in differentiation medium. Examination of the total reserve cell population showed that the CD34 – cell number comprised the majority (~ 88%) and CD34+ cells comprised ~ 12% (**figure 5.5a**). These results follow trends of previously reported ratios for CD34 – cells comprising ~ 67% and CD34+ cells comprising ~ 33% of total reserve cells in the C2.7 cell line after 4 days in DM[41].
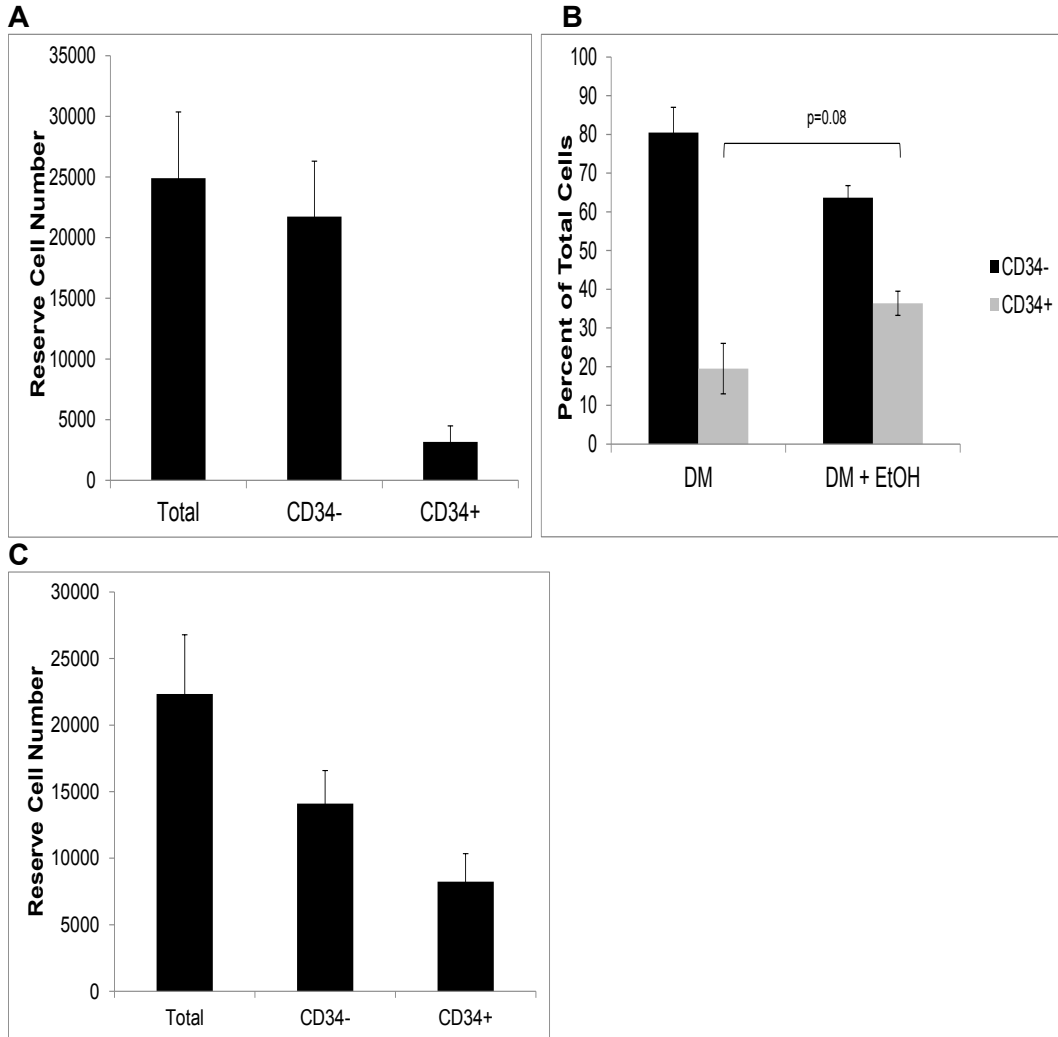
Figure 5.5: Ethanol shifts the ratio of CD34-/+ cells during differentiation.
C2C12 cells were induced to differentiate for 7 days in DM ± 100mM EtOH and
reserve cells were isolated (see Methods) and cell numbers were determined by
FACs **(A)** Total cell number and CD34 – and CD34+ cells in DM. **(B)** Percent of
total and CD34+/- cells in DM containing EtOH. **(C)** Total and CD34- and CD34+
% expressing cells in DM ± EtOH. The averages are shown ± SEM, *p≤ 0.05
(n=3).

The presence of ethanol nearly doubled the percentage of CD34+ cells to 36% compared to 19% present in controls (**figure 5.5b**) and this difference trended towards significance (p=0.08). The morphology of the reserve cells isolated from the control dishes was round which has been previously reported to describe quiescent cells whereas those in the ethanol treated dishes had a stellate appearance which suggests the cells in the ethanol dishes were displaying increased differentiation. Since the total number of reserve cells was not decreased by ethanol treatment (**figure 5.5c**) and the percent of CD34+ cells was increased, these results suggest that ethanol causes the premature differentiation of the CD34- population into CD34+ cells. Since the CD34- cells are reported to express Notch1, my previous findings that Notch1 expression disappears during ethanol induced C2C12 differentiation suggests that ethanol induces loss of Notch1 expressing cells early in differentiation to decrease the number of quiescent reserve cells.

Discussion

The present study demonstrates that ethanol activates Notch signaling during C2C12 differentiation to inhibit terminal differentiation events. Blocking ethanol induced Notch activation with a GSI completely restored the myogenic fusion index but was not sufficient to restore individual cellular parameters to the level seen in vehicle treated cells. Since this rescue was accompanied by an increase in MyoD of ~ 14%, this suggests that blocking ethanol induced Notch activation increases the number of committed cells participating in differentiation. Notch signaling has also been reported to inhibit myogenin independently of

MyoD[16]. The combination of MyoD dependent and independent effects on myogenin may increase its levels sufficiently to effect restoration of C2C12 differentiation. This hypothesis would need to be tested.

The data further suggest that a biological interaction occurs between ethanol and L-685, 458, perhaps this interaction occurs to impact fusion events between TnT+ cells. If ethanol causes a fusion defect then alleviation of this defect might explain the increase in myonuclear number, and the modest improvement seen in almost all cellular parameters. In *Drosophila*, Notch signaling regulates a protein that has been shown to regulate myoblast fusion[150]. The effect of Notch signaling and ethanol on myocyte fusion would need to be investigated further.

Since blocking Notch activation partially restored levels of MyoD this suggests that the increase in MyoD may be the causative factor which caused the partial rescue in differentiation. Notch signaling has been reported to inhibit C2C12 differentiation by a CBF1 and a CBF1 independent pathway[151]. The CBF1 independent pathway is reported to inhibit general cellular differentiation. In C2C12 cells in which Notch signaling is induced independently of CBF1, the transduction of MyoD causes differentiation to proceed[151]. It has been reported that the CBF1 dependent pathway functions to reinforce the general block in cellular differentiation and does not depend on Hes-1 expression [151]. This suggests that increasing MyoD levels further in C2C12 cells differentiating in the presence of ethanol may completely rescue differentiation.

The presence of ethanol and GSI partially restored ethanol induced decreases in N1-ICD protein. MyoD protein has been shown to activate Notch signaling by increasing Delta-1 expression[152]. Since Delta-1 activates Notch1 signaling, MyoD may be increasing levels of N1-ICD levels but this would need to be investigated further.

Ethanol was predicted to decrease reserve cell number independently of Notch activation. Ethanol shifted the ratio of CD34-:CD34+ reserve cell number towards an increase to the more differentiated CD34+ population without decreasing total cell number. It has been shown that reserve cells that are CD34- express Notch 1 and when the cells are treated with a GSI, their numbers decrease due to their differentiation and fusion into myotubes [41]. My data suggest that ethanol inhibits Notch1 signaling in reserve cells to decrease the number of Notch1; CD34- progenitor cells by promoting their differentiation. This hypothesis requires further investigation.

In summary the data suggest that ethanol modulates Notch signaling to inhibit C2C12 differentiation.

Chapter 6: Conclusions

In this thesis I investigated the hypothesis that ethanol affects the muscle stem cell population to inhibit myoblast differentiation which contributes to the etiology of alcoholic muscle disease. Using the C2C12 mouse myogenic cell line as a model to study events in muscle regeneration, I show that ethanol inhibits the differentiation of C2C12 cells (**figure 3.4**) decreases the expression of myogenic regulatory factors (**figure 4.3**) and activates the Notch signaling pathway to inhibit the myogenic fusion index (**figure 5.3**). In parallel I discovered that initially ethanol increases proliferation of reserve cells even at doses as low as 17mM (**figure 4.10a**) which may contribute to an initial increase of hypertrophic TnT+ cells (**figure 4.10d,f**) but the continued presence of ethanol during differentiation eventually reduces the number of reserve cells (**figure 4.10b,c; figure 3.4**), including the population of quiescent reserve cells (**figure 5.5**) and the myotubes which subsequently form are more numerous but smaller than those which form in controls (**figure 3.4**). My results indicate that blocking ethanol induced Notch activation during C2C12 differentiation restores fusion events in myocytes (**figure 5.3a**). Through transcriptional profiling I discovered that of all the MRFs reduced by ethanol during differentiation, MyoD was predicted to be the most affected by ethanol ($p=8.7X10^{-4}$) and network analysis (**figure 4.9**) predicted that one mechanism for inhibition of differentiation may be reduced MyoD acetylation. **Figure 6.1** displays a model to explain the pleiotropic effects of ethanol on C2C12 differentiation.
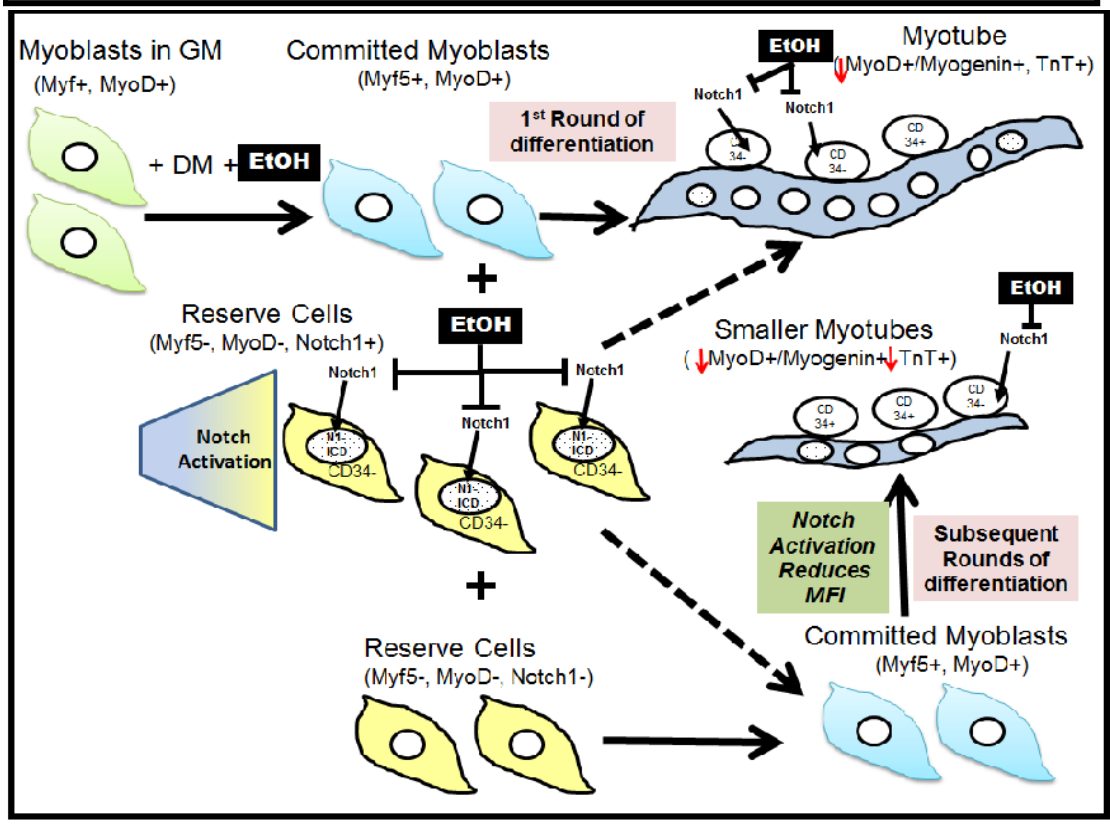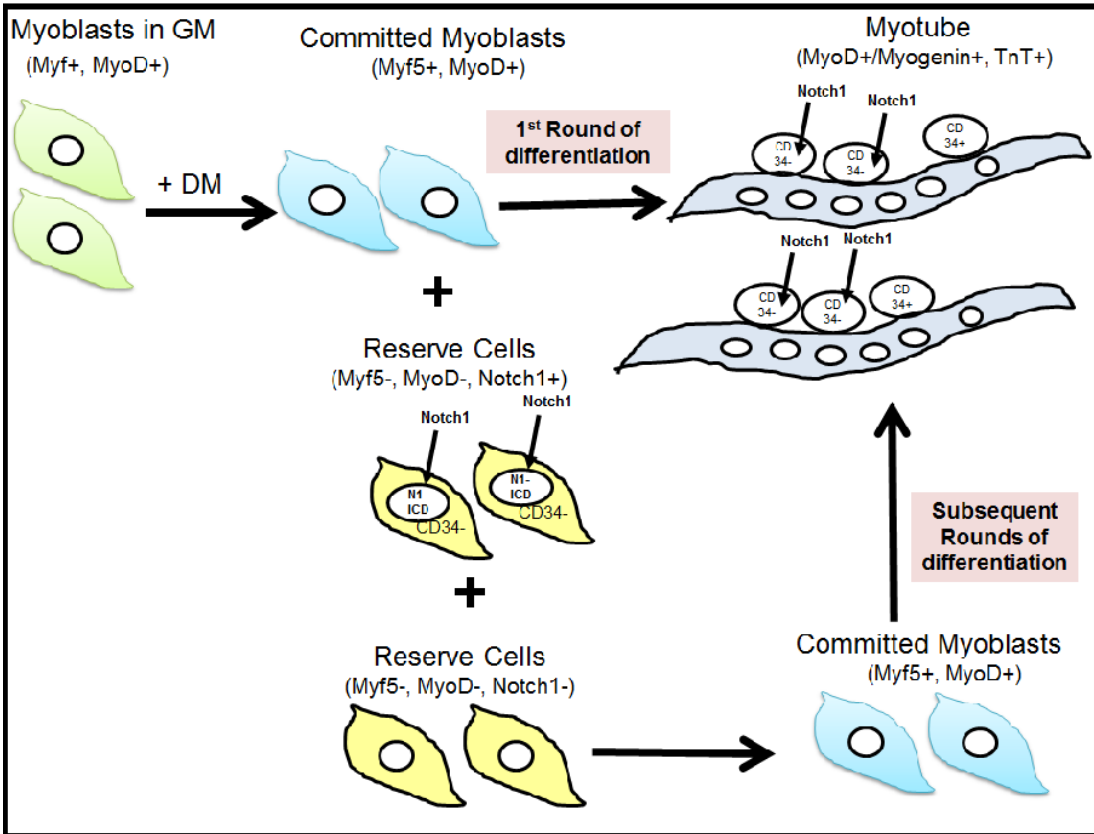
Figure 6.1: Ethanol accelerates differentiation of reserve cells and reduces differentiation capability of committed myoblasts to inhibit C2C12 myogenesis. Ethanol modulates Notch signaling and inhibits MyoD to inhibit C2C12 differentiation. Notch activation may increase the number of Notch1 expressing quiescent CD34- reserve cells. Ethanol inhibits Notch1 activation in quiescent CD34- reserve cells perhaps by interfering with receptor function. Prevention of Notch activation causes the Notch1 expressing CD34- quiescent reserve cells to differentiate and fuse causing formation of hypertrophic myotubes. With every consecutive round of ethanol driven differentiation the number of Notch1 expressing cells that ethanol can propel towards differentiation into myotubes is reduced. In committed myoblasts, ethanol inhibits MyoD, partially by inducing Notch activation and by other mechanisms, one of which may be a reduction in MyoD acetylation. Reduced MyoD functionality may impair the differentiation potential of committed cells and the inhibition of fusion events by Notch activation causes smaller myotubes to form during differentiation. Decreases in quiescent CD34- cells by ethanol are predicted to eventually deplete the satellite cell pool.

Verification of this model would require 1) testing whether Notch is activated by ethanol 7 days into differentiation 2) testing whether MyoD functionality is diminished due to reduced acetylation by ethanol during C2C12 differentiation and 3) tracking the Notch1 expressing cells during ethanol driven C2C12 differentiation and determining their identity as the CD34- cells.

Several proof-of-principle experiments can be envisaged. One experimental approach would be to over-express MyoD into C2C12 cells and see if ethanol driven differentiation is rescued. Another experiment would involve differentiation of C2C12 cells in the presence of ethanol for several days, followed by removal of ethanol and continuation of the differentiation for several more days and looking for any increase in the number of CD34- cells. To test whether the quiescent CD34- reserve cells are essential to maintain the C2C12 culture in the presence of ethanol one could differentiate the culture in the presence of ethanol and at multiple time points, measure the number of CD34- cells until the cultures dies off. If a correlation is found between cell death and reduced CD34- cell number in ethanol cultures, this would support the hypothesis that the quiescent reserve cells are essential for maintenance of the culture and that ethanol causes their depletion.

It would be useful to extend these studies to human myoblast cultures to see whether the findings in C2C12 cells are potentially translatable to humans. It would be interesting to perform in vivo studies in ethanol fed mice. Wild type mice have been reported to display abnormal muscle fiber morphology after ethanol feeding. Gene delivery of a MyoD or Notch1 transgene to the

gastrocnemius muscles of the alcohol fed mice would show whether these are sufficient to restore muscle mass and weakness and whether these therapies are well tolerated.

It is interesting that Notch and alcohol are implicated in many studies including the aspect of ethanol reward in studies of ethanol addiction in flies [153]. Currently there is no compelling evidence that there exists a ubiquitous alcohol receptor. Notch is an attractive candidate as the 'alcohol receptor'. Ethanol affects every system in the body and Notch signaling is critical for development, differentiation and homeostasis. It has been reported that ethanol interacts with a hydrophobic pocket on a neuronal membrane receptor[154]. There are reports of assays which measure ligand and ligand-independent Notch activation in real time at the single cell level [155, 156]. Ethanol may affect the Notch receptor upstream of GSI so studying the effect of ethanol on Notch signaling using one of these assays might yield an answer.

In this thesis I have provided experimental evidence for some of the harmful effects of ethanol on muscle cell differentiation which correlates with adverse effects reported by other researchers for ethanol's effects on skeletal muscle. As I researched this topic beyond the scope of myogenesis, I found even more evidence for the harmful effects of ethanol. Ethanol increases cancer risk by 10% in men and 3% in women and is the second leading cause of death in the industrialized world after tobacco[157]. Meta analyses of studies which claim cardioprotective effects of moderate ethanol consumption (1-2 drinks/day) report that these studies have systematically misclassified persons in ill health as

155

abstainers and heterogeneity across studies negates cardioprotective associations for moderate drinking in ischaemic heart disease[158-160]. There is increasing recognition that a randomized carefully controlled study is needed to truly assess whether ethanol has any protective effects against heart disease.

It is increasingly clear that ethanol should not be considered as a nutrient. There should be no place for it in the American Dietary Guidelines along with recommendations for consumption [161]. Finding ethanol in government guidelines suggests to young people that alcohol consumption is healthy. The alcohol industry aggressively promotes its products to youth[157] in much the same way as the tobacco industry did. There is concern that human adolescent brains are still developing and alcohol interferes with that development and increases the risk of addition [162]. Problem drinking during adolescence increases the number of adults with drinking problems and those who are addicted to alcohol. Yet the responsibility for problem drinking is squarely placed on the shoulders of the addict while the US$150 billion alcohol industry business is absolved of any responsibility for its marketing tactics[157]. It is time to take the alcohol industry to task, and it is possible, given that the tobacco industry has been brought to heel.

The alcohol industry funds alcohol research to demonstrate it is committed to social responsibility. However a review of the evidence suggests that the funding provided by the alcohol industry to scientific research will not contribute to breakthroughs nor alleviate in any meaningful way the health issues stemming from alcohol use[163]. Furthermore there is an increasing consensus that the

financial relationships of researchers has the potential to compromise research

results and that guidelines should be established to maintain scientific

integrity[164]. Awareness that the alcohol industry will continue to promote its

product as healthy and fun to the general public and cognizance of its increasing

influence in scientific research underscores the necessity of rigorous scientific

design and experimentation when investigating the effects of this drug.

Appendix

Journal 8 Algorithm

Z:\Equipment\ImageXpress\Michell...\Michelle_Arya_8.jnl
Page 1 of 8

New Journal

Open .tif image for shading correction.
IF ImageExists("Background") THEN
ELSE

1: Open("background")
END IF
2: Set Image Zoom("background", 20)
3: Zoom To Fit("background")
File name for DAPI and FITC images.
DAPI = "DAPI - Pos 1"
FITC = "FITC - Pos 2"
BGimage = "background"
LogicalRoute = 0
(Disabled)4: Clear All Regions("AND nuclei")

5: Clear All Regions("%FITC%")
(Disabled)6: Clear All Regions("FITCShadcorr")
7: Clear All Regions("DAPI - Pos 1")
(Disabled)8: Clear All Regions("Color Combine")
Resizing DAPI and FITC images for overlay.

9: Scale Image("%FITC%", NOAUTOSCALE, 70, 1500)
10: Scale Image("%DAPI%", NOAUTOSCALE, 255, 2000)
File name for overlay

11: Select Image("%DAPI%")
StageLabelModifier = instr(Image.StageLabel,":")
LeftStageLabelModifier = StageLabelModifier - 1
RightStageLabelModifier = INSTR(Image.StageLabel,"Site")
LeftStageLabel = LEFT(Image.StageLabel,LeftStageLabelModifier)

RightStageLabel = Right(Image.StageLabel,RightStageLabelModifier)
ModifiedStageLabel = LeftStageLabel+RightStageLabel
BaseDirectory =
"c"+Right(Journal.RunJournalLastDirectory,Len(Journal.RunJournalLastDirectory
)-1)
SaveDirectory = BaseDirectory + Review.PlateName +"_PlateID_"+
STR(Review.PlateID)+"\"+left(Image.StageLabel,3)+"\"
CreateSaveDirectory = BaseDirectory + Review.PlateName +"_PlateID_"+
STR(Review.PlateID)+"\"
SaveFileName = Review.PlateName+"-"+ModifiedStageLabel+" v"
LogSiteID = VAL(Right(Image.StageLabel,RightStageLabelModifier-5))
Create images save directory

12: DirectoryCreator = New(512, 480, 1, 0)
13: Setup Sequential File Names("c:\Journal Image Output\MA5\Michelle Plate 1
re-acquire - 1\", "DirectoryCreator", ALWAYSOVERWRITE, Base name =
"DirectoryCreator"
Directory = CreateSaveDirectory
14: Save Using Sequential File Name("DirectoryCreator")
15: Close("DirectoryCreator1")
Count total number of nuclei using DAPI

16: Pause Data Logging()
17: Stop/Resume Logging to Database(Stop Logging)
18: Configure Count Nuclei Data Log()
19: Overwrite "CountNuclei" = Count Nuclei(Src="%DAPI%")
20: Configure Count Nuclei Summary Log()
TotalNuclei = CountNuclei.TotalNuclei
TotalNuclearArea = CountNuclei.TotalArea
TotalIntegratedNuclearIntensity = CountNuclei.IntegratedIntensity
Shading correction (Newly added to improve the threshold performance).

21: Overwrite "FITCShadcorr" = Background and Shading Correction("%FITC%",
"%BGimage%", [None], 1, 1)
22: Scale Image("FITCShadcorr", NOAUTOSCALE, 70, 1000)

(Disabled)23: Close("background")

Create regions of FITC positive cell, modified, instead of "%FITC%" it is now "FITCShadcorr".

24: Threshold Image("FITCShadcorr", 80, 65535)
25: Overwrite "FITC Binary" = Binarize("FITCShadcorr"), 80, 65535
26: Integrated Morphometry - Load State("Green cell 75 lower area cutoff with no upper area cutoff")
27: Integrated Morphometry - Measure("FITCShadcorr", -1)
28: Create Regions Around Objects("FITCShadcorr")
29: Resequence Region Labels("FITCShadcorr")
30: Threshold Image("FITCShadcorr", 0, 65535)
Create images of DAPI overlap with FITC

31: Threshold Image("CountNuclei", 1, 65535)
32: Overwrite "NucleiBinary" = Binarize("CountNuclei"), 1, 65535
33: Overwrite "AND nuclei temp" = "%DAPI%" AND "NucleiBinary"
34: Overwrite "AND nuclei" = "AND nuclei temp" AND "FITC Binary"
35: Threshold Image("AND nuclei", 1, 65535)
36: Integrated Morphometry - Load State("Partial Nuclei cutoff by area and perimeter")
37: Integrated Morphometry - Measure("AND nuclei", -1)
38: Create Regions Around Objects("AND nuclei")
39: Resequence Region Labels("AND nuclei")
40: Transfer Regions("AND nuclei", "%DAPI%", ALLREGIONS and CLEARSOURCE)
41: Select Image("%DAPI%")
NumberOfNucleiRegion = val(Region.Label)
Condition test switches (should normally be disabled).
NumberOfNucleiRegion = 0
TotalNuclei = 0

Check to see if there is any nucleus or any nucleus with green cell. If there is none. All parameters expect

IF (NumberOfNucleiRegion = 0) or (TotalNuclei = 0) THEN

160

If there is no nuclei in green cells, all parameters except the following will be 0: TotalNonGreenNuclei, TotalNonGreenNuclearArea & TotalNonGreenIntegratedNuclearIntensity

Create DAPI/FITC combined images with FITC regions, annotations and some data.

42: Preferences()
43: Overwrite "Color Combine" = Color Combine([None], "FITCShadcorr", "%DAPI%")
44: Set Image Zoom("Color Combine", 50)
(Disabled)45: Transfer Regions("FITCShadcorr", "Color Combine", ALLREGIONS)
46: Select Region("Color Combine", "0")
47: Calibration Bar(X Position = 1300, Y Position = 1000)
48: Preferences()
Set all parameter to 0 should there is no nuclei in green cells.
CellArea = 0
CellIntegratedIntensity = 0
CellLength = 0
CellBreath = 0
CellShapeFactor = 0
CellPerimeter = 0
CellOrientation = 0
RegionalNucleiCount = 0
RegionalTotalNuclearIntensity = 0
RegionalNuclearArea = 0
DifferentiationFactor1 = 0
DifferentiationFactor2 = 0
DifferentiationFactor3 = 0
TotalGreenNuclei = 0
TotalGreenNuclearArea = 0
TotalGreenNuclearIntegratedIntensity = 0

TotalGreenArea = 0
TotalGreenAreaWithNuclei = 0
GreenCellWithNuclei = 0
CellNumber = 0
IF TotalNuclei = 0 THEN

TotalNonGreenNuclei = 0
TotalNonGreenNuclearArea = 0
TotalNonGreenIntegratedNuclearIntensity = 0
LogicalRoute = 1

ELSE
TotalNonGreenNuclei = TotalNuclei
TotalNonGreenNuclearArea = TotalNuclearArea
TotalNonGreenIntegratedNuclearIntensity = CountNuclei.IntegratedIntensity
LogicalRoute = 2

END IF

49: Stop/Resume Logging to Database(Resume Logging)
50: Set Cell Number for Database Logging()
Cell Number = 1
Object Data

51: Log Variable(LogSiteID, NEWLINE, HEADER)
52: Log Variable(CellArea, NEWLINE, HEADER)
53: Log Variable(CellIntegratedIntensity, NEWLINE, HEADER)
54: Log Variable(CellLength, NEWLINE, HEADER)
55: Log Variable(CellBreath, NEWLINE, HEADER)
56: Log Variable(CellShapeFactor, NEWLINE, HEADER)
57: Log Variable(CellPerimeter, NEWLINE, HEADER)
58: Log Variable(CellOrientation, NEWLINE, HEADER)
59: Log Variable(RegionalNucleiCount, NEWLINE, HEADER)
60: Log Variable(RegionalTotalNuclearIntensity, NEWLINE, HEADER)
61: Log Variable(RegionalNuclearArea, NEWLINE, HEADER)
62: Log Variable(DifferentiationFactor1, NEWLINE, HEADER)
63: Log Variable(DifferentiationFactor2, NEWLINE, HEADER)

64: Log Variable(DifferentiationFactor3, NEWLINE, HEADER)
Summary Data
65: Log Variable(CellNumber, NEWLINE, HEADER)
66: Log Variable(GreenCellWithNuclei, NEWLINE, HEADER)
67: Log Variable(TotalGreenAreaWithNuclei, NEWLINE, HEADER)
68: Log Variable(TotalNuclei, NEWLINE, HEADER)
69: Log Variable(TotalGreenNuclei, NEWLINE, HEADER)
70: Log Variable(TotalNonGreenNuclei, NEWLINE, HEADER)
71: Log Variable(TotalGreenNuclearArea, NEWLINE, HEADER)
72: Log Variable(TotalNonGreenNuclearArea, NEWLINE, HEADER)
73: Log Variable(TotalGreenNuclearIntegratedIntensity, NEWLINE, HEADER)
74: Log Variable(TotalNonGreenIntegratedNuclearIntensity, NEWLINE, HEADER)
Image header label and scale. (when no cells/nucleus or no green cell)
75: Text("Color Combine", 5, 1, 1, 0, 255, Arial, Bold, 20, "%Image.StageLabel% Cell:%GreenCellWithNuclei% Cell area 76: Stop/Resume Logging to Database(Stop Logging)
Images close down
77: Threshold Image("%DAPI%", 0, 65535)
78: Clear All Regions("%DAPI%")
79: Close("NucleiBinary")
80: Close("AND nuclei temp")
IF ImageExists("GreenNucleiPickTemp") THEN
81: Close("GreenNucleiPickTemp")
ELSE
END IF
82: Close("CountNuclei")
83: Close("FITC Binary")
(Disabled)84: Close("FITCShadcorr")

ELSE
If there is nuclei in green region

85: Threshold Image("%DAPI%", 1, 65535)
86: Select Region("%DAPI%", "1")
87: Overwrite "GreenNucleiPick" = Binarize("%DAPI%"), 1, 65535
k = 2
WHILE k <= NumberOfNucleiRegion DO
88: Select Region("%DAPI%", "%k%")
89: Overwrite "GreenNucleiPickTemp" = Binarize("%DAPI%"), 1, 65535
90: Overwrite "GreenNucleiPick" = "GreenNucleiPick" OR
"GreenNucleiPickTemp"
k = k + 1
WEND

91: Overwrite "AND nuclei" = "AND nuclei" AND "GreenNucleiPick"
92: Threshold Image("%DAPI%", 0, 65535)
93: Clear All Regions("%DAPI%")
94: Close("NucleiBinary")
95: Close("AND nuclei temp")
IF ImageExists("GreenNucleiPickTemp") THEN
96: Close("GreenNucleiPickTemp")
ELSE
END IF
97: Close("GreenNucleiPick")
98: Close("CountNuclei")
99: Close("FITC Binary")
Calculating various parameters of green cells.

100: Preferences()
101: Transfer Regions("FITCShadcorr", "AND nuclei", ALLREGIONS)
102: Select Image("AND nuclei")
NumberOfRegion = val(Region.Label)
Create DAPI/FITC combined images with FITC region

103: Preferences()
104: Overwrite "Color Combine" = Color Combine([None], "FITCShadcorr",
"%DAPI%")

105: Set Image Zoom("Color Combine", 50)
106: Transfer Regions("FITCShadcorr", "Color Combine", ALLREGIONS)
107: Select Region("Color Combine", "0")
108: Calibration Bar(X Position = 1300, Y Position = 1000)
109: Preferences()
Check to see if there is any green cell.
IF NumberOfRegion = 0 THEN
If there is not green cell, all green cell parameters are set to 0.

110: Stop/Resume Logging to Database(Resume Logging)
111: Set Cell Number for Database Logging()
Cell Number = 1
CellArea = 0
CellIntegratedIntensity = 0
CellLength = 0
CellBreath = 0
CellShapeFactor = 0
CellPerimeter = 0
CellOrientation = 0
RegionalNucleiCount = 0
RegionalTotalNuclearIntensity = 0
RegionalNuclearArea = 0
DifferentiationFactor1 = 0
DifferentiationFactor2 = 0

DifferentiationFactor3 = 0
CellNumber = 0
GreenCellWithNuclei = 0
TotalGreenNuclei = 0
TotalGreenNuclearArea = 0
TotalGreenNuclearIntegratedIntensity = 0
TotalGreenArea = 0
TotalNonGreenNuclei = TotalNuclei
TotalNonGreenNuclearArea = TotalNuclearArea
TotalNonGreenIntegratedNuclearIntensity = TotalIntegratedNuclearIntensity
TotalGreenAreaWithNuclei = 0
LogicalRoute = 3

112: Log Variable(LogSiteID, NEWLINE, HEADER)
113: Log Variable(CellArea, NEWLINE, HEADER)
114: Log Variable(CellIntegratedIntensity, NEWLINE, HEADER)
115: Log Variable(CellLength, NEWLINE, HEADER)
116: Log Variable(CellBreath, NEWLINE, HEADER)
117: Log Variable(CellShapeFactor, NEWLINE, HEADER)
118: Log Variable(CellPerimeter, NEWLINE, HEADER)
119: Log Variable(CellOrientation, NEWLINE, HEADER)
120: Log Variable(RegionalNucleiCount, NEWLINE, HEADER)
121: Log Variable(RegionalTotalNuclearIntensity, NEWLINE, HEADER)
122: Log Variable(RegionalNuclearArea, NEWLINE, HEADER)
123: Log Variable(DifferentiationFactor1, NEWLINE, HEADER)
124: Log Variable(DifferentiationFactor2, NEWLINE, HEADER)
125: Log Variable(DifferentiationFactor3, NEWLINE, HEADER)
126: Log Variable(CellNumber, NEWLINE, HEADER)
127: Log Variable(GreenCellWithNuclei, NEWLINE, HEADER)
128: Log Variable(TotalGreenAreaWithNuclei, NEWLINE, HEADER)
129: Log Variable(TotalNuclei, NEWLINE, HEADER)
130: Log Variable(TotalGreenNuclei, NEWLINE, HEADER)
131: Log Variable(TotalNonGreenNuclei, NEWLINE, HEADER)
132: Log Variable(TotalGreenNuclearArea, NEWLINE, HEADER)
133: Log Variable(TotalNonGreenNuclearArea, NEWLINE, HEADER)
134: Log Variable(TotalGreenNuclearIntegratedIntensity, NEWLINE, HEADER)
135: Log Variable(TotalNonGreenIntegratedNuclearIntensity, NEWLINE, HEADER)
Image header label and scale. (when no green cell)

136: Text("Color Combine", 5, 1, 1, 0, 255, Arial, Bold, 20, "%Image.StageLabel% Cell:%GreenCellWithNuclei% Cell 137: Stop/Resume Logging to Database(Stop Logging)
ELSE
If there are green cell region.
i = 1
TotalGreenNuclei = 0
TotalGreenArea = 0
TotalGreenNuclearArea = 0
TotalGreenNuclearIntegratedIntensity = 0
GreenCellWithNuclei = 0

138: Preferences()
139: Threshold Image("AND nuclei", 1, 65535)
140: Threshold Image("FITCShadcorr", 80, 65535)
WHILE i <= NumberOfRegion DO
Measure from green cells

141: Stop/Resume Logging to Database(Stop Logging)
142: Select Region("FITCShadcorr", "%i%")
143: Region Measurements("FITCShadcorr", CurrentPlane, Active Region, Milliseconds)
CellArea = RegionMeasurements.Measurements.Area
CellIntegratedIntensity = RegionMeasurements.Measurements.IntegratedIntensity
144: Integrated Morphometry - Load State("Green cell parameters measurement")

145: Integrated Morphometry - Measure("FITCShadcorr", -1)
146: Integrated Morphometry - Log Data("FITCShadcorr", OBJECTS, CURRENTDATA, 1, 2)
CellLength = IMAObjectData.Length
CellBreath = IMAObjectData.Breadth
CellShapeFactor = IMAObjectData.ShapeFactor
CellPerimeter = IMAObjectData.Perimeter
CellOrientation = IMAObjectData.Orientation
Measurement of nuclei
147: Select Image("AND nuclei")
148: Select Region("AND nuclei", "%i%")
149: Region Measurements("AND nuclei", CurrentPlane, Active Region, Milliseconds)
RegionalTotalNuclearIntensity = RegionMeasurements.Measurements.IntegratedIntensity
RegionalNuclearArea = RegionMeasurements.Measurements.ThresholdArea
150: Integrated Morphometry - Load State("NucleiMeasurement")
151: Integrated Morphometry - Measure("AND nuclei", -1)
152: Integrated Morphometry - Log Data("AND nuclei", SUMMARY, CURRENTDATA, 1, 2)
RegionalNucleiCount = IMASummary.Count
Check to see if there is nucleus in the green region
IF RegionalNucleiCount = 0 THEN
If there is no nucleus in the green region, all the green cell associated parameters are set to 0
TotalGreenNuclei = TotalGreenNuclei + 0
TotalGreenArea = TotalGreenArea + 0
TotalGreenNuclearArea = TotalGreenNuclearArea + 0
TotalGreenNuclearIntegratedIntensity = TotalGreenNuclearIntegratedIntensity + 0
GreenCellWithNuclei = GreenCellWithNuclei + 0
CellArea = 0
CellIntegratedIntensity = 0
CellLength = 0
CellBreath = 0
CellShapeFactor = 0
CellPerimeter = 0
CellOrientation = 0

153: Select Image("Color Combine")
154: Select Region("Color Combine", "%i%")

168

155: Delete Active Region()
ELSE
If there is nucleus in green region, all the parameters measured above is reported, and the site total parameters TotalGreenNuclei = TotalGreenNuclei + RegionalNucleiCount
TotalGreenArea = TotalGreenArea + CellArea
TotalGreenNuclearArea = TotalGreenNuclearArea + RegionalNuclearArea
TotalGreenNuclearIntegratedIntensity = TotalGreenNuclearIntegratedIntensity + RegionalTotalNuclearIntensity
GreenCellWithNuclei = GreenCellWithNuclei + 1
x = GreenCellWithNuclei
Log parameters into database
IF RegionalNucleiCount = 0 THEN

DifferentiationFactor1 = 0
DifferentiationFactor2 = 0
DifferentiationFactor3 = 0
CellDifferentiationFactor = 0

ELSE
DifferentiationFactor1 = CellArea / (RegionalNuclearArea + 0.000000000000001)
DifferentiationFactor2 = (CellArea / RegionalNuclearArea) / (CellShapeFactor + 0.000000000000001)
DifferentiationFactor3 = (CellArea / RegionalNuclearArea) / CellShapeFactor * RegionalNucleiCount
CellDifferentiationFactor = CellArea / CellShapeFactor * (CellIntegratedIntensity/CellArea)

END IF
DFpoint = INSTR(STR(DifferentiationFactor1),".") + 2
DF = LEFT(STR(DifferentiationFactor1),DFpoint)
CDF = LEFT(STR(CellDifferentiationFactor),4)

156: Stop/Resume Logging to Database(Resume Logging)
157: Set Cell Number for Database Logging()

Cell Number = x

158: Log Variable(LogSiteID, NEWLINE, HEADER)
159: Log Variable(CellArea, NEWLINE, HEADER)
160: Log Variable(CellIntegratedIntensity, NEWLINE, HEADER)
161: Log Variable(CellLength, NEWLINE, HEADER)
162: Log Variable(CellBreath, NEWLINE, HEADER)
163: Log Variable(CellShapeFactor, NEWLINE, HEADER)
164: Log Variable(CellPerimeter, NEWLINE, HEADER)
165: Log Variable(CellOrientation, NEWLINE, HEADER)
166: Log Variable(RegionalNucleiCount, NEWLINE, HEADER)
167: Log Variable(RegionalTotalNuclearIntensity, NEWLINE, HEADER)
168: Log Variable(RegionalNuclearArea, NEWLINE, HEADER)
169: Log Variable(DifferentiationFactor1, NEWLINE, HEADER)
170: Log Variable(DifferentiationFactor2, NEWLINE, HEADER)
171: Log Variable(DifferentiationFactor3, NEWLINE, HEADER)
(Disabled)172: Stop/Resume Logging to Database(Stop Logging)
Site objection summary generation
TBD.
Check to see if there is nucleus in the green region before drawing on the reference image.

IF RegionalNucleiCount <> 0 THEN
If there is nucleus, the region is drawn and labelled using the label positioning routine.
Label positioning routine.
IF Region.Left < 696 THEN

xpos = Region.Left + (Region.Width/2)
ELSE
xpos = Region.Left -100
END IF

173: Text("Color Combine", xPos, yPos, 0, 0, 255, Arial, Bold, 20, "R%x%N%RegionalNucleiCount%")
X Position = xpos
Y Position = Region.Top + Region.Height/2 + 5
ELSE

If there is no nucleus, no region is drawn.
END IF
END IF

i = i + 1
WEND

CellNumber = GreenCellWithNuclei
TotalNonGreenNuclei = TotalNuclei - TotalGreenNuclei
TotalNonGreenNuclearArea = TotalNuclearArea - TotalGreenNuclearArea
TotalNonGreenIntegratedNuclearIntensity = TotalIntegratedNuclearIntensity - TotalGreenNuclearIntegratedIntensity
TotalGreenAreaWithNuclei = TotalGreenArea
LogicalRoute = 4

174: Stop/Resume Logging to Database(Resume Logging)
175: Set Cell Number for Database Logging()
Cell Number = 1
176: Log Variable(CellNumber, NEWLINE, HEADER)
177: Log Variable(GreenCellWithNuclei, NEWLINE, HEADER)
178: Log Variable(TotalGreenAreaWithNuclei, NEWLINE, HEADER)
179: Log Variable(TotalNuclei, NEWLINE, HEADER)
180: Log Variable(TotalGreenNuclei, NEWLINE, HEADER)
181: Log Variable(TotalNonGreenNuclei, NEWLINE, HEADER)
182: Log Variable(TotalGreenNuclearArea, NEWLINE, HEADER)
183: Log Variable(TotalNonGreenNuclearArea, NEWLINE, HEADER)
184: Log Variable(TotalGreenNuclearIntegratedIntensity, NEWLINE, HEADER)
185: Log Variable(TotalNonGreenIntegratedNuclearIntensity, NEWLINE, HEADER)
186: Text("Color Combine", 5, 1, 1, 0, 255, Arial, Bold, 20, "%Image.StageLabel% Cell:%GreenCellWithNuclei% Cell (Disabled)187: Stop/Resume Logging to Database(Stop Logging)

Site summary data logJ.
TBD.
END IF
END IF

Comments below apply to all conditions.
Create Reference images

188: Preferences()
189: Select Region("Color Combine", "0")
190: Overwrite "Region Overlay" = As Displayed("Color Combine")
191: Setup Sequential File Names("c:\Journal Image Output\MA5\Michelle Plate 1 re-acquire - 1\", "Michelle Plate 1 re-acquire Base name = SaveFileName Directory = SaveDirectory
192: Save Using Sequential File Name("Region Overlay")
193: Close([Last Result])
Clean up files.

194: Threshold Image("AND nuclei", 0, 65535)
195: Threshold Image("%FITC%", 0, 65535)
196: Clear All Regions("FITCShadcorr")
197: Clear All Regions("AND nuclei")
198: Clear Overlays("FITCShadcorr", OBJECT)
199: Clear Overlays("%DAPI%", CUT and JOIN and OBJECT)
200: Close("AND nuclei")
201: Close("Color Combine")
202: Close("FITCShadcorr")

ABI Taqman Primers/Probes

Gene	TaqMan Primer Catalog Number
MyoD1	Mm00440387_m1
Myf5	Mm00435125_m1
Myogenin	Mm00446194_m1
Mef2c	Mm01340839_m1
Myl1	Mm00659043_m1
Atf3	Mm00476032_m1
Hey1	Mm00468865_m1
Hes1	Mm01342805_m1
Mgp	Mm00485009_m1
Notch1	Mm00435249_m1

References

1. Gilbert, S.F., *Developmental Biology*. 8th ed. 2006, Sunderland, MA: Sinauer Associates, Inc.

2. Kopan, R. and M.X. Ilagan, *The canonical Notch signaling pathway: unfolding the activation mechanism.* Cell, 2009. **137**(2): p. 216-33.

3. Wang, Y.X. and M.A. Rudnicki, *Satellite cells, the engines of muscle repair.* Nat Rev Mol Cell Biol, 2012. **13**(22186952): p. 127-133.

4. Tajbakhsh, S., *Skeletal muscle stem cells in developmental versus regenerative myogenesis.* J Intern Med, 2009. **266**(19765181): p. 372-389.

5. White, R.B., et al., *Dynamics of muscle fibre growth during postnatal mouse development.* BMC Dev Biol, 2010. **10**(20175910): p. 21-21.

6. Hawke, T.J. and D.J. Garry, *Myogenic satellite cells: physiology to molecular biology.* J Appl Physiol, 2001. **91**(11457764): p. 534-551.

7. Yoshida, N., et al., *Cell heterogeneity upon myogenic differentiation: down-regulation of MyoD and Myf-5 generates 'reserve cells'.* J Cell Sci, 1998. **111 (Pt 6)**: p. 769-79.

8. Seale, P., et al., *Pax7 is required for the specification of myogenic satellite cells.* Cell, 2000. **102**(6): p. 777-86.

9. Lepper, C., S.J. Conway, and C.-M. Fan, *Adult satellite cells and embryonic muscle progenitors have distinct genetic requirements.* Nature, 2009. **460**(19554048): p. 627-631.

10. Fukada, S.-i., et al., *Molecular signature of quiescent satellite cells in adult skeletal muscle.* Stem Cells, 2007. **25**(17600112): p. 2448-2459.

11. Braun, T. and M. Gautel, *Transcriptional mechanisms regulating skeletal muscle differentiation, growth and homeostasis.* Nat Rev Mol Cell Biol, 2011. **12**(21602905): p. 349-361.

12. Berkes, C.A. and S.J. Tapscott, *MyoD and the transcriptional control of myogenesis.* Semin Cell Dev Biol, 2005. **16**(16099183): p. 585-595.

13. Bentzinger, C.F., Y.X. Wang, and M.A. Rudnicki, *Building muscle: molecular regulation of myogenesis.* Cold Spring Harb Perspect Biol, 2012. **4**(22300977).

14. Buas, M.F. and T. Kadesch, *Regulation of skeletal myogenesis by Notch.* Exp Cell Res, 2010. **316**(20452344): p. 3028-3033.

15. Sun, J., et al., *Regulation of myogenic terminal differentiation by the hairy-related transcription factor CHF2.* J Biol Chem, 2001. **276**(21): p. 18591-6.

16. Buas, M.F., S. Kabak, and T. Kadesch, *Inhibition of myogenesis by Notch: evidence for multiple pathways.* J Cell Physiol, 2009. **218**(18727102): p. 84-93.

17. Shawber, C., et al., *Notch signaling inhibits muscle cell differentiation through a CBF1-independent pathway.* Development, 1996. **122**(9012498): p. 3765-3773.

18. Kuroda, K., et al., *Delta-induced Notch signaling mediated by RBP-J inhibits MyoD expression and myogenesis.* J Biol Chem, 1999. **274**(10066785): p. 7238-7244.

19. Jarriault, S., et al., *Signalling downstream of activated mammalian Notch.* Nature, 1995. **377**(7566092): p. 355-358.

20. Kopan, R., J.S. Nye, and H. Weintraub, *The intracellular domain of mouse Notch: a constitutively activated repressor of myogenesis directed at the basic helix-loop-helix region of MyoD.* Development, 1994. **120**(7956819): p. 2385-2396.

21. Charge, S.B.P. and M.A. Rudnicki, *Cellular and molecular regulation of muscle regeneration.* Physiol Rev, 2004. **84**(14715915): p. 209-238.

22. Fukada, S.-i., et al., *Hesr1 and Hesr3 are essential to generate undifferentiated quiescent satellite cells and to maintain satellite cell numbers.* Development, 2011. **138**(21989910): p. 4609-4619.

23. Kuang, S., et al., *Asymmetric self-renewal and commitment of satellite stem cells in muscle.* Cell, 2007. **129**(17540178): p. 999-991010.

24. Zammit, P.S., et al., *Muscle satellite cells adopt divergent fates: a mechanism for self-renewal?* J Cell Biol, 2004. **166**(15277541): p. 347-357.

25. Yaffe, D. and O. Saxel, *Serial passaging and differentiation of myogenic cells isolated from dystrophic mouse muscle.* Nature, 1977. **270**(563524): p. 725-727.

26. Stuelsatz, P., et al., *Down-regulation of MyoD by calpain 3 promotes generation of reserve cells in C2C12 myoblasts.* J Biol Chem, 2010. **285**(20139084): p. 12670-12683.

27. Parker, M.H., P. Seale, and M.A. Rudnicki, *Looking back to the embryo: defining transcriptional networks in adult myogenesis.* Nat Rev Genet, 2003. **4**(12838342): p. 497-507.

28. Buckingham, M. and D. Montarras, *Skeletal muscle stem cells.* Curr Opin Genet Dev, 2008. **18**(18625314): p. 330-336.

29. Tsivitse, S., *Notch and Wnt signaling, physiological stimuli and postnatal myogenesis.* Int J Biol Sci, 2010. **6**(20567496): p. 268-281.

30. Rand, M.D., et al., *Calcium depletion dissociates and activates heterodimeric notch receptors.* Mol Cell Biol, 2000. **20**(10669757): p. 1825-1835.

31. Barro, M., et al., *Myoblasts from affected and non-affected FSHD muscles exhibit morphological differentiation defects.* J Cell Mol Med, 2010. **14**(18505476): p. 275-289.

32. Buckingham, M., et al., *The formation of skeletal muscle: from somite to limb.* J Anat, 2003. **202**(12587921): p. 59-68.

33. Bryson-Richardson, R.J. and P.D. Currie, *The genetics of vertebrate myogenesis.* Nat Rev Genet, 2008. **9**(18636072): p. 632-646.

34. Iso, T., L. Kedes, and Y. Hamamori, *HES and HERP families: multiple effectors of the Notch signaling pathway.* J Cell Physiol, 2003. **194**(12548545): p. 237-255.

35. Chu, J., et al., *Repression of activator protein-1-mediated transcriptional activation by the Notch-1 intracellular domain.* J Biol Chem, 2002. **277**(11739397): p. 7587-7597.

36. Conboy, I.M. and T.A. Rando, *The regulation of Notch signaling controls satellite cell activation and cell fate determination in postnatal myogenesis.* Dev Cell, 2002. **3**(12361602): p. 397-409.

37. Schuster-Gossler, K., R. Cordes, and A. Gossler, *Premature myogenic differentiation and depletion of progenitor cells cause severe muscle hypotrophy in Delta1 mutants.* Proc Natl Acad Sci U S A, 2007. **104**(17194759): p. 537-542.

38. Dahlqvist, C., et al., *Functional Notch signaling is required for BMP4-induced inhibition of myogenic differentiation.* Development, 2003. **130**(14597575): p. 6089-6099.

39. Beauchamp, J.R., et al., *Expression of CD34 and Myf5 defines the majority of quiescent adult skeletal muscle satellite cells.* J Cell Biol, 2000. **151**(11121437): p. 1221-1234.

40. Beres, B.J., et al., *Numb regulates Notch1, but not Notch3, during myogenesis.* Mech Dev, 2011. **128**(21356309): p. 247-257.

41. Kitzmann, M., et al., *Inhibition of Notch signaling induces myotube hypertrophy by recruiting a subpopulation of reserve cells.* J Cell Physiol, 2006. **208**(16741964): p. 538-548.

42. Lang, C.H., et al., *Molecular mechanisms responsible for alcohol-induced myopathy in skeletal muscle and heart.* Int J Biochem Cell Biol, 2005. **37**(15982919): p. 2180-2195.

43. Pignataro, L., et al., *The regulation of neuronal gene expression by alcohol.* Pharmacol Ther, 2009. **124**(19781570): p. 324-335.

44. Fernandez-Sola, J., et al., *Molecular and cellular events in alcohol-induced muscle disease.* Alcohol Clin Exp Res, 2007. **31**(12): p. 1953-62.

45. Adachi, J., et al., *Alcoholic muscle disease and biomembrane perturbations (review).* J Nutr Biochem, 2003. **14**(14629892): p. 616-625.

46. Preedy, V.R., et al., *Chronic alcoholic myopathy: transcription and translational alterations.* FASEB J, 1994. **8**(7958620): p. 1146-1151.

47. Fernandez-Solà, J., J.M. Junyent, and A. Urbano-Marquez, *Alcoholic myopathies.* Curr Opin Neurol, 1996. **9**(8894418): p. 400-405.

48. Sakurama, K., *[Effects of long-term ethanol administration on the kidneys, bones and muscles of mice].* Nihon Arukoru Yakubutsu Igakkai Zasshi, 1998. **33**(10028828): p. 703-717.

49. Zakhari, S., *Overview: how is alcohol metabolized by the body?* Alcohol Res Health, 2006. **29**(17718403): p. 245-254.

50. Garriga, J., et al., *Ethanol inhibits skeletal muscle cell proliferation and delays its differentiation in cell culture.* Alcohol Alcohol, 2000. **35**(10869241): p. 236-241.

51. Lang, C.H., et al., *Alcohol myopathy: impairment of protein synthesis and translation initiation.* Int J Biochem Cell Biol, 2001. **33**(11331201): p. 457-473.

52. Preedy, V.R., et al., *Free radicals in alcoholic myopathy: indices of damage and preventive studies.* Free Radic Biol Med, 2002. **32**(11937294): p. 683-687.

53. Morrow, D., et al., *Alcohol inhibits smooth muscle cell proliferation via regulation of the Notch signaling pathway.* Arterioscler Thromb Vasc Biol, 2010. **30**(20930168): p. 2597-2603.

54. Morrow, D., et al., *Ethanol stimulates endothelial cell angiogenic activity via a Notch- and angiopoietin-1-dependent pathway.* Cardiovasc Res, 2008. **79**(18448572): p. 313-321.

55. Yu, H.-C., et al., *Canonical notch pathway protects hepatocytes from ischemia/reperfusion injury in mice by repressing reactive oxygen species production through JAK2/STAT3 signaling.* Hepatology, 2011. **54**(21633967): p. 979-988.

56. Ponnappa, B.C. and E. Rubin, *Modeling alcohol's effects on organs in animal models.* Alcohol Res Health, 2000. **24**(11199283): p. 93-9104.

57. Brodie, C. and A. Vernadakis, *Ethanol increases cholinergic and decreases GABAergic neuronal expression in cultures derived from 8-day-old chick embryo cerebral hemispheres: interaction of ethanol and growth factors.* Brain Res Dev Brain Res, 1992. **65**(1572068): p. 253-257.

58. Burattini, S., et al., *C2C12 murine myoblasts as a model of skeletal muscle development: morpho-functional characterization.* Eur J Histochem, 2004. **48**(15596414): p. 223-233.

59. Wagatsuma, A., et al., *Pharmacological inhibition of HSP90 activity negatively modulates myogenic differentiation and cell survival in C2C12 cells.* Mol Cell Biochem, 2011. **358**(21739150): p. 265-280.

60. Erbay, E. and J. Chen, *The mammalian target of rapamycin regulates C2C12 myogenesis via a kinase-independent mechanism.* J Biol Chem, 2001. **276**(11500483): p. 36079-36082.

61. Velica, P. and C.M. Bunce, *A quick, simple and unbiased method to quantify C2C12 myogenic differentiation.* Muscle Nerve, 2011. **44**(21996796): p. 366-370.

62.   Markworth, J.F. and D. Cameron-Smith, *Prostaglandin F2α stimulates PI3K/ERK/mTOR signaling and skeletal myotube hypertrophy.* Am J Physiol Cell Physiol, 2011. **300**(21191105): p. 671-682.

63.   Bryan, B.A., et al., *Coordinated vascular endothelial growth factor expression and signaling during skeletal myogenic differentiation.* Mol Biol Cell, 2008. **19**(3): p. 994-1006.

64.   Systems, I., *Ingenuity Systems Citation Guidelines.* 2011.

65.   Systems, I., *IPA 5.5 Help Manual version 1.* 2007.

66.   Systems, I., *Ingenuity Transcription Factor Analysis in IPA.* 2011.

67.   Preedy, V.R., et al., *The importance of alcohol-induced muscle disease.* J Muscle Res Cell Motil, 2003. **24**(12953836): p. 55-63.

68.   Andres, V. and K. Walsh, *Myogenin expression, cell cycle withdrawal, and phenotypic differentiation are temporally separable events that precede cell fusion upon myogenesis.* J Cell Biol, 1996. **132**(8647896): p. 657-666.

69.   Saggin, L., et al., *Cardiac troponin T in developing, regenerating and denervated rat skeletal muscle.* Development, 1990. **110**(2): p. 547-54.

70.   Tanaka, S., K. Terada, and T. Nohno, *Canonical Wnt signaling is involved in switching from cell proliferation to myogenic differentiation of mouse myoblast cells.* J Mol Signal, 2011. **6**(21970630): p. 12-12.

71.   Wagner, B.K., et al., *Small-molecule fluorophores to detect cell-state switching in the context of high-throughput screening.* J Am Chem Soc, 2008. **130**(18327938): p. 4208-4209.

72.   Yoon, M.S. and J. Chen, *PLD regulates myoblast differentiation through the mTOR-IGF2 pathway.* J Cell Sci, 2008. **121**(Pt 3): p. 282-9.

73.   Nowak, S.J., et al., *Nap1-mediated actin remodeling is essential for mammalian myoblast fusion.* J Cell Sci, 2009. **122**(19706686): p. 3282-3293.

74.   Watanabe, T.M., et al., *Chromatin plasticity as a differentiation index during muscle differentiation of C2C12 myoblasts.* Biochem Biophys Res Commun, 2012. **418**(22306010): p. 742-747.

75.   Linkhart, T.A., C.H. Clegg, and S.D. Hauschka, *Control of mouse myoblast commitment to terminal differentiation by mitogens.* J Supramol Struct, 1980. **14**(6454029): p. 483-498.

76.   Melcer, S. and E. Meshorer, *Chromatin plasticity in pluripotent cells.* Essays Biochem, 2010. **48**(20822497): p. 245-262.

77.   Ono, Y., et al., *BMP signalling permits population expansion by preventing premature myogenic differentiation in muscle satellite cells.* Cell Death Differ, 2011. **18**(20689554): p. 222-234.

78.   Shu, L. and P.J. Houghton, *The mTORC2 complex regulates terminal differentiation of C2C12 myoblasts.* Mol Cell Biol, 2009. **29**(19564418): p. 4691-4700.

79.   Hipp, J.A., et al., *Ethanol alters the osteogenic differentiation of amniotic fluid-derived stem cells.* Alcohol Clin Exp Res, 2010. **34**(20608908): p. 1714-1722.

80.   Adickes, E.D. and R.M. Shuman, *Fetal alcohol myopathy.* Pediatr Pathol, 1983. **1**(6687287): p. 369-384.

81.   Lepper, C., T.A. Partridge, and C.-M. Fan, *An absolute requirement for Pax7-positive satellite cells in acute injury-induced skeletal muscle regeneration.* Development, 2011. **138**(21828092): p. 3639-3646.

82.   Kerns, R.T. and M.F. Miles, *Microarray analysis of ethanol-induced changes in gene expression.* Methods Mol Biol, 2008. **447**(18369932): p. 395-410.

83. Tomczak, K.K., et al., *Expression profiling and identification of novel genes involved in myogenic differentiation.* FASEB J, 2004. **18**(14688207): p. 403-405.

84. Shen, X., et al., *Genome-wide examination of myoblast cell cycle withdrawal during differentiation.* Dev Dyn, 2003. **226**(12508234): p. 128-138.

85. Clemente, C.F.M.Z., et al., *Differentiation of C2C12 myoblasts is critically regulated by FAK signaling.* Am J Physiol Regul Integr Comp Physiol, 2005. **289**(15890789): p. 862-870.

86. Di Carlo, A., et al., *Hypoxia inhibits myogenic differentiation through accelerated MyoD degradation.* J Biol Chem, 2004. **279**(16): p. 16332-8.

87. Di Padova, M., et al., *MyoD acetylation influences temporal patterns of skeletal muscle gene expression.* J Biol Chem, 2007. **282**(52): p. 37650-9.

88. Duquet, A., et al., *Acetylation is important for MyoD function in adult mice.* EMBO Rep, 2006. **7**(17028574): p. 1140-1146.

89. Fleige, S. and M.W. Pfaffl, *RNA integrity and the effect on the real-time qRT-PCR performance.* Mol Aspects Med, 2006. **27**(16469371): p. 126-139.

90. Imbeaud, S., et al., *Towards standardization of RNA quality assessment using user-independent classifiers of microcapillary electrophoresis traces.* Nucleic Acids Res, 2005. **33**(15800207).

91. Guenin, S., et al., *Normalization of qRT-PCR data: the necessity of adopting a systematic, experimental conditions-specific, validation of references.* J Exp Bot, 2009. **60**(19264760): p. 487-493.

92. Udvardi, M.K., T. Czechowski, and W.-R. Scheible, *Eleven golden rules of quantitative RT-PCR.* Plant Cell, 2008. **20**(18664613): p. 1736-1737.

93. Alter, J. and E. Bengal, *Stress-induced C/EBP homology protein (CHOP) represses MyoD transcription to delay myoblast differentiation.* PLoS One, 2011. **6**(22242125).

94. Cabane, C., et al., *Regulation of C2C12 myogenic terminal differentiation by MKK3/p38alpha pathway.* Am J Physiol Cell Physiol, 2003. **284**(3): p. C658-66.

95. Travaglione, S., et al., *Cytotoxic necrotizing factor 1 hinders skeletal muscle differentiation in vitro by perturbing the activation/deactivation balance of Rho GTPases.* Cell Death Differ, 2005. **12**(1): p. 78-86.

96. Chen, S.L., et al., *The steroid receptor coactivator, GRIP-1, is necessary for MEF-2C-dependent gene expression and skeletal muscle differentiation.* Genes Dev, 2000. **14**(10817756): p. 1209-1228.

97. Ridgeway, A.G., S. Wilton, and I.S. Skerjanc, *Myocyte enhancer factor 2C and myogenin up-regulate each other's expression and induce the development of skeletal muscle in P19 cells.* J Biol Chem, 2000. **275**(1): p. 41-6.

98. Rajan, S., et al., *Analysis of early C2C12 myogenesis identifies stably and differentially expressed transcriptional regulators whose knock-down inhibits myoblast differentiation.* Physiol Genomics, 2012. **44**(22147266): p. 183-197.

99. Kuhn, K., et al., *A novel, high-performance random array platform for quantitative gene expression profiling.* Genome Res, 2004. **14**(11): p. 2347-56.

100. Page, G.P., et al., *A design and statistical perspective on microarray gene expression studies in nutrition: the need for playful creativity and scientific hard-mindedness.* Nutrition, 2003. **19**(14624952): p. 997-991000.

101. Breitling, R., *Biological microarray interpretation: the rules of engagement.* Biochim Biophys Acta, 2006. **1759**(16904203): p. 319-327.

102. Ou, X.-M., et al., *A novel role for glyceraldehyde-3-phosphate dehydrogenase and monoamine oxidase B cascade in ethanol-induced cellular damage.* Biol Psychiatry, 2010. **67**(20022592): p. 855-863.

103. Slonim, D.K. and I. Yanai, *Getting started in gene expression microarray analysis.* PLoS Comput Biol, 2009. **5**(19876380).

104. Bergstrom, D.A., et al., *Promoter-specific regulation of MyoD binding and signal transduction cooperate to pattern gene expression.* Mol Cell, 2002. **9**(11931766): p. 587-600.

105. de la Serna, I.L., et al., *MyoD targets chromatin remodeling complexes to the myogenin locus prior to forming a stable DNA-bound complex.* Mol Cell Biol, 2005. **25**(10): p. 3997-4009.

106. Gundogan, F., et al., *siRNA inhibition of aspartyl-asparaginyl beta-hydroxylase expression impairs cell motility, Notch signaling, and fetal growth.* Pathol Res Pract, 2011. **207**(9): p. 545-53.

107. Muthuchamy, M., L. Pajak, and D.F. Wieczorek, *Induction of endogenous myosin light chain 1 and cardiac alpha-actin expression in L6E9 cells by MyoD1.* J Biol Chem, 1992. **267**(1382061): p. 18728-18734.

108. Slonim, D.K., *From patterns to pathways: gene expression data analysis comes of age.* Nat Genet, 2002. **32 Suppl**(12454645): p. 502-508.

109. Porter, G.A., R.F. Makuck, and S.A. Rivkees, *Reduction in intracellular calcium levels inhibits myoblast differentiation.* J Biol Chem, 2002. **277**(12042317): p. 28942-28947.

110. Odemis, V., et al., *The chemokine SDF1 controls multiple steps of myogenesis through atypical PKCzeta.* J Cell Sci, 2007. **120**(17971416): p. 4050-4059.

111. Griffin, C.A., et al., *Chemokine expression and control of muscle cell migration during myogenesis.* J Cell Sci, 2010. **123**(Pt 18): p. 3052-60.

112. Hunger, C., V. Odemis, and J. Engele, *Expression and function of the SDF-1 chemokine receptors CXCR4 and CXCR7 during mouse limb muscle development and regeneration.* Exp Cell Res, 2012(22766125).

113. Ratajczak, M.Z., et al., *Expression of functional CXCR4 by muscle satellite cells and secretion of SDF-1 by muscle-derived fibroblasts is associated with the presence of both muscle progenitors in bone marrow and hematopoietic stem/progenitor cells in muscles.* Stem Cells, 2003. **21**(12743331): p. 363-371.

114. Luo, Y., et al., *SDF1alpha/CXCR4 signaling, via ERKs and the transcription factor Egr1, induces expression of a 67-kDa form of glutamic acid decarboxylase in embryonic hippocampal neurons.* J Biol Chem, 2008. **283**(36): p. 24789-800.

115. Casado, F.L., K.P. Singh, and T.A. Gasiewicz, *Aryl hydrocarbon receptor activation in hematopoietic stem/progenitor cells alters cell function and pathway-specific gene modulation reflecting changes in cellular trafficking and migration.* Mol Pharmacol, 2011. **80**(21791576): p. 673-682.

116. Tan, W., D. Martin, and J.S. Gutkind, *The Galpha13-Rho signaling axis is required for SDF-1-induced migration through CXCR4.* J Biol Chem, 2006. **281**(17056591): p. 39542-39549.

117. Mayer, U., *Integrins: redundant or important players in skeletal muscle?* J Biol Chem, 2003. **278**(17): p. 14587-90.

118. Huang, Y., et al., *The roles of integrin-linked kinase in the regulation of myogenic differentiation.* J Cell Biol, 2000. **150**(10953009): p. 861-872.

119. Dowling, J.J., et al., *Kindlin-2 is required for myocyte elongation and is essential for myogenesis.* BMC Cell Biol, 2008. **9**(18611274): p. 36-36.

120. Wu, Z., et al., *p38 and extracellular signal-regulated kinases regulate the myogenic program at multiple steps.* Mol Cell Biol, 2000. **20**(10805738): p. 3951-3964.

121. Keren, A., Y. Tamir, and E. Bengal, *The p38 MAPK signaling pathway: a major regulator of skeletal muscle development.* Mol Cell Endocrinol, 2006. **252**(16644098): p. 224-230.

122. Hong-Brown, L.Q., et al., *Alcohol and indinavir adversely affect protein synthesis and phosphorylation of MAPK and mTOR signaling pathways in C2C12 myocytes.* Alcohol Clin Exp Res, 2006. **30**(8): p. 1297-307.

123. Bhatnagar, S., et al., *Transforming growth factor-beta-activated kinase 1 is an essential regulator of myogenic differentiation.* J Biol Chem, 2010. **285**(20037161): p. 6401-6411.

124. Tran, P., et al., *TGF-beta-activated kinase 1 (TAK1) and apoptosis signal-regulating kinase 1 (ASK1) interact with the promyogenic receptor Cdo to promote myogenic differentiation via activation of p38MAPK pathway.* J Biol Chem, 2012. **287**(15): p. 11602-15.

125. Bachinski, L.L., et al., *Altered MEF2 isoforms in myotonic dystrophy and other neuromuscular disorders.* Muscle Nerve, 2010. **42**(21104860): p. 856-863.

126. Nakahara, T., et al., *Acute and chronic effects of alcohol exposure on skeletal muscle c-myc, p53, and Bcl-2 mRNA expression.* Am J Physiol Endocrinol Metab, 2003. **285**(12876071): p. 1273-1281.

127. Soddu, S., et al., *Interference with p53 protein inhibits hematopoietic and muscle differentiation.* J Cell Biol, 1996. **134**(8698814): p. 193-204.

128. Porrello, A., et al., *p53 regulates myogenesis by triggering the differentiation activity of pRb.* J Cell Biol, 2000. **151**(11121443): p. 1295-1304.

129. Yeilding, N.M., et al., *c-myc mRNA is down-regulated during myogenic differentiation by accelerated decay that depends on translation of regulatory coding elements.* J Biol Chem, 1998. **273**(9624173): p. 15749-15757.

130. Crescenzi, M., D.H. Crouch, and F. Tato, *Transformation by myc prevents fusion but not biochemical differentiation of C2C12 myoblasts: mechanisms of phenotypic correction in mixed culture with normal cells.* J Cell Biol, 1994. **125**(8195295): p. 1137-1145.

131. Weintraub, H., et al., *The myoD gene family: nodal point during specification of the muscle cell lineage.* Science, 1991. **251**(1846704): p. 761-766.

132. Tapscott, S.J., *The circuitry of a master switch: Myod and the regulation of skeletal muscle gene transcription.* Development, 2005. **132**(15930108): p. 2685-2695.

133. Epstein, J.A., et al., *Pax3 inhibits myogenic differentiation of cultured myoblast cells.* J Biol Chem, 1995. **270**(7744814): p. 11719-11722.

134. Collins, C.A., et al., *Integrated functions of Pax3 and Pax7 in the regulation of proliferation, cell size and myogenic differentiation.* PLoS One, 2009. **4**(19221588).

135. Gang, E.J., et al., *Pax3 activation promotes the differentiation of mesenchymal stem cells toward the myogenic lineage.* Exp Cell Res, 2008. **314**(18395202): p. 1721-1733.

136. Olguin, H.C. and B.B. Olwin, *Pax-7 up-regulation inhibits myogenesis and cell cycle progression in satellite cells: a potential mechanism for self-renewal.* Dev Biol, 2004. **275**(2): p. 375-88.

137. Zammit, P.S., et al., *Pax7 and myogenic progression in skeletal muscle satellite cells.* J Cell Sci, 2006. **119**(Pt 9): p. 1824-32.

138. Wen, Y., et al., *Constitutive Notch activation upregulates Pax7 and promotes the self-renewal of skeletal muscle satellite cells.* Mol Cell Biol, 2012. **32**(22493066): p. 2300-2311.

139. Systems, I., *IPA Network Generation Algorithm.* 2005.

140. Chen, I.H.B., et al., *Nuclear envelope transmembrane proteins (NETs) that are up-regulated during myogenesis.* BMC Cell Biol, 2006. **7**(17062158): p. 38-38.

141. Jia, W., et al., *Retinoic acid induces myoblasts transdifferentiation into premeiotic Stra8-positive cells.* Cell Biol Int, 2011. **35**(4): p. 365-72.

142. Schneider, K.J., et al., *Ethanol Administration Impairs Pancreatic Repair After Injury.* Pancreas, 2012.

143. Mason, M.N. and M.J. Mahoney, *Inhibition of gamma-secretase activity promotes differentiation of embryonic pancreatic precursor cells into functional islet-like clusters in poly(ethylene glycol) hydrogel culture.* Tissue Eng Part A, 2010. **16**(8): p. 2593-603.

144. Ruan, Y., et al., *Ethanol hypersensitivity and olfactory discrimination defect in mice lacking a homolog of Drosophila neuralized.* Proc Natl Acad Sci U S A, 2001. **98**(17): p. 9907-12.

145. Sathyan, P., H.B. Golden, and R.C. Miranda, *Competing interactions between micro-RNAs determine neural progenitor survival and proliferation after ethanol exposure: evidence from an ex vivo model of the fetal cerebral cortical neuroepithelium.* J Neurosci, 2007. **27**(32): p. 8546-57.

146. Prestifilippo, J.P., et al., *Effect of manganese on luteinizing hormone-releasing hormone secretion in adult male rats.* Toxicol Sci, 2007. **97**(1): p. 75-80.

147. Fryer, C.J., J.B. White, and K.A. Jones, *Mastermind recruits CycC:CDK8 to phosphorylate the Notch ICD and coordinate activation with turnover.* Mol Cell, 2004. **16**(4): p. 509-20.

148. Kuroda, K., et al., *Delta-induced Notch signaling mediated by RBP-J inhibits MyoD expression and myogenesis.* J Biol Chem, 1999. **274**(11): p. 7238-44.

149. Kitamoto, T. and K. Hanaoka, *Notch3 null mutation in mice causes muscle hyperplasia by repetitive muscle regeneration.* Stem Cells, 2010. **28**(12): p. 2205-16.

150. Artero, R.D., I. Castanon, and M.K. Baylies, *The immunoglobulin-like protein Hibris functions as a dose-dependent regulator of myoblast fusion and is differentially controlled by Ras and Notch signaling.* Development, 2001. **128**(21): p. 4251-64.

151. Nofziger, D., et al., *Notch signaling imposes two distinct blocks in the differentiation of C2C12 myoblasts.* Development, 1999. **126**(8): p. 1689-702.

152. Wittenberger, T., et al., *MyoD stimulates delta-1 transcription and triggers notch signaling in the Xenopus gastrula.* EMBO J, 1999. **18**(7): p. 1915-22.

153. Kaun, K.R., et al., *A Drosophila model for alcohol reward.* Nat Neurosci, 2011. **14**(5): p. 612-9.

154. Li, C., R.W. Peoples, and F.F. Weight, *Alcohol action on a neuronal membrane receptor: evidence for a direct interaction with the receptor protein.* Proc Natl Acad Sci U S A, 1994. **91**(17): p. 8200-4.

155. Hansson, E.M., et al., *Recording Notch signaling in real time.* Dev Neurosci, 2006. **28**(1-2): p. 118-27.

156. Ilagan, M.X., et al., *Real-time imaging of notch activation with a luciferase complementation-based reporter.* Sci Signal, 2011. **4**(181): p. rs7.

157. Barbour, V., et al., *Let's be straight up about the alcohol industry.* PLoS Med, 2011. **8**(5): p. e1001041.

158. Chikritzhs, T., K. Fillmore, and T. Stockwell, *A healthy dose of scepticism: four good reasons to think again about protective effects of alcohol on coronary heart disease.* Drug Alcohol Rev, 2009. **28**(4): p. 441-4.

159. Fillmore, K.M., et al., *Moderate alcohol use and reduced mortality risk: systematic error in prospective studies and new hypotheses.* Ann Epidemiol, 2007. **17**(5 Suppl): p. S16-23.

160. Roerecke, M. and J. Rehm, *The cardioprotective association of average alcohol consumption and ischaemic heart disease: a systematic review and meta-analysis.* Addiction, 2012. **107**(7): p. 1246-60.

161. US Department of Agriculture, U.D.o.H.a.H.S., *Dietary Guidelines for Americans 2010.* 2010.

162. Feinstein, E.C., L. Richter, and S.E. Foster, *Addressing the critical health problem of adolescent substance use through health care, research, and public policy.* J Adolesc Health, 2012. **50**(5): p. 431-6.

163. Babor, T.F., *Alcohol research and the alcoholic beverage industry: issues, concerns and conflicts of interest.* Addiction, 2009. **104 Suppl 1**: p. 34-47.

164. Stenius, K. and T.F. Babor, *The alcohol industry and public interest science.* Addiction, 2010. **105**(2): p. 191-8.

PERMISSIONS AGREEMENT

May 24, 2012

Permission granted to:
Michelle Arya
104 Rock Glen Road
Medford, MA 02155

Material to be reproduced:
Gilbert: *Developmental Biology, Eighth Edition*
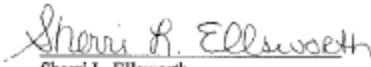Figure 14.11, page 451
Figure 14.12, page 452
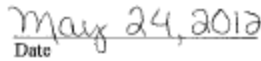Figure 14.13 A-E, page 454
PLEASE NOTE: We are unable to grant permission for you to reproduce 14.13 F and 14.13 G as we do not own the copyright. Please request permission from the copyright holder as noted in the figure caption (14.13 F: from Nameroff and Munar 1976; 14.13 G: courtesy of M. Nameroff).

To be reproduced in the work:
Michelle Arya's PhD Thesis entitled "The Effect of Ethanol on the Differentiation of C2C12 Mouse Myogenic Cells" to be published by Tufts University, Sackler School of Graduate Biomedical Sciences

Sinauer Associates owns copyright to the material described above and hereby grants permission for the one-time use of the material as specified, and for nonexclusive world rights provided that full and appropriate credit is given to the original source and that the work is for NON-COMMERCIAL use only. Please request permission for further use in subsequent editions, translations, or revisions of the work.

Sherri R. Ellsworth
Sherri L. Ellsworth
Permissions Coordinator

May 24, 2012
Date

Please acknowledge your acceptance of these terms by signing one copy of this form and returning it to Sinauer Associates. Permission Agreement is not valid until signed by applicant and received by Sinauer Associates.

Michelle Arya
Signature of Applicant

May 29, 2012
Date